REGULATION OF TRPML1 BY LIPIDS IN LYSOSOMES

by

Dongbiao Shen

A dissertation submitted in partial fulfillment
of the requirements for the degree of
Doctor of Philosophy
(Molecular, Cellular, and Developmental Biology)
in the University of Michigan
2012

Doctoral Committee:

        Associate Professor Haoxing Xu, chair
        Professor Richard I. Hume
        Professor John Y. Kuwada
        Associate Professor X.Z. Shawn. Xu
        Assistant Professor Catherine A. Collins

To my parents and my wife,

for their love and support

ACKNOWLEDGEMENTS

The completion of this work would not have been possible without the support from all the current and past members of the Xu lab. I would like to express my sincere gratitude and deep regards to my research advisor, Dr. Haoxing Xu for his invaluable guidance and constant encouragement throughout my entire graduate study. With great insight and passion for science, he showed me his approach to research the unknown, and instilled in me the importance of hard-working, perseverance and dedication, which I will always keep in mind for my future career. I feel extremely fortunate to be his student and have learned a lot from him both inside and outside science. My sincere thanks also go to Dr. Xiping Cheng and Dr. Xianping Dong, who are not only great colleagues and collaborators, but also great friends generously teaching me many techniques from the first day I joined the lab. The thesis work could not have been done without their support. I also owe my gratitude to Dr. Xiaoli Zhang, Xinran Li, Mohammad Samie and Zepeng Yao for their tremendous help with my research. We had close collaboration and their work has made indispensable contribution to my research projects. I want to thank Brian Eisinger and Andrew Goschka, our lab managers, for their wonderful job in organizing the laboratory work and kind personal assistance to me. I also thank Shannon Dibble, Eric Mills, Huan Meng, Lily Hu, Taylor Dawson, Jayne Knoff, Qiong Gao, Tony Zhou, Evan Gregg, Nicholas Rydzewski, Marlene Azar and all other members from the Xu lab, who are always ready for help and make the Xu lab a supportive and enjoyable place to stay.

I am extremely grateful to the members of my thesis committee, Dr. Richard Hume, Dr. John Kuwada, Dr. Catherine Collins and Dr. Shawn Xu, for being incredible available and helpful throughout my thesis work. Their suggestions on my research are all invaluable, not to mention their constant support on my study and career.

PREFACE

Some parts of Chapter 1 were modified from two invited reviews published in *BioEssays* 2011 Jun;33(6):448-57 and *FEBS Lett*. 2010 May 17;584(10) :2013-21. All the content in Chapter 2 has been published in *Nat. Commun.* 1:38 doi: 10.1038/ ncomms1037 (2010). All Figures in Chapter 3 (except Figure 3.1) have been published in *Nat. Commun.* 3:731 doi: 10.1038/ncomms1735 (2012). All the content in Chapter 3 (except some discussions) has been published in *Nat. Commun.* 3:731 doi: 10.1038/ncomms1735 (2012). Some parts of Chapter 5 were modified from the invited review published in *BioEssays* 2011 Jun;33(6):448-57. Figure 2.1were prepared by Xianping Dong and Xiang Wang. Figure 2.6 and 2.7 were prepared by Xiang Wang, Xianping Dong and me. Figure 2.14, 4.9 were prepared by Xiang Wang. Figure 3.2e,f and Fig 3.3 were prepared by Xiang Wang and Xiaoli Zhang. Figure 3.5b, 4.2a, 4.5b were prepared by Xinran Li.

TABLE OF CONTENTS

LIST OF FIGURES

Figure

LIST OF TABLES

Table

LIST OF ABBREVIATIONS

aSMase: acid sphingomyelinasse

BMP: bis(monoacylglycero)phosphate

Cer: ceramide

EE: early endosome

EEA1: early endosome antigen 1

Endolysosome: endosome and lysosome

HOPS: homotypic fusion and protein sorting

ILV: intraluminal vesicles

Lamp-1: the lysosome-associated membrane protein 1

LEL: late endosome and lysosome

LMP: lysosomal membrane protein

ML4: type IV mucolipidosis

MVB: multi-vesicular body

NP: Niemann-Pick

PC: phophatidylcholine

PE: phosphatidylethanolamine

PM: plasma membrane

PI: phosphatidylinositol

PS: phosphatidylserine

SM: sphingomyelin

SNARE: soluble NSF attachment protein receptor

TGN: *trans*-Golgi network

TM: transmembrane

TRP channels: Transient receptor potential channels

TRPML channels: the mucolipin family of the TRP channels

Abstract

TRPML1 is an inwardly-rectifying Ca^{2+}-permeable channel in late endosomes and lysosomes (LELs). Loss-of-function mutations on the human *TRPML1* gene cause a devastating pediatric neurodegenerative disease called type IV Mucolipidosis (ML4). Although it is well established that TRPML1 is involved in multiple late endocytic membrane trafficking processes, the regulatory mechanism for TRPML1 remains elusive. By directly patch-clamping endolysosomal membranes, we found that $PI(3,5)P_2$, a low abundance endolysosome-specific phosphoinositide, potently and specifically activates TRPML1 in both heterologous and endogenous systems (Chapter 2). Lipid-protein binding assays showed that $PI(3,5)P_2$ binds directly to the poly-basic region of the N terminus of TRPML1. Overexpression of TRPML1 rescued the enlarged vacuole phenotype in $PI(3,5)P_2$-deficient cells, suggesting that TRPML1 is a downstream effector of $PI(3,5)P_2$. Notably, this $PI(3,5)P_2$-dependent regulation of TRPML1 is evolutionarily conserved. In budding yeast, the activity of a yeast functional TRPML homologue is also $PI(3,5)P_2$-dependent. These results indicate that lysosomal $PI(3,5)P_2$ is a physiological regulator of TRPML1, providing a previously unknown link between these two important regulators of intracellular membrane trafficking.

In Chapter 3, a membrane-permeable small-molecule synthetic agonist for TRPMLs, Mucolipin-Synthetic Agonist 1 (ML-SA1), was identified. Electrophysiological results showed that ML-SA1 potently and specifically activates recombinant TRPMLs, as well as endogenous TRPML-like currents in many cell types. In addition, ML-SA1 evoked TRPML1-dependent Ca^{2+} release from endolysosomes in intact cells. ML-SA1 can therefore serve as a valuable tool for studying intracellular functions of TRPMLs.

By taking advantage of ML-SA1, the activity of TRPML1 was examined under a pathological context (Chapter 4). We found that TRPML1-mediated lysosomal Ca^{2+} release, measured using a genetically-encoded Ca^{2+} indicator (GCaMP3) attached directly to TRPML1, was dramatically reduced in Niemann-Pick (NP) disease cells. Patch-clamp analyses revealed that TRPML1 channel activity was inhibited by sphingomyelin, but potentiated by spingomyelinase. Importantly, increasing the expression/activity of TRPML1 was able to alleviate the lipid accumulation and trafficking defects in NPC cells. Our findings suggest that compromised channel activity of TRPML1 is the pathogenic cause for secondary lysosomal storage seen in many lysosomal storage disorders (LSDs). Thus manipulating TRPML1 channel activity by chemical agonists may provide therapeutic approaches not only for ML4, but also for other LSDs.

CHAPTER 1

INTRODUCTION

1. Overview of the lysosomal membrane dynamics

1.1. Lysosomes and their diverse functions

Efficient waste disposal is an essential and basic process in cells - the tiny, autonomous, functional units of our body. In eukaryotic cells, the major degradation centers are lysosomes discovered by Christian de Duve more than 50 years ago using a cell fractionation technique (de Duve 2005). Lysosomes are membrane-enclosed organelles of ~0.5 μm diameter and often have electron-dense cores (Luzio, Pryor et al. 2007). They are heterogeneous in morphology and comprise up to 5% of the intracellular volume (Luzio, Pryor et al. 2007; Saftig and Klumperman 2009). A hallmark feature of lysosomes is their acidic luminal environment that is enriched with more than 50 kinds of acid hydrolases, such as proteases, glycosidases, and phosphatases. Each of these hydrolases has its specific substrate, and collectively, they degrade the majority of cellular waste (Luzio, Pryor et al. 2007; Saftig and Klumperman 2009).

In addition to their degradation function, lysosomes are also involved in various physiological processes (Luzio, Pryor et al. 2007). They have been shown to mediate plasma membrane repair, antigen presentation, and neurite outgrowth via the exocytosis of lysosomal contents, i.e. lysosomal exocytosis (Rao, Huynh et al. 2004; Andrade and Andrews 2005; McNeil and Kirchhausen 2005). The release of lysosomal cathepsins is also implicated in the lysosome

mediated cell death pathway through direct activation of caspase 8, though the detailed mechanism is still unknown (Guicciardi, Leist et al. 2004; Conus, Pop et al. 2012). In addition, lysosomes are also involved in lipid metabolism. For example, cellular cholesterol homeostasis is largely regulated by lysosomal cholesterol efflux through lysosomal membrane proteins (Maxfield and Wustner 2002; Mesmin and Maxfield 2009). These multifaceted functions highlight the significance of the lysosome as a central and dynamic organelle for various cellular activities, as opposed to simply the "garbage-disposal unit" in the cell.

1.2. Major membrane trafficking routes to and from lysosomes

Lysosomes receive their substrates through fusion with endocytic, phagocytic, and autophagic vesicles (see **Fig 1.1**). During endocytosis, membrane proteins are internalized into primary endocytic vesicles. These vesicles undergo maturation and become early endosomes and later develop into late endosomes, on the time scale of minutes to tens of minutes (Luzio, Pryor et al. 2007; Cheng 2010). Both early and late endosomes can bud inwardly from their limiting membranes to form luminal vesicles referred to as multi-vesicular bodies (MVBs) (Gruenberg and Stenmark 2004; Slagsvold, Pattni et al. 2006; Malerod and Stenmark 2009; Raiborg and Stenmark 2009). During this inward budding process, ubiquitinated membrane proteins are sorted into MVBs and eventually delivered into lysosomes for degradation after late endosomes fuse with lysosomes (Hurley and Emr 2006; Saftig and Klumperman 2009). Lysosomes also receive substrates through fusion with phagosomes. This fusion process underlies the maturation of phagosomes to phagolysosomes in phagocytosis, and is essential for the cellular defense against pathogens (Desjardins 1995; Harrison, Bucci et al. 2003; Czibener, Sherer et al. 2006; Huynh, Eskelinen et al.

2007). The third pathway, autophagy, brings to lysosomes the obsolete intracellular components/organelles that have been sequestered in the autophagosome. This pathway is usually used for the turnover of cytoplasmic components in response to stress conditions, such as nutrition starvation in yeast cells (Levine and Klionsky 2004; Yang and Klionsky 2010).

The fusion of a lysosome with a late endosome, phagosome or autophagosome, produces an intermediate fusion-hybrid organelle, inside which the degradation of macromolecules takes place (Mullock, Bright et al. 1998; Saftig and Klumperman 2009). These fusion processes occur constantly and would eventually consume all the lysosomes if it were not for a process known as lysosome biogenesis (**Fig 1.1**) (Pryor, Mullock et al. 2000; Bright, Gratian et al. 2005; Luzio, Pryor et al. 2007). Lysosome biogenesis is the regeneration of lysosomes from the fusion-hybrid organelles. It involves two coupled but separate processes: firstly the formation of spherical or tubular structures oriented toward the surrounding cytosol and secondly the membrane scission (Eskelinen, Illert et al. 2002; Treusch, Knuth et al. 2004; Saftig and Klumperman 2009; Yu, McPhee et al. 2010). The first step requires multiple events of content condensation so that lysosomal specific membrane proteins and hydrolyses are again enriched. The second step is a membrane fission event that gives rise to new lysosomes (Eskelinen, Illert et al. 2002; Saftig and Klumperman 2009).

There are two major outgoing routes of membrane traffic from lysosomes, namely, lysosomal exocytosis and retrograde trafficking from lysosome to Golgi (**Fig 1.1**). Lysosomal exocytosis is essentially a fusion event between the limited lysosomal membrane and plasma membrane. This process is Ca^{2+}- and synaptotagmin VII- dependent, and delivers the membranes needed for plasma membrane repair or phagocytosis of large pathogen particles from extracellular

environment (Rao, Huynh et al. 2004; Andrade and Andrews 2005; McNeil and Kirchhausen 2005). Along with the exocytosis release the contents of the lysosomes, which are involved in cytokine secretion, antigen presentation and neurite outgrowth (Blott and Griffiths 2002; Chow, Toomre et al. 2002; Saftig and Klumperman 2009). The other outgoing route is the retrograde transportation to *trans*-Golgi network (TGN) of vesicles that bud off from late endosomes/lysosomes (LELs). In this way the degraded and recycled materials from lysosomes can be reused for synthesis of new proteins or lipids. In return, vesicles from the Golgi convey newly synthesized integral membrane proteins, hydrolyses, and lipids to endosome and lysosome membrane systems (endolysosomes, collectively) (Janvier and Bonifacino 2005; Luzio, Pryor et al. 2007).

1.3. Putative fusion/fission machinery in the endolysosome system

The various trafficking routes enable lysosomes to orchestrate their myriad cellular functions by specifically exchanging their contents and membranes with other organelles or plasma membrane. These trafficking routes must be tightly regulated to ensure their specificity and direction. Yet due to the inherent difficulties of studying intracellular organelles, the trafficking machineries and their regulators are still far from being fully characterized for endolysosomes. Here I will mainly discuss about the machinery for the fusion process, since membrane fission events are much less well understood - they are generally viewed as the reverse of membrane fusion events and therefore may share some common mechanisms with fusion processes. (Chernomordik and Kozlov 2003; Dong, Wang et al. 2010).

Extensive studies of exocytosis, particularly neurotransmission, have elucidated many of the essential components of membrane fusion events that take place during exocytosis (Suudhof

2008).   For example, soluble NSF attachment protein receptors (SNAREs) have been identified as

the basic structural components needed for membrane fusion events (Suudhof 2008; Wickner 2010).

For the regulation of pre-fusion steps (i.e., priming, tethering, and docking), Rab small GTPases,

Rab effectors, tethering factors, and phosphoinositides have been found to be important factors

(Martens and McMahon 2008; Suudhof 2008; Stenmark 2009; Wickner 2010; Yu and Hughson

2010).

Recent *in vitro* and *in vivo* studies have provided tantalizing glimpses of the similar

regulatory mechanisms shared by the exocytosis and the endolysosomal fusion processes (Hay

2007; Martens and McMahon 2008; Suudhof 2008).   These studies suggest that endolysosomal

fusions also involve sequential stages of tethering, docking and finally bilayer fusion (Luzio, Pryor

et al. 2007). Tethering, the initial interaction between membranes, requires the Rab GTPases, which

are compartmentalized in specific organelle membranes. For example, Rab5 is localized in the

early endosomes, while Rab7 is localized to late endosomes and lysosomes (Stenmark 2009;

Hutagalung and Novick 2011). Rab GTPases recruit their effectors to further determine the

organelle identity and transport specificity. These effectors include tethering factors such as early

endosome antigen 1 (EEA1) or homotypic fusion and protein sorting (HOPS) proteins which

bridge two endolysosomal membranes, lipid kinases/phosphotases that change the lipid

composition and thus the fusogenic potential of the opposing microdomains, as well as sorting

adaptors that redistribute membrane proteins (Grosshans, Ortiz et al. 2006; Stenmark 2009).

Tethered membranes are then brought into proximity by the formation of *trans*-SNARE complexes,

a highly stable, four-helix bundle comprised of three Q-SNAREs on one membrane, and one

R-SNARE on the opposing membrane (Martens and McMahon 2008).   In lysosomes, Vamp7 has

been identified as an R-SNARE, and Syntaxins -7 and -8 are Q-SNAREs (Luzio, Pryor et al. 2007).

After the formation of the *trans*-SNARE complex, a bilayer mixing reaction is initiated.

1.4. Calcium release from endolysosomes regulates membrane trafficking

Ca^{2+} is hypothesized to be another important regulator of endolysosomal membrane trafficking

(Peters and Mayer 1998; Burgoyne and Clague 2003; Hay 2007). Similar to the well-established

role of Ca^{2+} as a key regulator of synaptic vesicle fusion during neurotransmitter release (Suudhof

2008), the transient rise of the Ca^{2+} concentration near the endolysosomal fusion site is considered

as the final trigger of intracellular membrane fusion (Cheng, Shen et al. 2010; Shen, Wang et al.

2011). *In vitro* membrane fusion assays using cell extracts from yeast or mammalian cells have

shown that both homotypic and heterotypic fusion events between LELs are inhibited by BAPTA,

but not by EGTA (Peters and Mayer 1998; Pryor, Mullock et al. 2000). Although both BAPTA and

EGTA are Ca^{2+} chelators, the former binds to Ca^{2+} 10–100 times faster than the latter. The most

plausible explanation for this distinct difference in sensitivity to BAPTA versus EGTA is that the

putative fusion site is in close proximity to the Ca^{2+}-release site (Pryor, Mullock et al. 2000; Chen,

Ahluwalia et al. 2002; Hay 2007). By using membrane permeable forms of Ca^{2+} chelators, i.e.

BAPTA and EGTA fused with acetoxymethyl ester (AM), additional studies of intact cells have

further demonstrated that distinct BAPTA/ EGTA sensitivities are also associated with multiple

steps during endolysosomal transport, including endolysosomal fusion and retrograde trafficking

from endolysosomes to the TGN (Ahluwalia, Topp et al. 2001; Burgoyne and Clague 2003; Hay

2007). Thus, both *in vitro* and *in vivo* evidence suggests that Ca^{2+} release from endolysosomes

participates in most, if not all, fusion and fission events along the endolysosomal pathway.

Based on the ionic composition and electrical properties of endolysosomes, the capacity for endolysosomes to release Ca^{2+} during membrane trafficking has been considered (Dong, Wang et al. 2010). The luminal Ca^{2+} concentration of lysosomes is estimated to be 0.5 mM (Christensen, Myers et al. 2002; Lloyd-Evans, Morgan et al. 2008), while Ca^{2+} concentrations associated with endosomes have been shown to vary from 0.003 to 2 mM (Gerasimenko, Tepikin et al. 1998). Thus, both endosomes and lysosomes may represent sources of Ca^{2+} release along the endolysosome trafficking pathway. Dysregulation of luminal Ca^{2+} concentration is known to cause a block of phagosome maturation in macrophages (Shaughnessy, Hoppe et al. 2006), and trafficking defects in neurons and subsequent neurodegenerative diseases (Lloyd-Evans, Morgan et al. 2008; Lloyd-Evans, Waller-Evans et al. 2010)

Several putative endolysosome Ca^{2+}-release channels have been identified using Ca^{2+} imaging and a lysosomal patch-clamp technique (see **Fig 1.2b**). TRPMLs are the principle Ca^{2+} release channels on endolysosomes (Cheng, Shen et al. 2010). Two-pore channels (TPC1 and TPC2) are another type of Ca^{2+} channels that are ubiquitously expressed and are associated with endolysosomes. Recent studies have shown that TPCs may mediate nicotinic acid adenine dinucleotide phosphate (NAADP)-activated Ca^{2+} release from endolysosomes (Zhu, Ma et al. 2010), while overexpression of TPCs has been shown to cause defective membrane trafficking in endolysosomes (Galione, Morgan et al. 2010). Finally, TRPV2 and TRPM2 were detected as cell specific Ca^{2+} permeable channels present in endolysosomes (Saito, Hanson et al. 2007; Lange, Yamamoto et al. 2009). However, characterization of these channels in the membrane trafficking of endolysosomes is ongoing.

Currently, one of the most challenging questions in the field of endolysosomal trafficking is how Ca^{2+} release is tightly regulated *in vivo*. Emerging evidence suggests that while many components of the trafficking machinary, such as Rabs, SNAREs and phosphoinositides, have their own specific major functions (Martens and McMahon 2008; Wickner 2010), they may coordinate with each other and play additional roles as regulators of the Ca^{2+} signaling during fusion/fission process. For example, recent evidence suggests that in addition to their role as structural determinants of fusion, SNAREs can also regulate Rab effectors (Stenmark 2009) and plasma membrane Ca^{2+} channels (Dong, Wang et al. 2010). In yeast, *trans*-SNARE complex formation may directly induce Ca^{2+} release from the lumen of the vacuole (Merz and Wickner 2004). Similarly, phosphoinositides have been shown to be important not only for the recruitment of Rabs and tethering factors, but also for interactions with Ca^{2+} channels and Ca^{2+} sensors (Bai, Tucker et al. 2004).

This thesis will focuses on TRPMLs - the principle Ca^{2+} release channels on endolysosomes, and lipids on lysosomal membrane such as phosphoinosites, sphingolipid and cholesterol, and discuss how they interact with each other to regulate the Ca^{2+} signaling that fine-tune the endolysosomal dynamics. An overview of TRPMLs and lysosomal lipids will be presented in the next two sections.

2. TRPML channels: the principle Ca^{2+} release channels on endolysosomes

Transient receptor potential (TRP) channels are a large family of cation channels with diverse physiological functions particularly in sensory signaling (Clapham 2003; Wu, Sweet et al. 2010). TRPML channels are the mucolipin family of the TRP superfamily (Puertollano and Kiselyov 2009;

Cheng 2010). They are six transmembrane (TM) - spanning proteins with the amino-- and carboxy-terminal tails facing the cytosol. In mammals, there are three TRPML proteins (TRPML1-3). They share high amino acid similarity (~75%), especially in the putative pore region (>90%) between TM 5 and 6 (Puertollano and Kiselyov 2009). A long luminal loop spans across TM1 and TM2, and contains several N-glycosylation sites that may regulate TRPMLs activity. Another structural similarity shared by TRPMLs is the clusters of positively charged amino-acid residues on both amino-- and carboxy- terminus. These residues are important for the channels to interact with acidic lipids such as phosphoinositides (Dong, Shen et al. 2010).

2.1. Intracellular localization and tissue distribution of TRPMLs

At the subcellular level, TRPMLs primarily localize to the endolysosomal system. Overexpression studies using different epitope-tagged versions of TRPML1have revealed that TRPML1 primarily resides on LEL compartments, based on it co-localization with the lysosome-associated membrane protein 1 (Lamp-1) - a LEL specific marker (Dong, Wang et al. 2009; Puertollano and Kiselyov 2009; Cheng 2010). Immunostaining and gradient fractionation methods further confirmed that the endogenous TRPML1 proteins are also localized at LELs. Two acidic di-leucine motifs on both ends of the channel are proposed to be the important regulators for the delivery of TRPML1 to LELs (Pryor, Reimann et al. 2006; Vergarajauregui and Puertollano 2006). The di-leucine motif at N-termini mediates the direct trafficking pathway in which newly synthesized protein are transported from Golgi to LELs, while the di-leucine motif at C-termini mediates the indirect pathway where TRPML1 is first transported to the plasma membrane and then internalized and delivered to LELs. Mutations on both di-leucine motifs largely block the transport of TRPML1

from Golgi to LELs and trap the channel on the plasma membrane (Vergarajauregui and

Puertollano 2006).

Similar overexpression essays with tagged channel proteins revealed that TRPML2 and

TRPML3 are also localized in LEL compartments and co-localized with Lamp-1 (Cuajungco and

Samie 2008; Puertollano and Kiselyov 2009; Zeevi, Frumkin et al. 2009). Immunolocalization

studies have also shown that TRPML2 localizes to the vesicles along the long, tubular structures

within cells in addition to the LELs (Karacsonyi, Miguel et al. 2007). These long, tubular structures

correspond to the recycling endosomes of the GTPase ADP-ribosylation factor-6 (Arf-6) associated

pathway. By using cellular fractionation and primary antibodies raised against TRPML3, Kim et al.

provided evidence that TRPML3 localizes to LELs, early endosomes (EEs), and the plasma

membrane (Kim, Soyombo et al. 2009). The plasma membrane localization of TRPML3 is

consistent with the substantial whole-cell currents that can be recorded from TRPML3-expressing

HEK293 cells.

In the tissue level, TRPML1 has been shown to be ubiquitously expressed, with the highest

levels of expression located in the brain, kidney, spleen, liver, and heart (Cheng 2010). In contrast,

TRPML2 and TRPML3 are associated with a more restricted expression profile: Real-time PCR

analysis reveals that TRPML2 is mainly expressed in the thymus, kidney, and spleen; TRPML3 is

expressed in the cochlea, thymus, lung, kidney, spleen, eye and skin (Puertollano and Kiselyov

2009; Cheng 2010).

2.2. Channel properties of TRPMLs

TRPML3 was the first TRPML channel to be electrophysiologically characterized (Kim, Li et al.

2007; Xu, Delling et al. 2007; Kim, Li et al. 2008). As mentioned earlier, wild-type TRPML3 is present at the plasma membrane when it is overexpressed, and thus can be characterized using the conventional whole-cell patch clamp technique. These studies have shown that TRPML3 is an inwardly rectifying, Ca^{2+}-permeable cation channel. TRPML3-mediated current (I_{TRPML3}) is inhibited by an acidic extracellular (analogous to the luminal side) pH with H^+ presumably binding to multiple histidine residues within the TM1–TM2 loop (Kim, Li et al. 2007; Kim, Li et al. 2008). Interestingly, I_{TRPML3} is potentiated by the removal and subsequent re-addition of extracellular Na^+. The physiological implications of these two observations remain to be established. A amino acid mutation of mouse TRPML3 (A419P) causes the varitint-waddler (Va) phenotype, which is characterized by deafness, circling behavior, and pigmentation defects (Cuajungco and Samie 2008; Puertollano and Kiselyov 2009). Much larger currents were seen for TRPML3[A419P] (TRPML3[Va]) compared to WT TRPML3 under basal/non-stimulated conditions, consistent with the high open probability of $I_{TRPML3-Va}$ (Xu, Delling et al. 2007). $I_{TRPML3-Va}$ resembles I_{TRPML3} in the basic channel pore properties including current - voltage (I - V), single channel conductance, and ion selectivity. However, since $I_{TRPML3-Va}$ cannot be further activated by Na^+ manipulation, the Va mutation is likely to disrupt channel gating by locking the channel into an open state.

The channel properties of TRPML1 and TRPML2 are more difficult to be characterized due to their intracellular localization. Initial studies on the wild-type TRPML1 were carried out by using the standard whole cell patch clamp method (LaPlante, Falardeau et al. 2002; LaPlante, Ye et al. 2004; Soyombo, Tjon-Kon-Sang et al. 2006). But without an effective method of bringing TRPML1 to the plasma membrane and/or specific agonist for TRPML1, these observations are at best questionable. In fact, they give rise to contradicting results. For example, one group reported

TRPML1 as a monovalent cation channel permeable to and regulated by Ca^{2+}, and with linear conductance (LaPlante, Falardeau et al. 2002), while another group reported that TRPML1 is an outwardly rectifying monovalent cation channel that was blocked by Ca^{2+} (Soyombo, Tjon-Kon-Sang et al. 2006). There were also controversies over the H^+ permeability of TRPML1, which points to the debate whether TRPML1 regulates lysosomal pH (Raychowdhury, Gonzalez-Perrett et al. 2004; Soyombo, Tjon-Kon-Sang et al. 2006).

The application of Va activation-mutation approach facilitated the characterization of the pore properties of TRPML1-2 (Grimm, Cuajungco et al. 2007; Kim, Li et al. 2007; Xu, Delling et al. 2007). By introducing Va-like mutations to TRPML1 (V432P) and TRPML2 (A396P), a large proportion of the channels are mislocalized to the plasma membrane, and thus become accessible to whole cell patch clamp. Similar to TRPML3, $TRPML1^{Va}$ is identified as an inwardly rectifying channel that is permeable to Ca^{2+}- but not H^+. Interestingly, unlike I_{TRPML3}, $I_{TRPML1-Va}$ is potentiated by low pH (Xu, Delling et al. 2007).

Yet, since the Va mutation locks the channel into a constitutively open state, a concern remains that the mutation might change the pore properties of TRPML1 and TRPML2. A technique called lysosomal patch clamp was developed by directly record from isolated endo-lysosomes which were pharmacologically enlarged (from 0.5 to 2 - 3 µm) using the small molecule compound vacuolin-1 (Cerny, Feng et al. 2004; Dong, Cheng et al. 2008). This technique paved the way to study endolysosomal channels in their native membrane (LELs). It was found that lysosomal I_{TRPML1} and I_{TRPML2} exhibited almost identical pore properties as their Va-mutant counterparts (Dong, Cheng et al. 2008; Dong, Shen et al. 2010). Despite many previous controversial results, consensus now has been reached that TRPMLs constitute a family of inwardly rectifying, Ca^{2+}, Na^+,

K^+ permeable but proton-impermeable cation channels (Cheng 2010).

2.3. TRPMLs in membrane trafficking

Mutations of human TRPML1 causes type IV mucolipidosis (ML4) disease, a childhood neurodegenerative disease characterized by severe mental retardation, psychomotor defect and retinal degeneration. Human ML4 mutations cause the abnormal accumulation of sphingolipids, phospholipids, acidic mucopholysaccharides, and cholesterol in swollen/enlarged LEL-like vacuoles in all cell types (Bargal and Bach 1988; Chen, Bach et al. 1998). Consistent with this observation, abnormal lipid accumulation and enlarged LELs are also seen in cells from TRPML1 knockout mice, TRPML$^{-/-}$ (cup-5) C. elegans, and TRPML$^{-/-}$ Drosophila (Treusch, Knuth et al. 2004; Venugopal, Browning et al. 2007; Venkatachalam, Long et al. 2008). Electron microscopy (EM) studies suggest that enlarged LELs in TRPML$^{-/-}$ cells are likely to be the late endosome - lysosome hybrid organelles from which lysosomes are reformed under normal conditions (Piper and Luzio 2004). Since the hydrolase activity that is involved in lipid processing is relatively normal, the defect observed in TRPML$^{-/-}$ cells is most likely related to the sorting and trafficking processes of the endocytic pathway (Chen, Bach et al. 1998). Analyses of trafficking kinetics suggest that the defect is in the late endocytic pathways only. Specifically, the exit of lipids from the LELs to the TGN is defective in ML4 cells (Chen, Bach et al. 1998; Pryor, Reimann et al. 2006). In support of these observations, shRNA-mediated knockdown of TRPML1 expression in mouse macrophages results in a similar defect in retrograde lipid transport (Thompson, Schaheen et al. 2007). Taken together, TRPML1 is likely to be required for the formation of transport vesicles from the LEL compartments to the TGN and for the reformation of lysosomes from the late

endosome - lysosome hybrid organelles (Piper and Luzio 2004; Treusch, Knuth et al. 2004). This hypothesis is supported by the observation that TRPML1 expression is dramatically increased following induction of lysosome biogenesis (Sardiello, Palmieri et al. 2009). Since membrane fission and/or stabilization of transport vesicles is known to be dependent on luminal Ca^{2+} release (Pryor, Mullock et al. 2000; Luzio, Bright et al. 2007), it is likely that the Ca^{2+} permeability of TRPML1 is required for the membrane fission from LEL compartments or late endosome - lysosome hybrids and the biogenesis of both retrograde transport vesicles and lysosomes (**Fig. 1.1**). TRPML1 may also be required for the reformation of lysosomes from autolysosomes (Venkatachalam, Long et al. 2008; Vergarajauregui, Connelly et al. 2008).

Other trafficking defects are also observed in TRPML$^{-/-}$ cells. ML4 fibroblasts have been reported to exhibit a delay in the delivery of platelet-derived growth factor receptor (PDGFR) to lysosomes (Vergarajauregui, Connelly et al. 2008). In mouse macrophages where TRPML1 protein level has been reduced by shRNA, the transport of endocytosed molecules to lysosomes is delayed (Thompson, Schaheen et al. 2007). Autophagosomes have also been shown to accumulate in ML4 cells. This could be due to either increased autophagosome formation or delayed fusion of autophagosomes with lysosomes to form autolysosomes (AL) (**Fig. 1.1**) (Vergarajauregui, Connelly et al. 2008). ML4 fibroblasts also show a defect in ionomycin-induced lysosomal exocytosis (LaPlante, Sun et al. 2006). However, this effect could be a secondary observation, since ionomycin (a Ca^{2+} ionophore) presumably acts directly on the Ca^{2+} sensor synaptotagmin VII thereby bypassing upstream TRPML activation. Nevertheless, experiments showing that HEK293 cells transfected with a gain-of-function mutant of TRPML1 exhibit enhanced lysosomal exocytosis provide additional evidence that TRPML1 plays a role in this process (Dong, Wang et al.

2009). The gain-of-function mutation is likely to have mimicked an unidentified cellular stimulation to induce intralysosomal Ca^{2+} release since these experiments were performed using a Ca^{2+}-free extracellular solution to exclude the involvement of the gain-of-function TRPML1 channels at the plasma membrane. Taken together, TRPML1 plays a role in multiple membrane fusion processes related to late endosomes and lysosomes. TRPML1 may be tightly regulated to release Ca^{2+} as a mechanism of modulating the endocytic process in a correct spatiotemporal way.

In comparison to TRPML1, the role of TRPML2 and TRPML3 in regulating membrane trafficking is less understood. TRPML2 and TRPML3 may function indirectly through the formation of heteromultimers with TRPML1, since both heterologously-expressed (Venkatachalam, Hofmann et al. 2006) and endogenous (Zeevi, Frumkin et al. 2009) TRPMLs can physically associate with each other. However, the extent of co-localization appears to be limited (Zeevi, Frumkin et al. 2009). Therefore, it is more likely that TRPML2 and TRPML3 functions are primarily cell type specific. In LELs, it is reasonable to hypothesize that TRPML2/3 play a similar role in membrane trafficking as TRPML1. TRPML2 has been reported to traffic via the Arf6-associated recycling pathway in Hela cells (Karacsonyi, Miguel et al. 2007). While overexpression of TRPML2 promotes efficient activation of Arf6, inactivation of TRPML2 by a dominant-negative approach decreases recycling of CD59 proteins to the plasma membrane (Karacsonyi, Miguel et al. 2007). Thus, TRPML2 may interact and cross-talk with other trafficking regulators to control cargo sorting. The localization of TRPML3 is more dynamic with expression in multiple intracellular compartments. The diverse expression of TRPML3 may correlate with its role in membrane trafficking (Kim, Soyombo et al. 2009; Martina, Lelouvier et al. 2009). Overexpression of TRPML3 causes enlarged early-endosome-like structures and defective delivery

and degradation of EGF and EGFR that is consistent with its expression in EEs (Kim, Soyombo et al. 2009; Martina, Lelouvier et al. 2009). Since heterologously-expressed TRPMLs display basal activity in the LELs, it is possible that overexpression of TRPML3 promotes endosomal membrane fusion. Interestingly, knockdown of TRPML3 appears to enhance endocytosis and degradation (Zeevi, Frumkin et al. 2009), a result that is inconsistent with the role of TRPML1 in degradation and trafficking in the late endocytic pathways (LaPlante, Falardeau et al. 2002; Pryor, Reimann et al. 2006). It is possible that this observed effect is due to a function of TRPML3 in early endocytic pathways. The exact step where TRPML3 functions in the early endocytic pathway is still not clear. While Kim et al. showed that TRPML3 overexpression decreases constitutive and regulated endocytosis in HEK and HeLa cells (Kim, Soyombo et al. 2009), Martina et al. found that internalization of EGFR is not affected but that its delivery from the plasma membrane to the lysosome is impaired in human epithelial cells (Martina, Lelouvier et al. 2009). It is possible that these observed differences are due to the use of different cell types. Finally, TRPML3 may also be involved in the regulation of autophagy since both overexpression and knockdown of TRPML3 affect autophagy (Kim, Soyombo et al. 2009; Martina, Lelouvier et al. 2009).

It is yet unclear how TRPMLs coordinate with the other key regulators of vesicle trafficking such as GTPases (Rab and Arf) and phosphoinositides to control endolysosomal dynamics; however, we do know that dysfunctions of these regulators all cause similar cellular defects. Constitutive activation of Rab5 causes enlarged early endosomes by stimulating homotypic fusion (Stenmark 2009). This is reminiscent of the enlarged endosomes seen in cells with TRPML3 overexpression. It is possible that Rab5 may recruit effectors to activate TRPMLs. Alternatively, the activity of TRPMLs may regulate the activity of Rabs, as shown in the case of TRPML2 and

Arf6 GTPase (Karacsonyi, Miguel et al. 2007). Similarly, alterations of the levels of endolysosomal phosphoinositides (PI(3)P and PI(3,5)P$_2$) also results in enlarged endolysosomes and defective endosome-to-TGN retrograde trafficking (Roth 2004), a situation that is similar to the enlarged LELs and abnormal late endocytic trafficking phenotype seen in ML4 cells. It is possible that TRPMLs are regulated directly by phosphoinositides as shown for many other plasma membrane TRPs (Rohacs and Nilius 2007). Alternatively, TRPMLs may regulate key enzymes involved in the production or hydrolysis of phosphoinositides. Chapter 2 will discuss one of these possibilities.

3. Lipids on the lysosome membrane

Like all membranes, the limiting lysosomal membranes have a remarkably complex composition and organization of lipids, the function of which are only starting to be unraveled. The major types of lipids on the limiting lysosomal membrane include phophatidylcholine (PC), phosphatidylethanolamine (PE), phosphatidylserine (PS), phosphatidylinositol (PI), sphingolipids, cholesterol, as well as their various metabolic derivatives (Kolter and Sandhoff 2005; van Meer, Voelker et al. 2008; Lippincott-Schwartz and Phair 2010; Blom, Somerharju et al. 2011; Sztolsztener, Dobrzyn et al. 2012). These lipids on lysosomal membranes can affect the vast numbers of cellular processes that lysosomes are associated with in at least three principle ways. First, they serve as structural components of the lysosomal membrane and define its physical properties (Hannun and Obeid 2008; Graham and Kozlov 2010; Lingwood and Simons 2010; Lippincott-Schwartz and Phair 2010). The structural features of lipids can influence the flexibility, thickness and fusogenic potentials of membranes. For example, glycerophospholipids (GPLs, including PC, PE, PS and PI) mostly have unsaturated fatty acyl chains; thus the membrane

enriched with GPLs are highly flexible (Lippincott-Schwartz and Phair 2010). On the other hand, sphingolipids and cholesterol usually form more ordered and stiff membrane (Graham and Kozlov 2010; Lippincott-Schwartz and Phair 2010; Blom, Somerharju et al. 2011). In lysosomes, the concentrations of sphingolipids and cholesterol are lower than those in PM, thus providing a relatively flexible lipid environment suitable for dynamic fusion/fission process (van Meer, Voelker et al. 2008). Second, a variety of signaling factors and lipid enzymes can be recruited to and interact with specific lysosomal lipids (van Meer, Voelker et al. 2008; Breslow and Weissman 2010), generating a complicated regulatory network that modulate the trafficking and activity of lysosomes. Such regulatory network helps change the local shape of membranes, sort proteins into differentiated subdomains within membranes, and modulate the activity of integral membrane proteins. Third, some lysosomal lipids and their metabolic derivatives play critical roles as signaling molecules that regulate the activity of lysosomal enzymes and integrity of lysosmal membrane (Heinrich, Wickel et al. 2000; Breslow and Weissman 2010; Kirkegaard, Roth et al. 2010). For example, ceramide, a kind of sphingolipids, can function as an intracellular second messenger that binds to and activates a hydrolytic enzyme called cathepsin D in the lysosome (Heinrich, Wickel et al. 2000). A recent report provides another striking example that bis(monoacylglycero)phosphate (BMP), a membrane-bound, anionic phospholipid predominantly localized to the inner lysosomal membrane, can interact with heat-shock protein 70 (Hsp70) and help preserve the integrity of membranes under stress conditions (Kirkegaard, Roth et al. 2010).

In addition to the lipids on the limiting lysosomal membrane, a considerable number of membranes and lipids are passively delivered into lysosomes for degradation during the endocytosis, phagocytosis and autophagy processes (Saftig and Klumperman 2009; Kolter and

Sandhoff 2010). These membrane lipids reside on the internal vesicles in lysosomal lumen, where some of them are broken down into their "building blocks" such as fatty acid, or sphingoid base (Kolter and Sandhoff 2005; Kolter and Sandhoff 2010), while others like cholesterol are freed from the "lipid raft" (Gallala, Breiden et al. 2011; Gallala and Sandhoff 2011). This recycling and turnover process of membrane lipids in lysosomes is essential for overall cellular lipid metabolism, the failure of which leads to severe fatal neurodegenerative diseases (Nixon, Yang et al. 2008; Bellettato and Scarpa 2010; Kolter and Sandhoff 2010). Although these luminal lipids cannot directly affect integral lysosomal membrane proteins (LMPs), under pathological condition their storages at the lysosomal lumen may indirectly change the lipid composition of the limiting lysosomal membrane, and therefore modulate LMPs (Fraldi, Annunziata et al. 2010).

Whether any of these lipids in lysosomes can modulate TRPML1 is a question nobody had the answer three years ago when I began to work on the thesis; in fact, this question was barely explored at that time due to the inaccessibility of TRPML1 and these lipids. One clue to this question is that under pathological conditions, the dysregulation of the metabolism of several lipids in lysosomes causes the same late endocytic trafficking defects as those observed in TRPML1$^{-/-}$ cells (Chen, Patterson et al. 1999; Puri, Watanabe et al. 1999), suggesting that these lipids may function in the same signaling pathway as TRPML1, or may even directly regulate TRPML1. Among these lipids are PI(3,5)P$_2$, sphingomyelin and cholesterol, all of which could be potential regulators of TRPML1 and become the focuses of my thesis. In the following sessions, overviews of these three lipids and their critical role in endolysosomal dynamics will be presented.

3.1. PI(3,5)P$_2$ on the lysosome membrane

Phosphoinositides are a group of negatively charged phospholipids derived from phosphatidylinositol, which play key roles in cell signaling and membrane trafficking (Roth 2004; McCrea and De Camilli 2009; Poccia and Larijani 2009). Seven phosphoinositide isoforms have been identified: PI(3)P, PI(4)P, PI(5)P, PI(3,4)P$_2$, PI(3,5)P$_2$, PI(4,5)P$_2$, PI(3,4,5)P$_3$. They are concentrated on different parts of cellular membranes, with PI(4,5)P$_2$ mainly on plasma membranes, PI(4)P on Golgi, PI(3)P on the cytoplasmic side of endosomes, and PI(3,5)P$_2$ found on late endosome and lysosomes (see **Fig 1.2**). The best characterized phosphoinositides is PI(4,5)P$_2$, which modulates a number of plasma membrane channels (Suh and Hille 2008). My major focus here will be PI(3,5)P$_2$, a LEL specific phosphoinositide that has recently drawn the attention of many investigators.

3.1.1. PI(3,5)P$_2$ in late endosomes and lysosomes

PI(3,5)P$_2$ only represents ~0.05% of the total cellular phosphoinositides present in non-stimulated cells under basal conditions (Dove, Dong et al. 2009; Ikonomov, Sbrissa et al. 2011). This is ~10-fold less than the levels of PI(3)P that are normally maintained in cells (Zhang, Zolov et al. 2007). Due to its low abundance and lack of a specific detection probe (Kutateladze 2010), the majority of PI(3,5)P$_2$ studies have focused on PI(3,5)P$_2$-metabolizing enzymes, including PIKfyve/Fab1 and its regulators (Shisheva, Rusin et al. 2001; Chow, Zhang et al. 2007; Zhang, Zolov et al. 2007; Jin, Chow et al. 2008). PI(3,5)P$_2$ is generated from PI(3)P via PIKfyve/Fab1 (see **Fig 1.2a**), a PI 5-kinase that localizes to endolysosomes in both yeast and mammalian cells (Duex, Nau et al. 2006; Duex, Tang et al. 2006; Botelho, Efe et al. 2008; Dove, Dong et al. 2009; Poccia and Larijani 2009; Ikonomov, Sbrissa et al. 2011). Therefore, PI(3,5)P$_2$ is hypothesized to predominantly localize to the LELs

(Bonangelino, Nau et al. 2002; Chow, Zhang et al. 2007; Zhang, Zolov et al. 2007; Dove, Dong et al. 2009). The activity of PIKfyve/Fab1 has been shown to be positively regulated by several associated proteins such as Fig4 and Vac14 (Chow, Zhang et al. 2007; Zhang, Zolov et al. 2007; Jin, Chow et al. 2008; Dove, Dong et al. 2009). On the other hand, $PI(3,5)P_2$ can be hydrolyzed to $PI(5)P$ by the myotubularin (MTM/MTMR)-family of PI-3 phosphatase (Dove, Dong et al. 2009; Poccia and Larijani 2009; Shen, Yu et al. 2009). Although the global concentration of $PI(3,5)P_2$ is very low, the local concentration in PIKfyve-enriched microdomains is likely to increase in response to stimuli (Botelho, Efe et al. 2008; Ikonomov, Sbrissa et al. 2009), and can reach levels similar to those of $PI(4,5)P_2$ at the plasma membrane (~10 μM) (Whiteford, Brearley et al. 1997; Duex, Nau et al. 2006; Duex, Tang et al. 2006). Mutations in $PI(3,5)P_2$-metabolizing enzymes have been shown to be responsible for a variety of neurodegenerative diseases including amyotrophic lateral sclerosis (ALS) and Charcot-Marie-Tooth (CMT) disease in humans (Chow, Zhang et al. 2007; Chow, Landers et al. 2009; Dove, Dong et al. 2009).

3.1.2. Cellular consequences of $PI(3,5)P_2$ deficiency

At the cellular level, $PI(3,5)P_2$-deficient cells, such as fibroblasts from Fig4 or Vac14 KO mice, exhibit enlarged endolysosomes/vacuoles and trafficking defects in the late endocytic pathways, which include retrograde LEL-to-TGN trafficking, MVB formation, autophagosome-lysosome fusion, and exocytosis (Berwick, Dell et al. 2004; Chow, Zhang et al. 2007; Zhang, Zolov et al. 2007; Jin, Chow et al. 2008; Ferguson, Lenk et al. 2009). In studies of $Vac14^{-/-}$ cells, immunoreactivity of a cation-independent mannose-6- phosphate receptor (ciM6PR), a membrane protein that shuttles between TGN and the LELs, was detected in Lamp1-positive compartments

rather than in the TGN (Zhang, Zolov et al. 2007), suggesting that reformation of ciM6PR-positive transport vesicles from LELs was compromised. Consistent with this model, suppression of PIKfyve by small interfering RNA or by treatment with YM201636, a potent inhibitor of Pikfyve, also induces defective endosome to TGN retrograde traffic and the formation of swollen endosomal structures (Rutherford, Traer et al. 2006; Jefferies, Cooke et al. 2008). The detailed molecular mechanism for the $PI(3,5)P_2$ dependent retrograde trafficking effect is largely unknown, though Atg18 is reported to mediate the effect (Dove, Piper et al. 2004). In addition, $PI(3,5)P_2$ is implicated to be important for sorting proteins to MVBs. Several proteins required for protein sorting to MVBs are reported to bind to $PI(3,5)P_2$, such as Ent3p and VPS24 (Friant, Pecheur et al. 2003) (Whitley, Reaves et al. 2003). $PI(3,5)P_2$ may function together with $PI(3)P$ as important recruitment markers for ESCRT complex formation in endolysosomal compartments. Disrupting the balance between $PI(3)P$ and $PI(3,5)P_2$ may affect the proper sorting of macromoleculars to MVBs, as shown in the case that MVB protein sorting is impaired in yeast mutants with deficient $PI(3,5)P_2$ synthesis (Dove, Dong et al. 2009). $PI(3,5)P_2$ has also been shown to have an essential role in the fusion of late endosomes or lysosomes with other organelles, including autophagosomes (Ferguson, Lenk et al. 2009). Consistent with a role for $PI(3,5)P_2$ in exocytosis, PIKfyve has been implicated in the translocation of several ion channels and transporters to the plasma membrane (Hill, Hudson et al. 2010).

3.1.3. The effectors of $PI(3,5)P_2$

$PI(3,5)P_2$ exerts its effect through the recruitment of effector proteins that bind to $PI(3,5)P_2$. Several effector proteins have been identified, but considering the multifaceted functions that $PI(3,5)P_2$

associates with, future research promises the discoveries of many more downstream effectors. Atg18 is a protein that potentially mediates retrograde trafficking following its binding of PI(3,5)P$_2$ in yeast (Dove, Piper et al. 2004). Similarly, WIP1 has been shown to bind both PI(3)P and PI(3,5)P$_2$ to affect ciM6PR recycling in mammalian cells, suggesting that it is an effector of PI(3,5)P$_2$ (Proikas-Cezanne, Ruckerbauer et al. 2007). Chapter 2 will demonstrate that mucolipin subfamily of Transient Receptor Potential channels (TRPMLs) are novel PI(3,5)P$_2$ effectors that mediate the release of Ca^{2+} from endolysosomes (Dong, Shen et al. 2010).

3.2. Sphingomyelin in lysosomes

Sphingomyelin (SM) is the most abundant sphingolipid in mammalian cells and exists virtually in all membranes (Gault, Obeid et al. 2010). It consists of a ceramide backbone linked to a polar phosphorylcholine group, which makes it barely able to flip-flop across bilayers and almost water insoluble (Hannun and Obeid 2008; Breslow and Weissman 2010; Gault, Obeid et al. 2010). The major synthesis site of SM is the Golgi (Gault, Obeid et al. 2010). From there, SMs were delivered via vesicle transport to the plasma membrane, where they mainly localize on the outer leaflet of PM, although a small proportion may also exist on the inner leaflet. Upon endocytosis, SMs proceed through the endocytic pathway and reach the lysosome compartments. Here they predominantly localize on the luminal leaflet of endosomal and lysosomal membranes or internal vesicles in the lumen (see **Fig 1.3a**). The breakdown of SM is mediated by the sphingomyelinase family, which hydrolyse SM to ceramide and free phosphocholine (Perrotta and Clementi 2010). Three groups of sphingomyelinase have been identified in mammals based on their optimal pH: acid sphingomyelinasse (aSMase) (Gatt 1963; Gatt 1976), alkaline sphingomyelinases (Duan,

Hertervig et al. 1996) and the neutral sphingomyelinases (Yamaguchi and Suzuki 1978). Among them, aSMase predominantly localizes at lysosomes, while the others concentrate at membranes of other cellular compartment, such as Golgi and plasma membrane (Gault, Obeid et al. 2010).

The catabolism of SM in lysosomes is tightly controlled by aSMase (Perrotta and Clementi 2010). First discovered by the pioneering work of Shimon Gatt in 1963 (Gatt 1963), aSMase is identified as a glycoprotein with *in vitro* pH optimum between 4.5 and 5, and presents in most human tissues (Fowler 1969). The protein is first glycosylated in ER and then phosphorylated in Golgi (Schissel, Keesler et al. 1998; Gault, Obeid et al. 2010). These modifications not only stabilize the enzyme, but also ensure its proper delivery to lysosomes and protect it from proteolysis. In lysosomes, aSMase metabolizes SMs, and its importance is highlighted by the discovery that mutations on aSMase gene, *SMPD1*, leads to Niemann-Pick (NP) type A and type B diseases, progressive neurodegenerative diseases of high lethality (Brady, Kanfer et al. 1966). For type A NP (NPA) disease, the enzyme activity of aSMase is almost gone, leading to severe symptoms including psychomotor retardation, hepatosplenomegaly and premature death (Brady, Kanfer et al. 1966; Perrotta and Clementi 2010). For type B NP (NPB) disease, patients survive into adulthood due to residual aSMase enzyme activity, but many of them suffer from hepatosplenomegaly and lung diseases (Schuchman 2007; Gault, Obeid et al. 2010). In both types, SMs build up in the lysosomes of cells in multiple tissues, such as the liver, spleen, and bone marrow, resulting in multiple cellular defects such as dysfunction of lysosomal degradation and impaired lysosomal membrane trafficking (Schuchman 2007; Smith and Schuchman 2008; Gault, Obeid et al. 2010). The NP disease phenotype was recapitulated in the aSMase^{-/-} mouse (Horinouchi, Erlich et al. 1995; Marathe, Miranda et al. 2000), which has proved to be an

invaluable tool to study the function of SM and aSMase.

The various cellular defects observed in aSMase$^{-/-}$ cells point to the fact that SMs have multiple roles besides serving as structural components of lysosomal membranes. Numerous studies have unraveled SMs as an important precursor for the ceramide-based signaling pathway (Kitatani, Idkowiak-Baldys et al. 2008). In lysosomes, the breakdown of SMs by aSMase provides a significant source for generating ceramide, a bioactive messenger involved in many cellular processes of physiological and pathophysiological importance (Bikman and Summers 2011). Multiple stress stimuli, such as ultraviolet (UV), death receptor activation, chemotherapeutic agents, and pathogens (Smith and Schuchman 2008), can activate aSMase and increase the concentration of ceramide, which further activates the downstream effectors (Yu, Nikolova-Karakashian et al. 2000; Paris, Fuks et al. 2001; Grassme, Cremesti et al. 2003; Dimanche-Boitrel, Meurette et al. 2005). This stress response is largely abolished in aSMase mutant cells (from NP disease patients) (Lozano, Menendez et al. 2001), aSMase$^{-/-}$ mice (Garcia-Barros, Paris et al. 2003), or aSMase siRNA knockdown cells (Zeidan, Wu et al. 2008). The activity of aSMase also plays a key role in maintaining the integrity of the lysosomal membrane, as the cells from NPA or NPB patients show a marked decrease in lysosomal stability (Kirkegaard, Roth et al. 2010). In addition to the lysosomal signaling functions of aSMase, upon oxidative stress or cytokine (such as TNF-a, IL-1b) stimulation, aSMase can be secreted into extracellular environment, where they catabolize SMs to ceramides on the outer leaflet of plasma membrane (Zeidan and Hannun 2007; Jenkins, Canals et al. 2010). This translocation of aSMase is likely to be mediated by the exocytosis of membrane proximal lysosomes, as the secretion can occur within seconds of stimulation (Jaiswal, Andrews et al. 2002; Jin, Yi et al. 2008).

In addition, aSMase^{-/-} cells exhibit defects in endolysosomal trafficking (Chen, Patterson et al. 1999; Puri, Watanabe et al. 1999; Smith and Schuchman 2008). Recent research has revealed an intriguing mechanism by which accumulated SM in aSMase^{-/-} cells might affect endolysosomal membrane dynamics (fusion/fission process) (Chernomordik and Kozlov 2003; Trajkovic, Hsu et al. 2008; Graham and Kozlov 2010). Due to its zwitterionic headgroup, SM has zero spontaneous curvature (Graham and Kozlov 2010). On the other hand, ceramide, without the phosphocholine headgroup, has a negative spontaneous curvature (Graham and Kozlov 2010). This property difference suggests that aSMase activity could change the physical property of the membrane, such as its curvature, so as to increase its fusogenic potential (or its potential to fission). Trajkovic,K et al recently provide striking evidence that the formation of intraluminal vesicles (ILVs), which are vesicles that bud into the lumen of the endosome, is driven by the hydrolysis of SMs to Ceramides (Trajkovic, Hsu et al. 2008). This is further supported by the facts that ILVs are enriched with ceramides, and application of SMase inhibitors abrogates the ILV formation (Trajkovic, Hsu et al. 2008). Thus the conversion from SMs to ceramides on the cytosolic leaflet of the endosome promotes the budding of ILVs into the lumen space (ceramide is engulfed into the lumen of ILVs). Interestingly, when aSMase is secreted during lysosomal exocytosis, increased ceramide concentration on the outer leaflet of plasma membrane induces inward budding of endocytic vesicles (again, ceramide is engulfed into the lumen of vesicles) (Tam, Idone et al. 2010). Therefore, it is likely that the activity of aSMase in the lumen of lysosomes, which increase ceramide concentration on the luminal leaflet of lysosomes, might drive the budding of vesicles to cytosol side and promote the formation of retrograde trafficking vesicles. Consistent with this idea, in aSMase^{-/-} fibroblasts, the retrograde trafficking from LELs (budding off vesicles) to Golgi is

largely impaired (Puri, Watanabe et al. 1999).

Whether the SM-based pathway regulates endolysosomal Ca^{2+} signaling is still an open question. Yet several groups have reported that SM is involved in maintenance of cellular Ca^{2+} homeostasis in other cellular compartments (Church, Hessler et al. 2005; Ginzburg and Futerman 2005; Hannun and Obeid 2008). For example, aSMase^{-/-} mice have defects in ER Ca^{2+} homeostasis due to reduced expression levels of SERCA and of the inositol 1,4,5-triphosphate receptor (IP3R), which may contribute to the onset of neuropathology in NPA disease (Ginzburg and Futerman 2005). It is possible that in lysosomes, SM metabolism might also play an important role in regulating the Ca^{2+} transport machineries, either by modulating their expression level (like the previous example), or by directly regulating their activity. Indeed, a recent study revealed that the phospho-head of SM can stabilize the positively charged voltage sensor of voltage-activated K^+ (K_v) channels on the plasma membrane (Xu, Ramu et al. 2008). This stabilization effect provides a novel mechanism by which hydrolysis of SM regulates Kv channels (Xu, Ramu et al. 2008). A similar mechanism might also exist in the lysosomal environment. In Chapter 4, I will test whether SMs negatively regulate TRPML1, and whether lysosomal Ca^{2+} signaling is impaired in aSMase^{-/-} cells due to the dysfunction of TRPML1.

3.3. Cholesterol in lysosomes

Cholesterol is a key component of mammalian membranes, serving not only as a structural lipid but also an important regulator for membrane proteins (Maxfield and Wustner 2002; Mesmin and Maxfield 2009; Rosenbaum and Maxfield 2011). Cholesterol forms "lipid rafts" with other sphingolipids (mainly SM), which largely determines the fluidity of a membrane. The proper

cholesterol level on the membrane ensures the function of many receptors and enzymes as well as membrane sorting and trafficking processes (Maxfield and Wustner 2002; Mesmin and Maxfield 2009; Lingwood and Simons 2010). Cells can generate cholesterol through *de novo* synthesis in the ER, or alternatively, through the uptake of low density lipoprotein (LDL) particles via endocytosis (Mesmin and Maxfield 2009; Blom, Somerharju et al. 2011). It is interesting that ER, the site of cholesterol synthesis, has a very low concentration of cholesterol (0.5-1% of total). Instead, the majority of cellular cholesterol (60-80% of total) is delivered to the plasma membrane (Blom, Somerharju et al. 2011). Along the endocytic pathway, early endosomes or recycling endosomes are cholesterol rich, while LELs contain much less cholesterol. The regulation of cholesterol level in different intracellular organelles is of fundamental importance and governed by multiple tightly interconnected mechanisms (Maxfield and Wustner 2002; Mesmin and Maxfield 2009).

LELs are critical stations for the redistribution of cholesterol to other intracellular compartments (Mesmin and Maxfield 2009; Rosenbaum and Maxfield 2011). When lipoprotein or endocytosed pieces of membrane are delivered into the lumen of LEL, an acidic hydrolase called lysosomal acid lipase liberates cholesterol from cholesteryl ester (Anderson and Sando 1991) (see **Fig 1.3a**). The unesterified cholesterols then efflux from LELs and transport to the plasma membrane, the endoplasmic reticulum or other intracellular membranes (Mesmin and Maxfield 2009). The mechanism of cholesterol efflux from LELs is an area of active investigation. Two proteins, Niemann-Pick C1 (NPC1) (Carstea, Morris et al. 1997) and Niemann-Pick C2 (NPC2) (Naureckiene, Sleat et al. 2000), are essential for the efflux, although the precise molecular mechanism remains elusive. The best supported model is that liberated cholesterols can bind to NPC2 and are later transferred from NPC2 to NPC1 (Cheruku, Xu et al. 2006; Infante, Wang et al.

2008). NPC1, which is located on the lysosomal membrane, then transports cholesterol out of the lysosomal compartments (Higgins, Davies et al. 1999; Neufeld, Wastney et al. 1999; Davies and Ioannou 2000) (**Fig 1.3a**). The concerted action of NPC1 and NPC2 are tightly regulated and can be modulated by the lipids in lysosomes. For example, *in vitro* studies have shown that NPC2 activity can be stimulated by BMP (Cheruku, Xu et al. 2006) or ceramide (Abdul-Hammed, Breiden et al. 2010), but inhibited by SM (Abdul-Hammed, Breiden et al. 2010).

The significance of lysosomal cholesterol metabolism is underscored by its association with a fatal, autosomal recessive neurodegenerative disorder called Niemann Pick type C (NPC) disease (Schiffmann 2010), which is caused by mutations of NPC1 (~95% of patients), or NPC2 (~5% of patients). The major symptoms of NPC patients include progressive cognitive impairment, seizures, dystonia, liver dysfunction and early mortality (Higgins, Patterson et al. 1992; Vanier 2010). At the cellular level, NPC cells accumulate abnormally large amounts of cholesterol, SM and saturated fatty acids in LEL compartments (Rosenbaum and Maxfield 2011; Sztolsztener, Dobrzyn et al. 2012). This primary defect leads to secondary defects such as the disturbance of endolysosomal trafficking processes, which further worsen the cellular pathology (Choudhury, Sharma et al. 2004; Pipalia, Hao et al. 2007). For example, in NPC cells, although the formation of autophagosome is reported to be normal, the degradation of contents of autophagosomes is largely impaired, indicative of the defective fusion process of lysosome and autophagosome (Liao, Yao et al. 2007; Pacheco, Kunkel et al. 2007; Fraldi, Annunziata et al. 2010). Studies have also shown that lipid transport along the endocytic pathway and retrograde trafficking from LELs to TGN are also compromised in NPC cells (Chen, Patterson et al. 1999; Puri, Watanabe et al. 1999; Fraldi, Annunziata et al. 2010; Knez and Peake 2010). Potential therapies that target primary or secondary

defects have proved to be effective on the cellular level, but there is still no cure for patients yet (Vanier 2010).

The mechanism by which mutations of NPC1 or NPC2 cause endolysosomal trafficking defects remains to be clarified. One possibility is that the failure of efflux of cholesterol may lead to the excessive formation of cholesterol/SM-rich microdomains on the lysosomal membrane, which makes the membrane more "rigid" and thus less likely to undergo fusion/fission processes (Graham and Kozlov 2010; Lippincott-Schwartz and Phair 2010). Indeed, increasing cholesterol-enriched regions on lysosomal membrane by cholesterol loading significantly impairs the fusion of lysosomes with endosomes and with autophagic vacuoles, while lowering cholesterol in diseased cells rescued normal lysosomal fusion (Fraldi, Annunziata et al. 2010). Another possibility is that the build-up of cholesterol might have a direct effect on integral lysosomal membrane proteins including channels or transporters that are important regulators of membrane trafficking. Extensive studies have shown that cholesterol alters the function of many ion channels on plasma membrane (Hampshire, Burghel et al. 2010; Levinger, Howlett et al. 2010). For example, elevation of membrane cholesterol decrease the open probability of large-conductance Ca^{2+} dependent K^+ channels (Chang, Reitstetter et al. 1995), inhibits L-type Ca^{2+} channels (Jennings, Xu et al. 1999), and decreases the current density of inwardly rectifying K^+ channels by changing the number of active channels (Romanenko, Rothblat et al. 2002). Due to the intracellular localization of the lysosome membrane, which defies conventional patch clamp analysis, the effect of cholesterol on lysosomal channels has been barely investigated. However, with the advance of lysosomal patch clamp technique first described by Xu lab, it is now possible to examine whether the accumulation of cholesterol in diseased conditions changes the activity of channels in

lysosomes, and how these changes relate to trafficking defects.

4. Lysosomal storage disease

The aforementioned Mucolipidosis type IV and Niemann Pick disease(type A,B,C) all belong to

lysosomal storage diseases (LSDs), which are a group of inherited diseases caused by the

deficiency of lysosomal hydrolases, membrane proteins, or other proteins important for normal

functions of lysosomes (Bellettato and Scarpa 2010; Vitner, Platt et al. 2010; Schultz, Tecedor et al.

2011; Shachar, Lo Bianco et al. 2011).   Over 50 LSDs have been identified, and the common

hallmark of LSDs is the abnormal accumulation of undigested substrates in lysosomal

compartments (Vitner, Platt et al. 2010). The storage does not follow a one-enzyme, one-substrate

relationship; instead, there is often secondary storage of other lipids unrelated to the primary defect

and such accumulation is progressive (Schultz, Tecedor et al. 2011). Failure to degrade the

accumulated substrates eventually impairs lysosomal function, causes cell death and leads to

debilitating symptoms such as mental retardation, loss of motor ability and premature death.

Neurons are especially vulnerable to such accumulation; thus most of LSDs involve central

nervous system dysfunction (Bellettato and Scarpa 2010). There are currently no effective cures for

most LSDs (Schultz, Tecedor et al. 2011).

Although caused by different genetic defects, LSDs share many common trafficking defects (Vitner,

Platt et al. 2010; Schultz, Tecedor et al. 2011). For instance, the perturbation of LEL-to-Golgi

trafficking is observed in a number of LSDs (i.e. Niemann-Pick disease, Mucolipidosis IV, GM1

gangliosidosis, GM2 gangliosidosis, Fabry disease) (Chen, Patterson et al. 1999; Puri, Watanabe et

al. 1999)(See **Fig 1.3b**). The fusion of lysosomes with autophagosomes is also impaired in many LSDs, leading to autophagosome accumulation and cell death (Fukuda, Roberts et al. 2006; Jennings, Zhu et al. 2006; Pacheco, Kunkel et al. 2007; Settembre, Fraldi et al. 2008; Venugopal, Mesires et al. 2009; Curcio-Morelli, Charles et al. 2010). In addition, defective intracellular Ca^{2+} signaling is also a common factor in LSDs (Korkotian, Schwarz et al. 1999; Lloyd-Evans, Pelled et al. 2003; Pelled, Lloyd-Evans et al. 2003; Ginzburg and Futerman 2005; Ginzburg, Li et al. 2008; Lloyd-Evans, Morgan et al. 2008). These similar cellular defects suggest that the common regulatory machineries for intracellular membrane trafficking pathways are impaired in LSDs, despite their distinct primary causes. Understanding which and how the regulatory machineries are affected in LSDs will not only bring us new insight into lysosomal physiology, but also lay critical foundations for future therapeutic development (Shachar, Lo Bianco et al. 2011). Chapter 4 will discuss that TRPML1, an important regulator for endolysosomal trafficking, is compromised in several LSDs, and the dysfunction of TRPML1 contributes to the trafficking defects and secondary lysosomal storage seen in these LSDs' cells. This work is the first functional investigation into the effect of accumulated luminal lipids on lysosomal channels, and raises an intriguing possibility that enhancing TRPML1 activity may speed membrane trafficking and thus up-regulate the waste disposal ability of diseased cells.
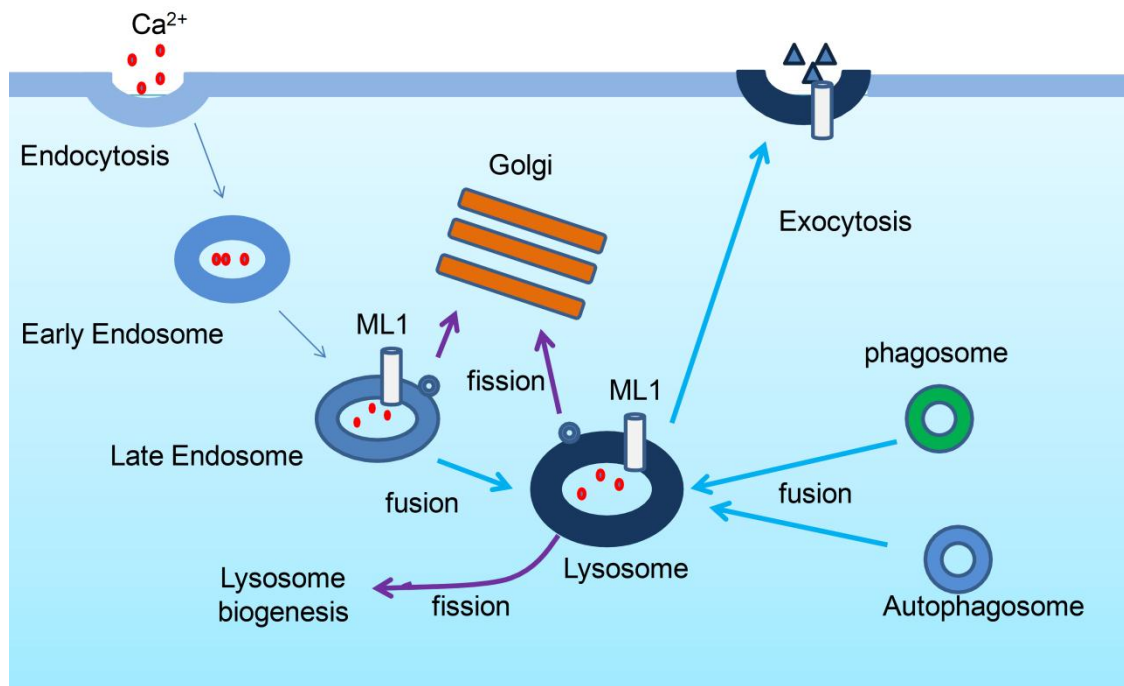
Figure 1.1: Overview of the endocytic pathway and lysosomal fusion/ fission processes.
Endolysosomes are Ca^{2+} stores, with a luminal Ca^{2+} concentration estimated to be approximately
0.5 mM. Early endosomes (EEs; pH 6.0) are derived from the primary endocytic vesicles after
endocytosis. EEs can undergo maturation through membrane trafficking to become late endosomes
(LEs; pH 5.5). LEs can fuse with lysosomes (LYs; pH 4.5) to form late endosome and lysosome
hybrids (LELHs). LYs can be reformed from LELHs in a fission-dependent mechanism (referred to
as lysosome biogenesis). Besides fusion with LEs, LYs also fuse with autophagosomes (APs) to
form autolysosomes (ALs), fuse with phagosome to form phagolysosome, or fuse with the plasma
membrane during exocytosis. Retrograde transport vesicles, derived from LEs or LYs upon
membrane fission, transport lipids and proteins in a retrograde direction to the *trans*-Golgi Network
(TGN).
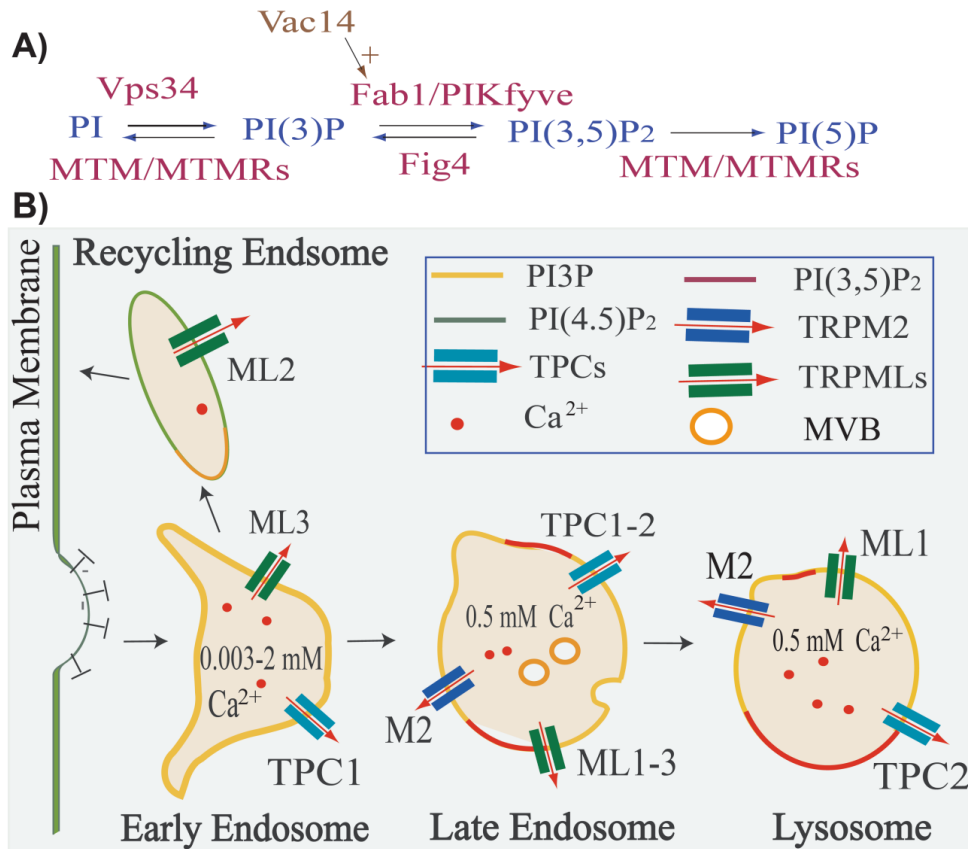
Fig 1.2: Phosphoinositides and Ca²⁺ channels in endolysosomes.

A: An overview of phosphoinositide (PI) synthesis in endolysosomes. PI(3)P is synthesized from PI via a PI 3-kinase (Vps34) present in endosomes, while PI(3,5)P_2 is synthesized from PI(3)P via a PI 5-kinase (PIKfyve/Fab1). PIKfyve is a PI(3)P effector that is associated with late endosomes and lysosomes (LELs), and is positively regulated by Vac14. PI(3,5)P_2 can be dephosphorylated by Fig4 or MTM/MTMRs to generate PI(3)P or PI(5)P, respectively.

B: The distribution of PI(3)P and PI(3,5)P_2 associated with the membranes of early and late endosomes, as well as lysosomes, are represented by yellow and red outlines at the membrane of these vesicle types. respectively (Dove, Dong et al. 2009). TRPML1-3, TRPM2, and TPC1-2 are putative Ca²⁺ release channels associated with endolysosomal membranes that are also labeled in this diagram (Cheng, Shen et al. 2010; Dong, Wang et al. 2010; Zhu, Ma et al. 2010). TRPML1-3 channels are predominantly localized to LELs, while TRPML2 and TRPML3 are also associated with recycling and early endosomes, respectively. TPC2 is mainly localized in the LELs, and TPC1 is mainly associated with early and late endosomes. TRPM2 is expressed in specific cell types, and is associated with LELs as well as the plasma membrane. The concentration of Ca²⁺ stores associated with each vesicle type is also indicated, with luminal [Ca²⁺] estimated to be in the micro- to millimolar ranges.
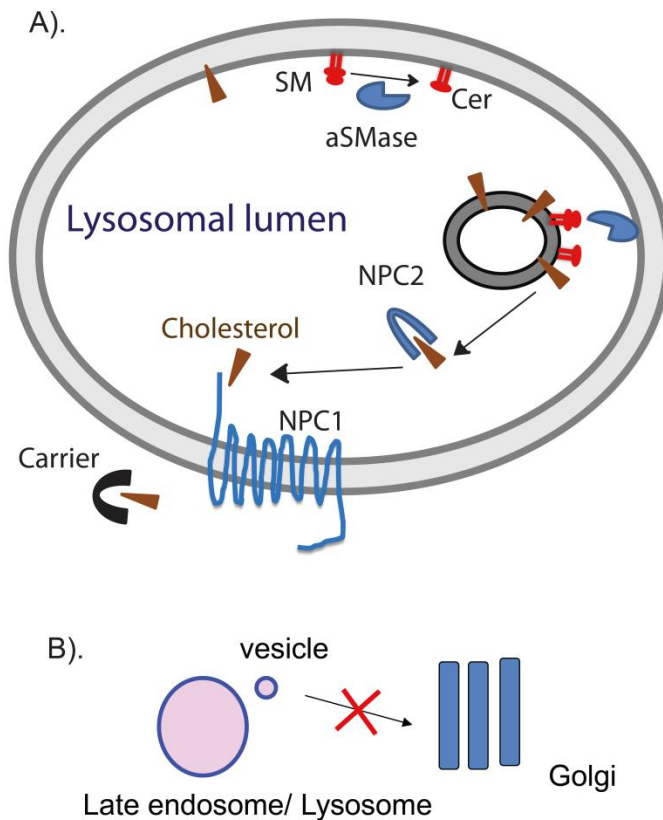
Fig 1.3: Sphingomyelin and cholesterol in late endosomes/lysosomes. A). The breakdown of sphingomyelins (SMs) in lysosome is mediated by acid sphingomyelinase (aSMase), which hydrolyse SM to ceramide (Cer) and free phosphocholine. aSMase is a glycoprotein with *in vitro* pH optimum between 4.5 and 5. It metabolizes both the SMs on the luminal leaflet of the limiting lysosomal membrane and those on the outer leaflet (luminal side) of internal vesicles. Late endosomes/lysosomes are also critical stations for the metabolism of cholesterol. Cholesteryl esters are hydrolyzed by lysosomal acid lipase to produce free cholesterol and fatty acid. Free cholesterol is transferred to NPC2, and then to NPC1. NPC1 help free cholesterol flip to the cytosolic side, where cytoplasmic carrier protein transport free cholesterol to its various destinations in the cell. **B).** In NP fibroblasts, accumulation of SMs or cholesterol in LELs causes LEL-to-Golgi trafficking defects. Same defects are also observed in PI(3,5)P$_2$-deficient cells (Zhang, Zolov et al. 2007), ML4 fibroblasts (Chen, Bach et al. 1998; Shen, Wang et al. 2011), as well as fibroblasts from several other sphingolipid LSDs (Chen, Patterson et al. 1999; Puri, Watanabe et al. 1999), which suggest that SMs, cholesterol, PI(3,5)P$_2$ and TRPML1 may function in the same pathway that regulates the LEL-to-Golgi trafficking process.

CHAPTER 2

PI(3,5)P$_2$ DIRECTLY BINDS AND ACTIVATES MUCOLIPIN CA^{2+} RELEASE CHANNELS IN ENDOLYSOSOME

Abstract

PI(3,5)P$_2$ is a low abundance endolysosome-specific phosphoinositide (PIP), the deficiency of which causes enlarged endolysosomes and endocytic trafficking defects in cells. Similar trafficking defects are also observed in mammalian cells that lack TRPML1, a Ca^{2+}-permeable channel primarily localized on membranes of late endosomes and lysosomes. Here we hypothesized that endolysosomal Ca^{2+} release through TRPML channels is regulated by PI(3,5)P$_2$. By directly patch-clamping endolysosomal membranes, we found that PI(3,5)P$_2$ potently and specifically activates TRPML1 in both heterologous and endogenous systems. Lipid-protein binding assays showed that PI(3,5)P$_2$ binds directly to the N terminus of TRPML1. The multiple positively charged amino acid residues are critical for the binding, and mutations on these residues abolished the PI(3,5)P$_2$ sensitivity of TRPML1. Overexpression of TRPML1 rescued the enlarged vacuole phenotype in PI(3,5)P$_2$- deficient cells, suggesting that TRPML1 is a downstream effector of PI(3,5)P$_2$. Notably, this PI(3,5)P$_2$-dependent regulation of TRPML1 is evolutionarily conserved. In budding yeast, hyperosmotic stress induces Ca^{2+} release from the vacuole. Here, we showed that this release requires both PI(3,5)P$_2$ production and a yeast functional TRPML homolog. We propose that TRPMLs regulate membrane trafficking by transducing information about PI(3,5)P$_2$ levels into changes in juxtaorganellar Ca^{2+}, thereby triggering membrane fusion/fission events.

Introduction

Ca^{2+} is a key regulator of synaptic vesicle fusion during neurotransmission. Similarly, Ca^{2+} is thought to regulate other, more general membrane trafficking pathways (Hay 2007). However, in these cases, the source of Ca^{2+} is unknown. For these general pathways, it has been postulated that Ca^{2+} is released through unidentified Ca^{2+} channels from the lumen of vesicles and organelles (Peters and Mayer 1998; Hay 2007; Luzio, Pryor et al. 2007). Transient receptor potential (TRP) proteins are a superfamily of Ca^{2+}-permeable cation channels that are localized in the plasma membrane and/or membranes of intracellular organelles (Dong, Wang et al. 2010). For example, mucolipin TRPs (TRPML1-3) are localized in the membranes of endosomes and lysosomes (collectively endolysosomes) (Puertollano and Kiselyov 2009; Cheng, Shen et al. 2010). Mutations in the human *TRPML1* gene cause mucolipidosis type IV (ML4) neurodegenerative disease (Sun, Goldin et al. 2000; Nilius, Owsianik et al. 2007). Cells that lack TRPML1 exhibit enlarged endolysosomes and trafficking defects in the late endocytic pathway (reviewed in Refs. (Puertollano and Kiselyov 2009; Cheng, Shen et al. 2010)). TRPMLs are, therefore, natural candidate channels for Ca^{2+} release in the endolysosome.

$PI(3,5)P_2$ is a low-abundance endolysosome-specific phosphoinositide (Bonangelino, Nau et al. 2002; Chow, Zhang et al. 2007; Zhang, Zolov et al. 2007; Dove, Dong et al. 2009). $PI(3,5)P_2$ can be generated from $PI(3)P$ through PIKfyve/Fab1, a PI 5-kinase that is localized in the endolysosome of both yeast and mammalian cells (Duex, Nau et al. 2006; Botelho, Efe et al. 2008; Dove, Dong et al. 2009; Poccia and Larijani 2009). The activity of PIKfyve/Fab1 can be positively regulated by several associated proteins such as Fig4, Vac14, and Vac7 (Chow, Zhang et al. 2007; Zhang, Zolov et al. 2007; Jin, Chow et al. 2008; Dove, Dong et al. 2009). On the other hand, $PI(3,5)P_2$ can be metabolized into $PI(5)P$ through the myotubularin (MTM/MTMR)-family of PI-3 phosphatase (Dove, Dong et al. 2009; Poccia and Larijani 2009; Shen, Yu et al. 2009). Human mutations in $PI(3,5)P_2$-metabolizing enzymes and their regulators cause a variety of neurodegenerative diseases including amyotrophic lateral

sclerosis (ALS) and Charcot-Marie-Tooth (CMT) disease (Chow, Zhang et al. 2007; Chow, Landers et al. 2009; Dove, Dong et al. 2009). At the cellular level, PI(3,5)P$_2$-deficient cells reportedly exhibit enlarged endolysosomes/vacuoles and trafficking defects in the endocytic pathways (Chow, Zhang et al. 2007; Zhang, Zolov et al. 2007; Jin, Chow et al. 2008; Dove, Dong et al. 2009).

Because the cellular phenotypes in PI(3,5)P$_2$-deficient cells are similar to those observed in cells lacking TRPML1, we hypothesized that TRPML1 may act as an endolysosomal Ca^{2+}-release channel that is regulated by PI(3,5)P$_2$. In this study, by directly patch-clamping of the endolysosomal membrane, we found that PI(3,5)P$_2$ activates TRPMLs with striking specificity and potency. Protein-lipid interaction and mutational analyses revealed that PI(3,5)P$_2$ binds directly to the N-terminus of TRPML1. Overexpression of TRPML1 suppresses the enlarged vacuole phenotype observed in PI(3,5)P2-deficient cells. We conclude that PI(3,5)P2 controls endolysosomal membrane trafficking by regulating TRPML channels to change juxtaorganellar Ca^{2+} levels.

Methods

Molecular biology and biochemistry. Full-length mouse TRPML1, 2, and 3 were cloned into the EGFP-C2 (Clontech) or mCherry vector (Xu, Delling et al. 2007; Dong, Cheng et al. 2008; Dong, Wang et al. 2009). TRPML1 non-conducting pore mutant (D471K/D472K; abbreviated TRPML1-KK) and PIP$_2$-insensitive mutant (R42Q/R43Q/R44Q/K55Q/R57Q/R61Q/K62Q; abbreviated TRPML1-7Q) were constructed using a site-directed mutagenesis kit (Qiagen). For glutathione S-transferase (GST) fusion constructs, DNA fragments corresponding to the N- (amino acid residues 1-69) terminal regions of mouse TRPML1 were generated by PCR amplification and cloned into the Eco*RI* and Xho*I* site of pGEX4T1, in frame to generate GST-fusion protein plasmids (pGEX-ML1-N). For overexpression of TRPML1 in yeast, full-length mouse TRPML1 was cloned into the Xho*I* and Eco*RI* site of the pCuGFP416 vector, and the XhoI and Hind III site of the pVT102U-GFP vector. FKBP*2 fragment was PCR-amplified from EGFP-FKBP12-Rab5 and inserted into the HindIII and XhoI site

of EGFP-Rab7 vector. RFP-FRB-MTM1 and EGFP-FKBP*2-Rab5 were kind gift from Dr.Banasfe Larijani. All constructs were confirmed by sequencing, and protein expression was verified by Western blot. HEK293T, Cos-1, human fibroblasts, or mouse primary fibroblast cells were transiently transfected with TRPML1-3 and the TRPML1 mutants for electrophysiology, biochemistry, live-cell imaging, and confocal imaging. Confocal images were taken using a Leica (TCS SP5) microscope. TRPML1 Western blot analyses were performed with an anti-GFP monoclonal antibody (Covance).

Endolysosomal electrophysiology. Endolysosomal electrophysiology was performed in isolated endolysosomes using a modified patch-clamp method (Dong, Cheng et al. 2008; Dong, Wang et al. 2009). HEK293 or Cos-1 cells were used for all the heterologous expression experiments and were transfected using Lipofectamine 2000 (Invitrogen) with TRPML1 or mutants fused to GFP or mCherry. Human skin fibroblast cells from a ML4 patient (TRPML1$^{-/-}$, clone GM02048) and age-matched control (TRPML1$^{+/+}$, clone GM00969) were obtained from the Coriell Institute for Medical Research (NJ, U.S.A). LEL size is usually < 0.5 μm, which is suboptimal for patch clamping. We therefore treated cells with 1 μM vacuolin-1, a lipid-soluble polycyclic triazine that can selectively increase the size of endosomes and lysosomes, for ~1h (Huynh and Andrews 2005). Large vacuoles (up to 5 μm; capacitance = 0.68 ± 0.05 pF, N = 44 vacuoles) were observed in most vacuolin-treated cells. Occasionally, enlarged LELs were obtained from TRPML1-transfected cells without vacuolin-1 treatment. No significant difference in TRPML channel properties were seen for enlarged LELs obtained with or without vacuolin-1 treatment. Vacuoles positive for both mCherry-TRPML1 and EGFP-Lamp1 were considered enlarged LELs. Whole-endolysosome recordings were performed on isolated enlarged LELs. In brief, a patch pipette (electrode) was pressed against a cell and quickly pulled away to slice the cell membrane. Enlarged LELs were released into a dish and identified by monitoring EGFP-TRPML1, the mCherry-TRPML1 or EGFP-Lamp1 fluorescence. Unless otherwise stated, bath (internal/cytoplasmic) solution contained 140 mM K-Gluconate, 4 mM NaCl, 1 mM EGTA, 2 mM Na$_2$-ATP, 2 mM MgCl$_2$, 0.39 mM CaCl$_2$, 0.1 mM GTP, 10 mM HEPES (pH adjusted with KOH to 7.2; free [Ca^{2+}]$_i$ approximately 100 nM). Pipette (luminal) solution was pH 4.6 standard

extracellular solution (modified Tyrode's) with 145 mM NaCl, 5 mM KCl, 2 mM $CaCl_2$, 1 mM $MgCl_2$, 20 mM HEPES, 10 mM glucose (pH adjusted with NaOH). All bath solutions were applied via a fast perfusion system to achieve a complete solution exchange within a few seconds. Data were collected using an Axopatch 2A patch clamp amplifier, Digidata 1440, and pClamp 10.0 software (Axon Instruments). Whole-endolysosome currents were digitized at 10 kHz and filtered at 2 kHz. All experiments were conducted at room temperature (21-23ºC), and all recordings were analyzed with pCLAMP10 (Axon Instruments, Union City, CA), and Origin 8.0 (OriginLab, Northampton, MA). All PIP antibodies are from Echelon Biosciences Inc. All PIPs are from A.G. Scientific, Inc.

GST fusion proteins. To purify GST-tagged proteins, *Escherchia coli* BL21DE3 was transformed with empty pGEX vectors or pGEX-TRPML1-N (abbreviated as pGEX-ML1-N). After growth to approximately $OD_{600} = 0.6$ in a SuperBroth medium supplemented with ampicillin, expression was induced with IPTG (1 mM) for 7 h at 37°C. Cells were collected and resuspended in 30 ml of ice-cold PBS supplemented with protease inhibitor cocktail, 0.5 mM EDTA, and deoxytibonuclease, and lysed with a French press. Cell lysates in 1% Triton-X100 were incubated with 2 mL mixed glutathione Sepharose (GE Healthcare) for 1 h at 4°C. After three washes with 30 mL PBS, proteins were eluted with 7 mL elution buffer (10 mM Glutathione, 50 mM Tris, pH 8).

Lipid Strip Binding Assay. Lipid binding analysis of GST-ML1-N and GST-ML1-7Q-N fusion proteins was conducted using PIP Strips (Echelon Biosciences Inc.), with each spot containing 100 pmol active lipids. Membranes were blocked with Phosphate Buffered Saline Tween (PBST) solution (supplemented with 3% fatty acid-free bovine serum albumin) for 1 h at room temperature, and incubated with 0.5-3 μg GST-fusion protein in blocking buffer overnight. After six washes, the membranes were incubated with a mouse anti-GST antibody (1:5000, Sigma) for 1 h at room temperature, and secondary antibody HRP-labeled goat anti-mouse (1:5000) was added before detection by enhanced chemiluminescence.

PIP bead binding assay. Purified GST fusion proteins (10 μg) were diluted in 1 mL binding buffer (50 mM Tris, 150 mM NaCl, 0.25% NP-40, pH 7.5) and incubated with 50 μl of 50% lipid-conjugated Sepharose beads (Echelon Biosciences Inc.) for 2 h. After three washes, proteins were eluted from the PIP beads by heating at 50°C for 10 min in 2X SDS-PAGE sample buffer and visualization by Western blot.

Liposome binding assay. Purified GST fusion proteins (3 μg) were incubated with 20 μl liposome (Echelon Biosciences Inc.) in 1 mL binding buffer (50 mM Tris, 150 mM NaCl, 0.05% Nonidet P-40, pH 7.5) for 10 min. Liposomes were pelleted at 16,000 x g for 10 min and washed multiple times with binding buffer. Bound fractions were analyzed by Western blot.

Yeast Strains

Wild-type and mutant yeast strains are listed in Table 2.1 (next page). Strains were grown at 24°C or 30°C in either YPD (yeast extract/peptone/glucose) or synthetic complete (SC) minimal medium.

Yeast Ca^{2+} imaging. Yeast Ca^{2+} imaging experiments were performed using an aequorin-based genetic Ca^{2+} sensor method (Denis and Cyert 2002). PEVP11/AEQ plasmid was kindly provided by Dr. Patrick H. Masson (University of Wisconsin-Madison, Madison, WI). Transformed yeasts were inoculated from a saturated overnight culture to OD$_{600}$ ~ 0.3 in a synthetic defined (SD) medium with 3 μM coelenterazine, and grown overnight (OD$_{600}$ = 2–3) at 24°C or 30°C to convert apo-aequorin to aequorin. For each experiment, an aliquot of 250 μl was harvested, re-suspended in 100 μl SD medium, and transferred to 94-well plates for luminescence measurement. Baseline luminescence was recorded every 3 s for 30 s using a PHERAstar plate reader (BMG Labs). Hyperosmotic shock was performed by adding an equal volume of SD medium (100 μl) containing 1.8 M NaCl to a final concentration of 0.9 M. All experiments were concluded with 14% ethanol or 0.03 % SDS, which resulted in maximal luminescence and served as a positive control for aequorin transformation.

Table 2.1 Yeast strains.

Genotype	Strains	Genetic background	References
WT	LWY7217	MATa leu2,3-112 ura3-52 his3-Δ200 trp1-Δ901 lys2-Δ801 suc2-Δ9	Ref. (Duex, Tang et al. 2006)
vac7Δ	LWY2054	LWY 7217; vac7Δ::HIS3	Ref. (Duex, Tang et al. 2006)
WT	LWY 7235	MATa leu2,3-112 ura3-52 his3-Δ200 trp1-Δ901 lys2-Δ801 suc2-Δ9	Ref. (Duex, Tang et al. 2006)
vac14Δ	LWY 5177	LWY 7235; vac14Δ::TRP1	Ref. (Duex, Tang et al. 2006)
fig4Δ	LWY 6474	LWY 7235; fig4Δ::TRP1	Ref. (Duex, Tang et al. 2006)
yvc1Δ	LWY 6848	LWY 7235; yvc1Δ::Kan	This study
WT	SEY6210	MATa leu2-3,112 ura3-52 his3-Δ200 trp1-Δ901 lys2-Δ801 suc2-Δ9	Ref. (Botelho, Efe et al. 2008)
fab1Δ	fab1Δ2	SEY6210; fab1Δ::HIS3	Ref. (Botelho, Efe et al. 2008)
vma3Δ	Vma3Δ	MATa his3-Δ1 leu2Δ0, Met15Δ0 ura3Δ0 vmaΔ:: Kan MX	Open Biosystems

Yeast vacuole labeling. Log-phase yeast cells were labeled with FM4-64 dye (Molecular Probes) (Duex, Tang et al. 2006). Phase contrast and fluorescence images were taken using a Zeiss microscope with a 100X objective.

Mouse fibroblast vacuole assay. Vac14$^{-/-}$ mouse fibroblast cells were isolated and cultured as described previously (Zhang, Zolov et al. 2007). Briefly, fibroblasts were transiently transfected by electroporation (260 V, 950 μF) with 100 μg of the following expression constructs: mCit, mCit-Vac14, GFP-ML1, GFP-ML1-KK, or GFP-ML1-7Q. Cells were grown on 100-mm plates to 90% confluence and distributed to six 35-mm plates after electroporation. Cells were fixed with 4% paraformaldehyde 24 h after electroporation. Fibroblasts were considered to be vacuolated if they had

at least one enlarged (> 3 μm) cytoplasmic vacuole.

Confocal imaging. All   images were taken using a Leica (TCS SP5) confocal microscope. Lamp1 antibody was from the Iowa Hybridoma Bank.

Data analysis.   Data are presented as the mean ± standard error of the mean (SEM).   Statistical comparisons were made using analysis of variance (ANOVA).   A *P* value < 0.05 was considered statistically significant.

Results

Activation of endolysosomal TRPML channels by PI(3,5)P$_2$

TRPML1 is primarily localized on membranes of late endosomes and lysosomes (LELs) (Pryor, Reimann et al. 2006; Cheng, Shen et al. 2010), which are inaccessible to conventional electrophysiological approaches. Using our recently-established modified patch-clamp method (Dong, Wang et al. 2009; Dong, Wang et al. 2010), native LEL membranes were directly patched. HEK293T or Cos-1 cells were transfected with either EGFP-TRPML1 alone, or co-transfected with mCherry-TRPML1 and EGFP-Lamp1 (a marker for LEL). Whole-endolysosome recordings (see **Fig 1.1a**; note that the inward current indicates cations flowing out of the endolysosome) were performed on enlarged vacuoles manually isolated from cells pre-treated with vacuolin-1 (Dong, Cheng et al. 2008), which caused an increase in the diameter of the vacuoles from < 0.5 μm to up to 5 μm (mean capacitance = 0.68 ± 0.05 pF, N = 44 vacuoles). The majority (> 85%) of mCherry-TRPML1-positive vacuoles were also EGFP-Lamp1-positive, confirming that the TRPML1-positive vacuoles were enlarged LELs (Dong, Cheng et al. 2008).   In the TRPML1-positive enlarged LELs, small basal inwardly rectifying currents (72 ± 12 pA/pF at -140 mV, N = 65 vacuoles) were seen under the whole-endolysosome configuration (**Fig 2.1b, 2.1c**). Bath application of 100 nM PI(3,5)P$_2$ in a water-soluble diC8 form, rapidly and dramatically activated TRPML1-mediated current (I_{TRPML1}; $\tau = 15 \pm 4$ s at -

140 mV, N = 8 vacuoles; 18.3 ± 2.7-fold increase of basal activity, N = 20 vacuoles) (**Fig 2.1b-e**). PI(3,5)P_2-dependent activation was dose-dependent (EC$_{50}$= 48 ± 14 nM, Hill slope (n) = 1.9, N = 7 vacuoles). On average, I_{TRPML1} in the presence of 100 nM diC8 PI(3,5)P_2 was 982 ± 150 pA/pF at - 140 mV (N = 23 vacuoles).

In yeast, PI(3,5)P_2 is exclusively produced from PI(3)P by the PIKfyve/Fab1 PI 5-kinase (Cooke, Dove et al. 1998; Gary, Wurmser et al. 1998; Bonangelino, Nau et al. 2002). PI(3,5)P_2 can be quickly metabolized into PI(3)P by Fig4, or to PI(5)P by MTMR-family phosphatases (Rudge, Anderson et al. 2004; Duex, Nau et al. 2006; Dove, Dong et al. 2009; Shen, Yu et al. 2009). Neither PI(3)P (1 μM; 1.05 ± 0.17 fold increase of basal, N = 4; **Fig 2.1e**) nor PI(5)P (1 μM; 0.98 ± 0.05 fold increase of basal, N=3; **Fig 2.1e**) activated I_{TRPML1}. PI(3)P and PI(3,5)P_2 are localized in the endolysosome system. Other PIPs such as PI(3,4)P_2, PI(4,5)P_2, and PI(3,4,5)P_3, are localized in the plasma membrane, or in other intracellular organelles, and are sequestered from endolysosomes (Poccia and Larijani 2009). I_{TRPML1} was not activated by these other PIPs (**Fig 2.1e**). Thus, PI(3,5)P_2 activated I_{TRPML1} with a striking specificity. TRPML2 and TRPML3 are also localized in the endolysosome (Cheng, Shen et al. 2010). PI(3,5)P_2, but not PI(3)P activated whole-endolysosome I_{TRPML2} and I_{TRPML3} (data not shown). Since PI(3,5)P_2 and TRPMLs are both primarily localized in the LEL (Refs. (Cheng, Shen et al. 2010)[,] (Dove, Dong et al. 2009); see **Fig 2.2**), the insensitivity of I_{TRPML1} to PI(3)P or PI(5)P, and its robust activation by PI(3,5)P_2 suggested that TRPML1 might be acutely regulated by the activities of PIKfyve/Fab1, or by Fig4 or MTMR phosphatases in the LEL.

Activation of endogenous TRPML-like currents by PI(3,5)P_2

Next, we investigated whether PI(3,5)P_2 activated endogenous TRPMLs. In enlarged LELs isolated from wild-type (TRPML1$^{+/+}$) human fibroblast cells, PI(3,5)P_2–activated $I_{TRPML-L}$ was detected in 5 of 5 tested vacuoles (**Fig 2.1f**), with an average current amplitude 239 ± 37 pA/pF at -140 mV (N = 5; **Fig 2.1g**). In contrast, enlarged LELs from human ML4 (TRPML1$^{-/-}$ or abbreviated as ML1$^{-/-}$) fibroblasts showed no significant PI(3,5)P_2–activated $I_{TRPML-L}$ (15.7 ± 5.2 pA/pF at -140 mV, N = 6; **Fig 2.1g**). These results indicated that PI(3,5)P_2 activated endogenous TRPMLs, and that TRPML1

was the primary or sole functional TRPML channel in the endolysosome of human fibroblast, although a previous study reported the expression of TRPML2 and TRPML3 in human fibroblasts (Zeevi, Frumkin et al. 2009).

Binding of PI(3,5)P$_2$ to the N-terminus of TRPML1 *in vitro*

Phosphoinoitides are known to bind with high affinity to PI-binding modules such as PH or FYVE domain, or to poly-basic region with unstructured clusters of positively-charged amino acid residues, such as Arg and Lys, in an electrostatic manner (Suh and Hille 2008). PI(4,5)P$_2$ can bind directly to the cytoplasmic N- and C- termini of several plasma membrane TRPs (Kwon, Hofmann et al. 2007; Nilius, Owsianik et al. 2008). Notably, the intracellular N terminus of TRPML1 has a poly-basic region (Nilius, Owsianik et al. 2008) (see **Fig 2.3a**). To test whether PI(3,5)P$_2$ binds directly to TRPML1, we fused GST to the entire N-terminus of mouse TRPML1, up to residue 69 (see **Fig 2.3a** for putative membrane topology). The protein, GST-TRPML1-N (abbreviated as GST-ML1-N), was used to probe phosphoinositides immobilized on a nitrocellulose membranes (Kwon, Hofmann et al. 2007; Nilius, Owsianik et al. 2008; Suh and Hille 2008)(**Fig 2.3b**). GST-ML1-N, but not GST alone, bound to PIP$_3$ and PIP$_2$s, but not to other PIPs or phospholipids (**Fig 2.4a**). A liposome assay showed that GST-ML1-N strongly associated with PI(3,5)P$_2$, but not PI(3)P or control liposomes (**Fig 2.4b**). In a pull-down assay, agarose beads conjugated with PI(3,5)P$_2$, but not control lipids, pulled down GST-ML1-N (**Fig 2.4c**). Taken together, these results suggested that PI(3,5)P$_2$ bound directly *in vitro* to the cytoplasmic N-terminus of TRPML1.

Critical amino-acid residues in PI(3,5)P$_2$ binding

To further map the PI(3,5)P$_2$ binding sites, we systematically replaced positively-charged amino acid residues (Arg and Lys) within and adjacent to the poly-basic region with non-charged Gln residues and assayed Gln-substituted, purified GST-fusion proteins for PI(3,5)P$_2$ binding. We also tested whether PI(3,5)P$_2$ activated Gln-substituted TRPML1 channels using whole-endolysosome recordings. A most dramatic decrease in PI(3,5)P$_2$ binding and activation (**Fig 2.5, 2.6**) was observed in a 7Q

mutant, with seven substitutions (R42Q/R43Q/R44Q/K55Q/R57Q/R61Q/K62Q). In contrast to GST-ML1-N, GST-ML1-7Q-N failed to bind significantly to $PI(3,5)P_2$ or to other PIPs in the PIP strip and pull down assays (**Fig 2.5a, 2.5b**). Considering the specificity of $PI(3,5)P_2$ for TRPML1 activation, one plausible explanation for the apparent discrepancy between our biochemical assays (see **Fig 2.5a**) and electrophysiological measurements (see **Fig 2.1e**) is that the purified GST-ML1-N protein fragment did not recapitulate the specificity of PIP-binding of full length TRPML1 in the endolysosomal membrane. Nevertheless, the binding affinity of ML1-N to $PI(3,5)P_2$ was dramatically reduced by removing the charges with the 7Q mutations (**Fig 2.5a, 2.5b**), suggesting that multiple positively charged amino acid residues are critical for $PI(3,5)P_2$ binding.

Compared to wild type (WT) TRPML1, TRPML1-7Q was only weakly activated by high concentrations of $PI(3,5)P_2$, with a maximal response (efficacy) that was approximately 20% of I_{TRPML1} (EC_{50}= 2.2 ± 2 μM, Hill slope (n) = 0.8, N = 6 vacuoles) (**Fig 2.6a, 2.6b**). Like TRPML1^{Va}, TRPML1^{Va}-7Q also exhibited large basal currents (**Fig 2.6c**), suggesting a relatively specific effect of 7Q mutations on $PI(3,5)P_2$-dependent activation. Consistent with the $PI(3,5)P_2$ binding-assay results, we found that GST-ML1-N, but not GST-ML1-7Q-N, competitively reduced the activation effect of $PI(3,5)P_2$ (**Fig 2.7a, 2.7b**). Collectively, our results suggested that $PI(3,5)P_2$ bound directly to the cytoplasmic N-terminus of TRPML1, resulting in conformational changes that favor opening of TRPML1.

$PI(3,5)P_2$ in vacuolar Ca^{2+} release in yeast

TRPML1 is a Ca^{2+}-permeable channel (Grimm, Cuajungco et al. 2007; Xu, Delling et al. 2007), so activation by $PI(3,5)P_2$ may lead to Ca^{2+} release from endolysosomes. Although PIKfyve/Fab1 is a PI 5-kinase responsible for $PI(3,5)P_2$ generation in both yeast and mammalian cells (Duex, Nau et al. 2006; Botelho, Efe et al. 2008; Dove, Dong et al. 2009; Poccia and Larijani 2009), the extracellular signals that lead to activation of PIKfyve in mammalian cells have not been identified. Furthermore, endolysosomal Ca^{2+} release has been difficult to detect in mammalian cells because of the small size of the endolysosome (Calcraft, Ruas et al. 2009; Cheng, Shen et al. 2010). In contrast, Fab1-mediated

PI(3,5)P$_2$ production has been well documented in yeast (Duex, Nau et al. 2006; Dove, Dong et al. 2009). For example, hyperosmotic shock increases PI(3,5)P$_2$ levels more than 20-fold within a few minutes (Duex, Nau et al. 2006; Dove, Dong et al. 2009). Interestingly, hyperosmotic shock is also known to induce Ca^{2+} release from yeast vacuoles, which share many similar features with mammalian lysosomes. Induction of Ca^{2+} release is through Yvc1/TRPY1, a TRP-channel homolog in yeast, and occurs with a slightly faster, but otherwise comparable time-course of PI(3,5)P$_2$ elevation (Denis and Cyert 2002). Based on our data, we hypothesized that hyperosmolarity-induced vacuolar Ca^{2+} release would be dependent on elevated PI(3,5)P$_2$ levels. To test this, we used an a luminescence assay based on aequorin, a genetic Ca^{2+} sensor, (Denis and Cyert 2002) to measure changes in cytosolic Ca^{2+} ([Ca^{2+}]$_{cyt}$) levels . Consistent with previous reports (Denis and Cyert 2002), hyperosmotic shock by addition of 0.9 M NaCl to the culture medium induced a rapid and dramatic increase of [Ca^{2+}]$_{cyt}$. The time required for peak [Ca^{2+}]$_{cyt}$ increase was 48 ± 4 sec, (N = 10 yeast colonies/experiments); the increase of luminescence was 700 ± 94% over basal (N = 4; **Fig 2.8a, 2.8b**). In the *yvc1Δ* mutant, however, no significant increase in [Ca^{2+}]$_{cyt}$ was seen (29 ± 6 % over basal, N = 4), consistent with the hypothesis that the [Ca^{2+}]$_{cyt}$ increase resulted primarily from vacuolar release through Yvc1(Denis and Cyert 2002). Interestingly, in the *fab1Δ* mutant, hyperosmotic shock also failed to induce any significant increase in [Ca^{2+}]$_{cyt}$ (20 ± 8 %, N = 4; **Fig 2.8a, 2.8b**), in comparison with 700 % for the wild-type cells. Both *yvc1Δ* and *fab1Δ* cells responded to 14% ethanol or 0.03 % SDS (data not shown), which is known to induce Ca^{2+} influx (Denis and Cyert 2002). Consistent with previous studies (Duex, Nau et al. 2006; Dove, Dong et al. 2009), *fab1Δ* mutant yeasts failed to exhibit vacuolar fragmentation in response to hyperosmotic shock (**Fig. 2.9**).

Fab1 kinase activity is regulated by Vac7, Vac14 and Fig4, mutations in which cause a partial or nearly complete loss of Fab1-mediated PI(3,5)P$_2$ production (Duex, Nau et al. 2006; Duex, Tang et al. 2006; Zhang, Zolov et al. 2007; Dove, Dong et al. 2009; Poccia and Larijani 2009). All these mutants exhibited reduced vacuolar Ca^{2+} release: 533 ± 60 % (N = 4) for *fig4Δ*, 357 ± 77 % (N = 4) for *vac14Δ*, and 106 ± 18 % (N = 4) for *vac7Δ* (**Fig 2.8a, 2.8b**). The degree of Ca^{2+}-release reduction

($fab1\Delta$ > $vac7\Delta$ > $vac14\Delta$ > $fig4\Delta$) correlated well with the severity of the defect of PI(3,5)P$_2$ production in these strains (Dove, Dong et al. 2009). The loss of Ca^{2+} response in $fab1\Delta$ cells was not due to reduced expression of Yvc1 (**Fig 2.10d, 2.10e**), as transformation of Yvc1-GFP failed to restore the response. In contrast, when wild-type yeast *FAB1* was transformed into $fab1\Delta$ mutant yeast, hyperosmolarity-induced [Ca^{2+}]$_{cyt}$ increase was largely restored (**Fig 2.11f, 2.11g**). Mutant $fab1\Delta$ yeast reportedly hypo-acidify the vacuole (Duex, Nau et al. 2006; Dove, Dong et al. 2009), which could result in reduced Ca^{2+} release because of a decrease in H$^+$-dependent refilling of vacuolar Ca^{2+} stores mediated by Vcx1 (vacuolar Ca^{2+}-H$^+$ exchanger) (Baars, Petri et al. 2007). However, $vcx1\Delta$ cells exhibit normal Ca^{2+} release in response to hyperosmotic shock (Denis and Cyert 2002), indicating that the alternate Pmc1 (vacuolar Ca^{2+} ATPase)-mediated refilling system is sufficient to maintain vacuolar Ca^{2+} stores. In support, we found that hypo-acidified cells lacking *vma3*, an essential component of the vacuolar ATPase (Baars, Petri et al. 2007), exhibited normal [Ca^{2+}]$_{cyt}$ release (**Fig 2.12**). These results suggested that the Fab1-mediated PI(3,5)P$_2$ generation system was required for hyperosmolarity-induced, Yvc1-dependent vacuolar Ca^{2+} release. Although TRPML1 shares a degree of sequence homology to Yvc1, they differ significantly in their channel properties (Palmer, Zhou et al. 2001; Cheng, Shen et al. 2010) . To test whether TRPML1 functions in yeast, we overexpressed TRPML1 in both a wild-type and $yvc1\Delta$ background. Overexpression of TRPML1 in wild-type yeast resulted in a significant increase in Ca^{2+} release in response to hyperosmotic shock (**Fig 2.13a**, **2.13b**). In $yvc1\Delta$ cells, overexpression of TRPML1, but not a non-functional pore mutant of TRPML1 (TRPML1-KK), resulted in a partial rescue of the [Ca^{2+}]$_{cyt}$ response, with a 114 $\pm$ 14% increase over basal luminescence (N = 9) (**Fig 2.13d**). In contrast, overexpression of TRPML1 in $fab1\Delta$ failed to result in significant [Ca^{2+}]$_{cyt}$ response (**Fig 2.13c**), while overexpression of YVC1 in $yvc1\Delta$ cells completely restored the [Ca^{2+}]$_{cyt}$ response (**Fig 2.13e**). The rescue might be incomplete because Yvc1, but not TRPML1, is activated by cytoplasmic Ca^{2+} and mechanical force (Palmer, Zhou et al. 2001), both of which might have synergistic effects with PI(3,5)P$_2$. Nevertheless, these results suggested that regulation of lysosomal Ca^{2+} channels by PI(3,5)P$_2$ might be a conserved mechanism in

eukaryotic cells.

TRPML1 and PI(3,5)P$_2$ in endolysosomal trafficking

The data presented here suggest that TRPMLs might be activated downstream of the PI(3,5)P$_2$ increase, to trigger membrane fusion and fission. If this hypothesis is correct, expression of TRPML1, which often exhibits substantial basal activity in heterologous systems (Cheng, Shen et al. 2010), might alleviate trafficking defects in PI(3,5)P$_2$-deficient cells. In cultured Vac14$^{-/-}$ fibroblast cells, the trafficking defects from PI(3,5)P$_2$ deficiency were reflected by enlarged vacuoles/LELs (> 3 up to 12 μm in diameter) in 79 ± 7% of the cells (N = 3 experiments with >100 cells) (**Fig 2.14a**; Ref. (Zhang, Zolov et al. 2007)). Only approximately 5-10 % of WT cells were vacuolated (< 4 μm; data not shown). Transfection of a wild-type Vac14 construct was sufficient to restrict vacuoles to 15 ± 2% of cells (N = 3 experiments; **Fig 2.14a**). Interestingly, we were able to rescue the vacuolar phenotype by transfection of TRPML1, which showed vacuolation in 18 ± 1 % cells (N = 6), but not pore-mutant TRPML1 (ML1-KK) with 69 ± 6% vacuolation (N = 3), or the PI(3,5)P$_2$-insensitive mutant TRPML1 (ML1-7Q) with 75 ± 7% vacuolation (N = 3) (**Fig 2.14a,b**). These results suggested that TRPML1 channel activity and PI(3,5)P$_2$ sensitivity played important roles in controlling vacuole size.

Discussion

We used biochemical binding assays to demonstrate that PI(3,5)P$_2$ binds directly to the N-terminus of TRPML1. Using whole-endolysosomal patch-clamp recordings, we showed that PI(3,5)P$_2$ robustly activates TRPML1 in the endolysosome. The effect of PI(3,5)P$_2$ was strikingly specific; none of the other PIPs activated TRPML1. Using a spectrum of yeast mutant strains with variable degrees of PI(3,5)P$_2$ deficiency, we established a high-degree of correlation between the amount of vacuolar Ca^{2+} release and the levels of PI(3,5)P$_2$. Finally, we showed that overexpression of WT, but not the PIP$_2$-insensitive variant of TRPML1, was sufficient to rescue the trafficking defects in PI(3,5)P$_2$-deficient

mammalian cells, as demonstrated by the observation of enlarged vacuoles. Our identification of an endolysosome-localizing Ca^{2+} channel that is activated by endolysosome-specific $PI(3,5)P_2$ provides a previously unknown link between these two important regulators of intracellular membrane trafficking.

Similar trafficking defects are seen in both TRPML1$^{-/-}$ and $PI(3,5)P_2$-deficient cells. For example, LEL-to-Golgi retrograde trafficking, a process that requires membrane fission, is defective in both TRPML1$^{-/-}$ cells (Chen, Bach et al. 1998; Treusch, Knuth et al. 2004; Pryor, Reimann et al. 2006; Thompson, Schaheen et al. 2007; Cheng, Shen et al. 2010), and in $PI(3,5)P_2$-deficient cells (Duex, Nau et al. 2006; Duex, Tang et al. 2006; Zhang, Zolov et al. 2007; Botelho, Efe et al. 2008; Dove, Dong et al. 2009; Poccia and Larijani 2009). Furthermore, both TRPML1 and $PI(3,5)P_2$-metabolizing enzymes are implicated in membrane-fusion processes like exocytosis (Dong, Wang et al. 2009; Dove, Dong et al. 2009; Poccia and Larijani 2009), and lysosomal fusion with autophagosomes (Ferguson, Lenk et al. 2009; Puertollano and Kiselyov 2009). Thus, both TRPML1 and $PI(3,5)P_2$ play active roles in membrane fission and fusion. However, the cellular defects of $PI(3,5)P_2$-deficient cells are generally more severe than those of TRPML1$^{-/-}$ cells. $PI(3,5)P_2$ is proposed to have at least five independent functions, including: recruitment of cytosolic proteins to define organelle specificity; functional regulation of endolysosomal membrane proteins; determination of physical properties and fusogenic potential of endolysosomal membranes; serving as precursor for $PI(3)P$ or $PI(5)P$; and modulation of endolysomal pH (Bonangelino, Nau et al. 2002; Dove, Dong et al. 2009; Poccia and Larijani 2009). Hence, activation of TRPML1 might define a subset of the multiple functions of $PI(3,5)P_2$. Such activation, however, may provide an essential spatial and temporal regulation of endolysosomal dynamics. Membrane fusion and fission are highly coordinated processes requiring an array of cytosolic and membrane-bound proteins and factors. A local increase in $PI(3,5)P_2$ likely recruits protein complexes required to generate the membrane curvature necessary for membrane fusion and fission (Poccia and Larijani 2009). A local increase in $PI(3,5)P_2$ could also activate TRPML1 to elevate juxtaorganellar Ca^{2+}, which binds to a putative Ca^{2+} sensor protein such as Synaptotagmin/CaM (Luzio, Pryor et al. 2007) or ALG-2 (Vergarajauregui, Martina et al. 2009), to exert effects on SNARE proteins or lipid bilayer fusion (Roth 2004; Poccia and Larijani 2009). A

similar mechanism might be employed by NAADP and TPC channels to regulate membrane trafficking in the endolysosome (Calcraft, Ruas et al. 2009; Zhu, Ma et al. 2010).

The remarkable specificity of $PI(3,5)P_2$ in activating TRPML1 is consistent with the role of Ca^{2+} in controlling the direction and specificity of membrane traffic (Hay 2007; Luzio, Pryor et al. 2007). Although we identified several positively charged amino acid residues as potential $PI(3,5)P_2$ binding sites, electrostatic interaction alone is unlikely to provide a high affinity $PI(3,5)P_2$ binding pocket (Nilius, Owsianik et al. 2008; Suh and Hille 2008). Thus, additional structural determinants such as hydrophobic amino acid residues must also contribute to specificity by interacting with the lipid portion of $PI(3,5)P_2$. Because of the low abundance of $PI(3,5)P_2$ (Dove, Dong et al. 2009), such specificity might be a pre-requisite for $PI(3,5)P_2$ and TRPML1 to control the trafficking direction in the late-endocytic pathway. In other organelles, however, other PIPs and intracellular Ca^{2+} channels are likely to provide machinery necessary for Ca^{2+}-dependent membrane fission and fusion. Within LELs, membrane fusion and fission are likely to occur in sub-organellar compartments that are enriched for both TRPMLs and PIKfyve. While TRPML-mediated juxtaorganellar Ca^{2+} transients might be captured using real-time live-imaging methods, these seemingly "spontaneous" events may correlate with membrane fusion and fission events that can be simultaneously monitored with fluorescence imaging approaches.

a Pipette (Luminal) Solution

LEL

Inward

PI(3,5)P$_2$

Bath (Internal/Cytoplasmic) Solution

b TRPML1   ○ −140 mV

■ Internal Solution
■ 100 nM PI(3,5)P$_2$

I (pA)

Time (s)

c TRPML1   Vm (mV)

—— Basal
—— 100 nM PI(3,5)P$_2$

I (pA)

d TRPML1

EC$_{50}$ = 48 nM
n = 1.9

Current Density (pA/pF)

PI(3,5)P$_2$ (μM)

e TRPML1

Increase of current (fold)

(4) (3) (4) (20) (4) (3)

***

PI(3)P PI(5)P PI(3,4)P$_2$ PI(3,5)P$_2$ PI(4,5)P$_2$ PI(3,4,5)P$_3$

f WT (TRPML1$^{+/+}$) Human Fibroblast

Vm (mV)

—— Basal
—— 10 μM PI(3,5)P$_2$

I (pA)

g (pA/pF)

WT (TRPML1$^{+/+}$) Human Fibroblast

ML4 (TRPML1$^{-/-}$)

Whole-endolysosome $I_{TRPML-L}$

(5) (5) (6) (6)

***   NS

Basal PI(3,5)P$_2$ Basal PI(3,5)P$_2$

Figure 2.1. PI(3,5)P$_2$ activates recombinant and endogenous TRPML channels in the endolysosomal membranes. (Prepared by Xianping Dong and Xiang Wang) a) Illustration of a whole-endolysosome recording configuration. Pipette (luminal) solution was a standard external (Tyrode's) solution adjusted to pH 4.6 to mimic the acidic environment of the lysosome lumen. Bath (internal/cytoplasmic) solution was a K$^+$-based solution (140 mM K$^+$-gluconate). Putative membrane topology of TRPML channels is illustrated in the late endosome and lysosome (LEL). Note that the inward current indicates cations flowing out of the endolysosome (see red arrow for the direction). **b)** Bath application of PI(3,5)P$_2$ (diC8, 100 nM) activated inwardly rectifying whole-endolysosome TRPML1-mediated current (I_{TRPML1}) in an enlarged endolysosome/vacuole from a TRPML1-EGFP-expressing Cos-1 cell that was pre-treated with vacuolin-1. I_{TRPML1} was elicited by repeated voltage ramps (-140 to +140 mV; 400 ms) with a 4-s interval between ramps. I_{TRPML1} exhibited a small basal current prior to PI(3,5)P$_2$ application; bath application of PI(3,5)P$_2$ to the cytoplasmic side of the endolysosome resulted in maximal activation of 18-fold of baseline within a minute, measured at -140 mV of I_{TRPML1}. **c)** Representative traces of I_{TRPML1} before (black) and after (red) PI(3,5)P$_2$ at two time points, as shown in **a** (black and red circles). Only a portion of the voltage protocol is shown; holding potential = 0 mV. **d)** Dose-dependence of PI(3,5)P$_2$-dependent activation (EC$_{50}$ = 48 nM, n = 1.9). **e)** Specific activation of TRPML1 by PI(3,5)P$_2$ (in 100 nM), but not other diC8 PIPs (all in 1 μM). **f)** An endogenous inwardly rectifying TRPML-like current ($I_{TRPML1-L}$) activated by PI(3,5)P$_2$ (10 μM) in a vacuole isolated from wild type (WT) human skin fibroblast cell. **g)** Endogenous PI(3,5)P$_2$-activated $I_{TRPML-L}$ in WT and TRPML1$^{-/-}$ human fibroblasts. Note that PI(3,5)P$_2$ doesn't activate a significant $I_{TRPML1-L}$ vacuoles isolated from a human ML4 (TRPML1$^{-/-}$) skin fibroblast cell. For histogram graphs of all figures including panels (**e,g**) of this figure, data are presented as the mean ± standard error of the mean (SEM); the n numbers are in parentheses. Statistical comparisons were made using analysis of variance (ANOVA): *P* value < 0.05 was considered statistically significant and indicated with asterisks (*, 0.01< *P* < 0.05; **, *P* < 0.01; ***, *P* < 0.001).
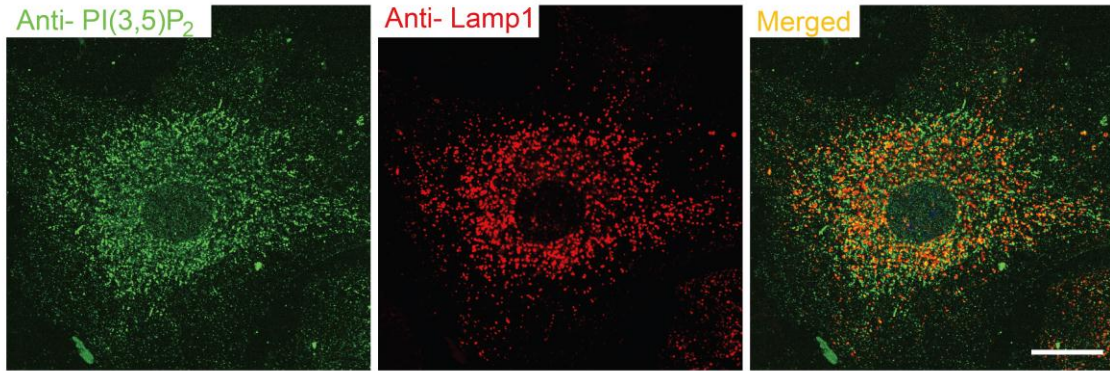
Figure 2.2. Immuofluorescence of PI(3,5)P$_2$ in Lamp1-positive compartments. Mouse fibroblast cells were immunostained with anti-PI(3,5)P$_2$ (green) and anti-Lamp1 (red). The majority of Lamp1-positive compartments were immunostained by anti-PI(3,5)P$_2$, which also recognized some Lamp1-negative compartments. Scale Bar = 10 μm.
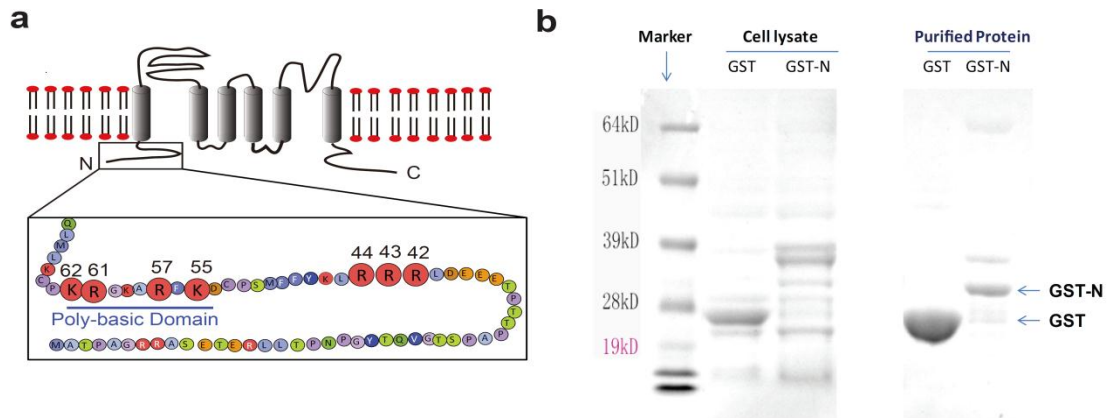

Figure 2.3. Purification of TRPML1 N-terminus peptides. a) The cytoplasmic N-terminus of TRPML1 contains a poly-basic region and clusters of positively charged amino acid residues as potential PI(3,5)P$_2$ binding sites. The positively charged amino acid residues (Arg and Lys) that were mutated into neutral amino acids Gln (Q) in this study are shown with enlarged circles and their amino acid residue numbers. **b**) commassie blue staining of the purified GST peptide and GST-tagged TRPML1 N-terminus peptide.

54
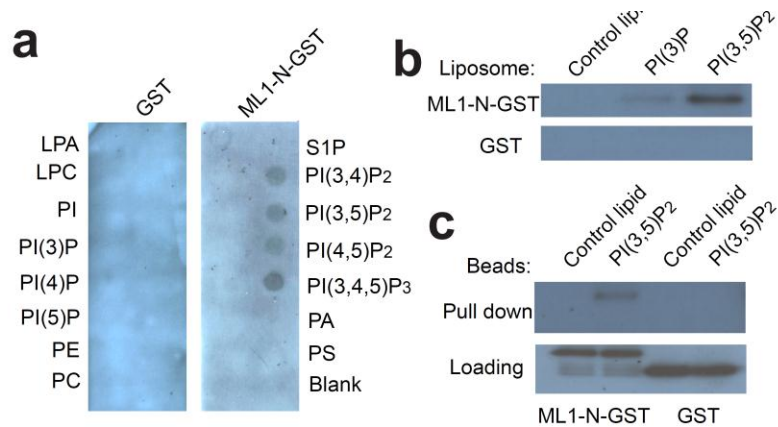
Figure 2.4. TRPML1 N-terminus peptide binds to PI(3,5)P$_2$. a) Protein-lipid strip assay. The strip contained 15 different types of lipids: PA, phosphatidic acid; S1P, sphingosine-1-phosphate. Three purified proteins were used to probe the strip: GST alone (left panel), GST-fused to the N-terminal fragment of TRPML1 (ML1-N-GST; right panel). Proteins were detected with anti-GST antibodies. **b**) Liposome pull-down assay. Liposomes were incubated with purified GST-fusion proteins, centrifuged, and associated proteins visualized by Western blot with GST antibodies. **c**) Binding of GST-ML1-N to agarose beads conjugated to PI(3,5)P$_2$, but not control lipids; GST alone failed to pull down PI(3,5)P$_2$-conjugated beads.
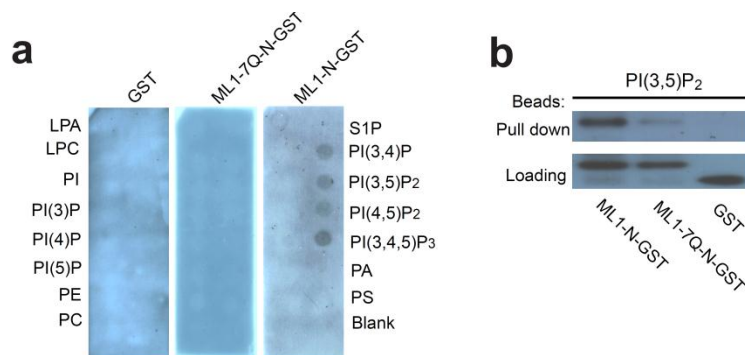

Figure 2.5. 7Q mutations on TRPML1 N-terminus renders the peptide unable to bind to PI(3,5)P$_2$. a) Protein-lipid strip assay. Gln-substituted mutant of ML1-N-GST (ML1-7Q-N-GST; middle) fails to bind to PI(3,5)P$_2$. Proteins were detected with anti-GST antibodies.) Compared to GST-ML1-N, GST-ML1-7Q-N exhibited significantly weaker binding to PI(3,5)P$_2$-conjugated agarose beads.
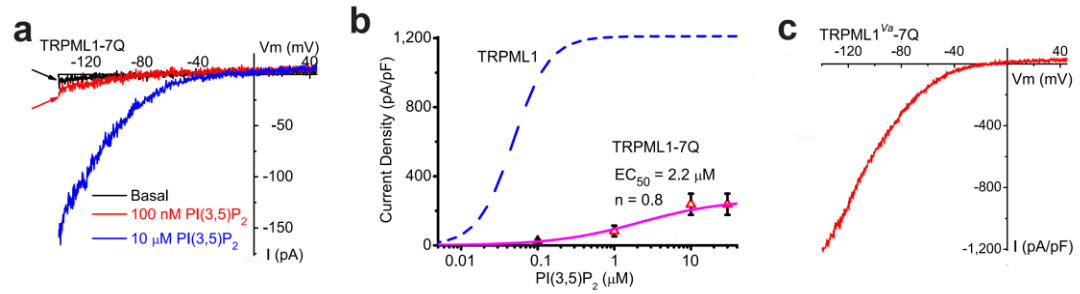
Figure 2.6. 7Q mutations on TRPML1 N-terminus renders the channel insensitive to PI(3,5)P$_2$. a) Whole-endolysosome $I_{TRPML1\text{-}7Q}$ was weakly activated by high concentrations of PI(3,5)P$_2$. b) PI(3,5)P$_2$ dose dependence of $I_{TRPML1\text{-}7Q}$. Dotted line indicates the dose dependence of I_{TRPML1} (repotted from Fig. 1d). c) Large basal whole-endolysosome $I_{TRPML1\text{-}Va\text{-}7Q}$. Charge-removing Gln substitutions (7Q) were introduced into the gain-of-function *Va* background.
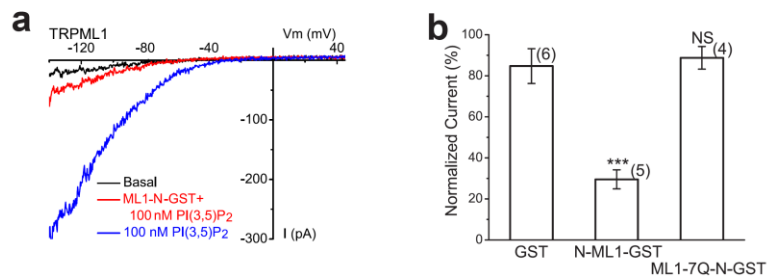

Figure 2.7. TRPML1 N-terminus peptides, but not the 7Q mutants, competitively reduce the activation effect of PI(3,5)P$_2$. **a**) GST-ML1-N peptide (5 μg/ml) reduced PI(3,5)P$_2$-dependent activation of whole-endolysosome I_{TRPML1}. **b**) Charge-removing Gln-substituted substitutions (7Q) abolished the inhibitory effect of GST-ML1-N peptide.
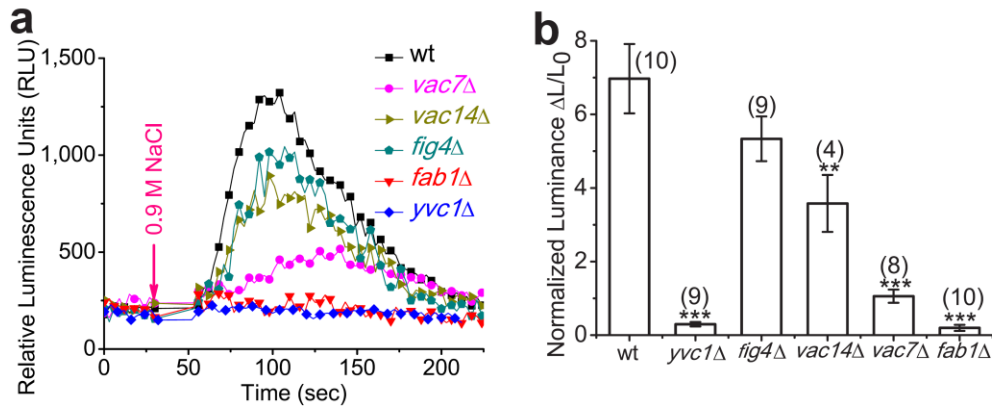
Figure 2.8 Ca^{2+} release from yeast vacuoles after hyperosmostic shock is dependent on PI(3,5)P$_2$ production. a) Representative Ca^{2+} response measured with aequorin-mediated luminescence in wild-type (wt), *yvc1Δ*, and PI(3, 5P)$_2$-deficient strains (*vac7Δ, vac14Δ, fig4Δ, fab1Δ*) upon hyperosmotic shock induced by addition of 0.9 M NaCl. **b**) Quantitative data to show luminescence responses upon hyperosmotic shock in different yeast strains. Fold-response was normalized to basal luminescence prior to shock. For b, data are presented as the mean ± standard error of the mean (SEM); the n numbers are in parentheses. Statistical comparisons were made using analysis of variance (ANOVA): *P* value < 0.05 was considered statistically significant and indicated with asterisks (*, $0.01< P < 0.05$; **, $P < 0.01$; ***, $P < 0.001$).
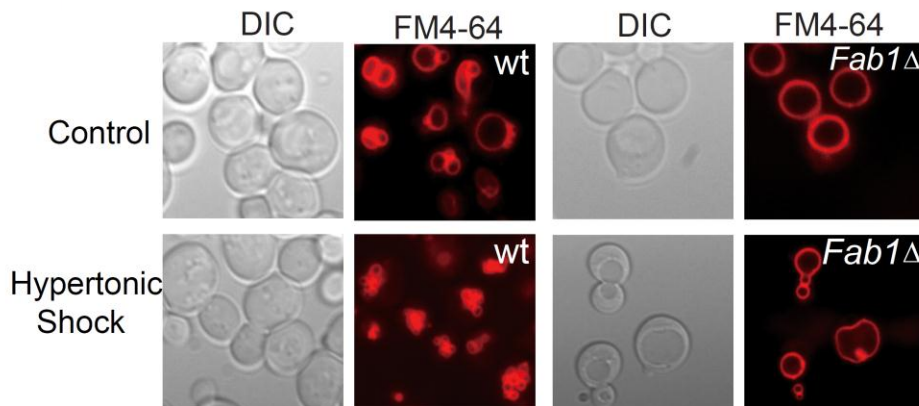
Figure 2.9. *fab1Δ* yeast cells fail to undergo vacuolar fragmentation in response to hyperosmotic shock. Hyperosmotic shock increases the number of vacuoles and decreases the vacuolar volume in wild type, but not fab1 mutant yeast strains. Both WT and *fab1Δ* cells were labeled with FM4-64 dye to visualize vacuole volume and the number of vacuole lobes. Cells were treated with 0.45M NaCl and viewed by fluorescence microscopy.

57
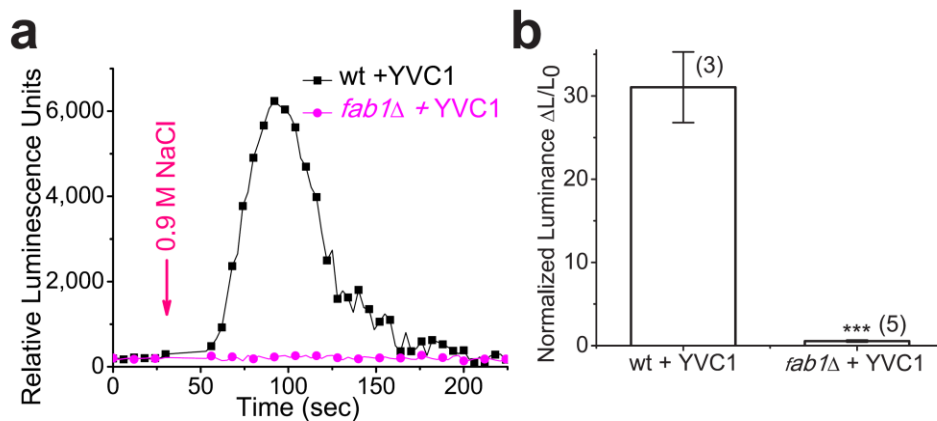
Figure 2.10. Overexpression of YVC1 in *fab1Δ* cells fails to restore hyperosmolarity-induced Ca^{2+} response. a) Representative Ca^{2+} response measured with aequorin-mediated luminescence in wild-type or *fab1Δ* cells with overexpression of YVC1 channel. **b**)Quantitative data to show luminescence responses upon hyperosmotic shock in wild-type or *fab1Δ* cells with overexpression of YVC1 channel. Fold-response was normalized to basal luminescence prior to shock. Data are presented as the mean ± standard error of the mean (SEM); the n numbers are in parentheses. ***, $P < 0.001$
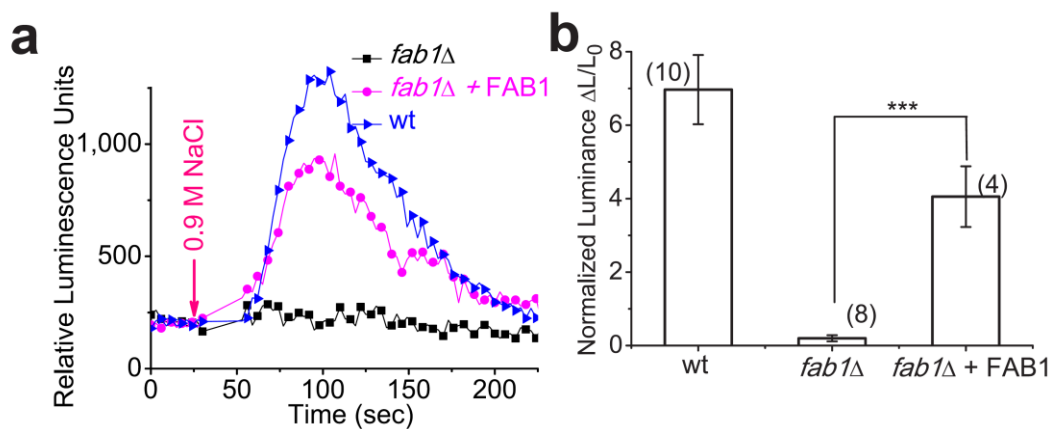
Figure 2.11. Overexpression of *FAB1* in *fab1Δ* cells restores hyperosmolarity-induced Ca^{2+} response. a) Representative Ca^{2+} response measured with aequorin-mediated luminescence in wild-type, *fab1Δ*, and *fab1Δ* cells rescued with FAB1. **b**) Quantitative data to show luminescence responses upon hyperosmotic shock in wild-type, *fab1Δ*, and *fab1Δ* cells rescued with FAB1. Fold-response was normalized to basal luminescence prior to shock. Data are presented as the mean ± standard error of the mean (SEM); the n numbers are in parentheses. ***, $P < 0.001$
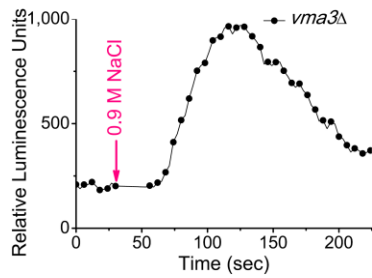
Figure 2.12. Hyperosmotic shock induces vacuolar Ca^{2+} release in *vma3* mutant yeast strains. Showing here is a representative Ca^{2+} response measured with aequorin-mediated luminescence in vma3-/- cells
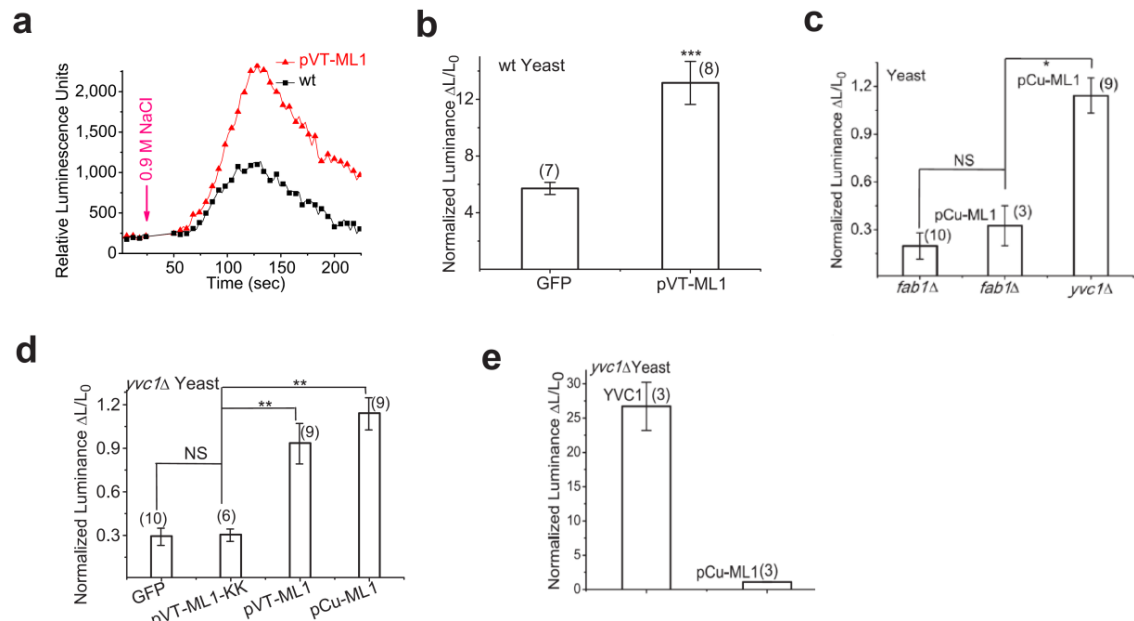
Figure 2.13. Hyperosmotic shock induces vacuolar Ca^{2+} release though TRPML1 in WT or *yvc1Δ* cells, but not *fab1Δ* cells. a,b) Overexpression of TRPML1 in WT yeast cells increased hyperosmolarity-induced Ca^{2+} response. Hyperosmolarity-induced Ca^{2+} responses were measured using the aequorin-mediated luminescence assay. Hyperosmotic shock was induced by addition of 0.9 M NaCl. **c**) Overexpression of TRPML1 in *fab1Δ* cells failed to restore hyperosmolarity-induced Ca^{2+} response. Hyperosmolarity-induced Ca^{2+} responses (normalized with baseline luminescence before hyperosmotic shock) from *fab1Δ* cells, and pCu-ML1-transformed *yvc1Δ* cells were re-plotted from Fig. 8b and 13d for comparison. **d**) Overexpression of TRPML1, but not pore mutant TRPML1-KK (in pCu and pVT expression vectors), in *yvc1Δ* yeast cells resulted in small but significant hyperosmolarity-induced Ca^{2+} response. **E**) Overexpression of YVC1 in *yvc1Δ* cells restored hyperosmolarity-induced Ca^{2+} response. Hyperosmolarity-induced Ca^{2+} responses from pCu-ML1-transformed *yvc1Δ* cells were re-plotted from Fig. 13d for comparison. Data are presented as the mean ± standard error of the mean (SEM); the n numbers are in parentheses. (*, 0.01< P < 0.05; **, P < 0.01; ***, P < 0.001).
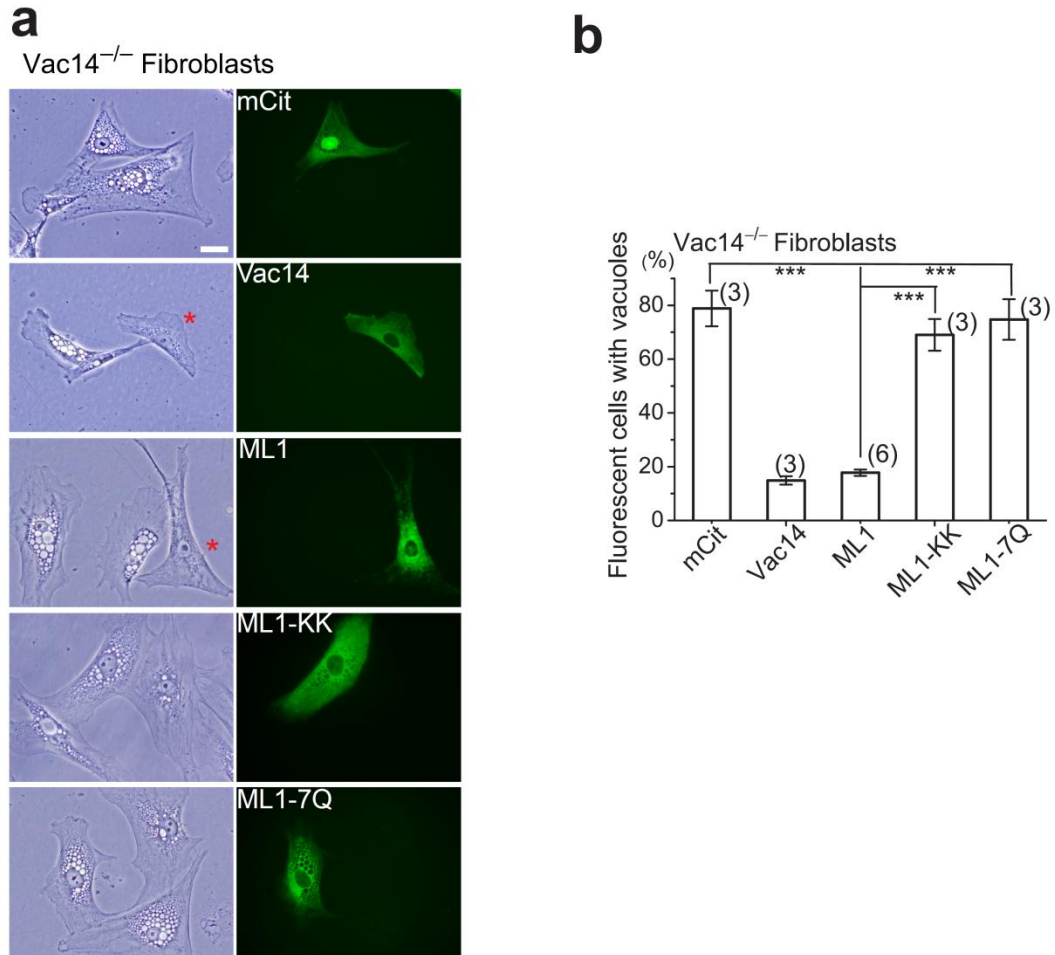
Figure 2.14 Overexpression of TRPML1 rescues the enlarged endolysosome phenotype of PI(3,5)P$_2$-deficient mouse fibroblasts. (Prepared by Xiang Wang)
a) The effects of overexpression of WT TRPML1 and pore (ML1-KK) or PI(3,5)P$_2$-insensitive (ML1-7Q) mutant TRPML1 on the number and size of the vacuoles in Vac14$^{-/-}$ fibroblasts. Cultured Vac14$^{-/-}$ mouse fibroblast cells exhibited variable numbers (1-20) of large (> 3 μm) vacuoles/endolysosomes. Non-vacuolated cells are indicated with asterisk. Scale Bar = 20 μm. b) Large vacuoles in 75% of vector (mCit) -transfected Vac14$^{-/-}$ fibroblast cells. Overexpression of Vac14-mCit or EGFP-ML1 reduced the percentage (of enlarged vacuoles) to approximately 15%, while the 75% of EGFP-ML1-KK or EGFP-ML1-7Q-transfected cells contained enlarged vacuoles. Data are presented as the mean ± standard error of the mean (SEM); the n numbers are in parentheses. (***, $P < 0.001$).

CHAPTER 3

A SMALL-MOLECULE SYNTHETIC AGONIST EVOKES TRPML1-DEPENDENT CA^{2+} RELEASE FROM ENDOLYSOSOMES

Abstract

TRPML1 is an inwardly-rectifying Ca^{2+}-permeable channel in late endosomes and lysosomes. Loss-of-function mutations on human TRPML1 gene cause a devastating pediatric neurodegenerative disease called type IV Mucolipidosis (ML4). In the preceding chapter, I described PI(3,5)P$_2$, a phosphoinositide localized predominantly in the late endosomes and lysosomes, as an endogenous activator of TRPML1. Here I will report a membrane-permeable small-molecule synthetic agonist for TRPML1, Mucolipin-Synthetic Agonist 1 (ML-SA1). ML-SA1 potently activates recombinant TRPML1, as well as endogenous TRPML-like currents in several cell types, including human fibroblasts, macrophages and Chinese Hamster Ovary cells. The activation effect of ML-SA1 can be further potentiated by PI(3,5)P$_2$, suggestive of a synergism between the two agonists. By using lysosome-targeting GCaMP3-based Ca^{2+} sensors, I found that ML-SA1 evokes TRPML1-dependent Ca^{2+} release from endolysosomes in intact cells. Therefore this TRPMLs-specific chemical agonist can be used as a valuable tool for studying intracellular functions of TRPMLs. Future studies on the agonist may lead to a novel therapeutic approach for treating ML4 disease.

Introduction

Identification of specific ligands and activators is important for ion channel study, since characterization of the properties or physiological roles of ion channels often heavily relies on the availability of such tools as channel activators. Recent studies on TRP channels have identified a number of agonist or antagonists for many TRP channels (Ramsey, Delling et al. 2006; Patapoutian, Tate et al. 2009); however, there are still no chemical activators or selective inhibitors found for TRPML1. This is mainly due to the intracellular localization of TRPML1, which make the channel inaccessible to conventional patch clamp method. By using a modified patch-clamp method (Dong, Cheng et al. 2008; Dong, Shen et al. 2010), Xu lab recently identified Phosphatidylinositol 3,5-bisphosphate(PI(3,5)P$_2$) as the first endogenous TRPML1 activator. Yet due to the membrane impermeability of PI(3,5)P$_2$, its effectiveness as a TRPML1 agonist for cellular assays is greatly comprised. Although intracellular delivery of PIP is feasible (Ozaki, DeWald et al. 2000), this method is time-consuming and requires extra carrier molecules that may introduce unexpected complications. Identification of a plasma membrane permeable chemical agonist for TRPML1 is necessary, and such an agonist will provide a useful tool to study the biophysical and physiological features of TRPML1.

Recently Stefan Heller's group identified several small molecular activators of TRPML3 through compound library screening(Grimm, Jors et al. 2010). Given the high similarity of amino acid sequences shared by TRPML1 and TRPML3, we tested whether any of these chemicals can activate TRPML1 on the endolysosomal membrane. We found several chemicals that can weakly activate TRPML1. Interestingly, they can also activate the di-leucine mutant of TRPML (TRPML-4A) on plasma membranes, which contains four amino acid mutations on both di-

leucine motifs that trap a portion of TRPML1 channels on the plasma membrane (Vergarajauregui and Puertollano 2006; Grimm, Jors et al. 2010)). By modifying the structure of one of the chemicals - SF51, we found another chemical (ML-SA1) that potently activates both recombinant and endogenous TRPML1 channel using lysosomal patch clamp technique. Notably, ML-SA1 evokes Ca^{2+} release from endolysosomes by activating intracellular TRPMLs in intact cells, suggesting that the agonist is membrane permeable. Therefore this TRPMLs-specific chemical agonist can be used as a valuable tool for studying intracellular functions of TRPMLs. Future studies on the agonist may lead to a novel therapeutic approach for treating ML4 disease.

Methods

Molecular biology and biochemistry. The GCaMP3-ML1 construct was made by inserting the full length GCaMP3 sequence (Tian, Hires et al. 2009) between the HindIII and BamHI sites of a pcDNA6 plasmid that contains the mouse TRPML1 cDNA at the XhoI site. TRPML1-L^{15}L/AA-L577L/AA (abbreviated as ML1-4A) and the TRPML1 non-conducting pore mutant (D471K/D472K; abbreviated ML1-KK) were constructed using a site-directed mutagenesis kit (Qiagen). All constructs were confirmed by sequencing, and protein expression was verified by western blot. CHO, HEK293T, Cos-1, and human fibroblast cells were transiently transfected with GCaMP3-ML1 for electrophysiology, Ca^{2+} imaging, and confocal imaging.

Preparation and culture of mouse macrophages. Bone marrow cells from femurs and tibias were harvested and cultured in macrophage differentiation medium (RPMI-1640 medium with 10%

fetal bovine serum (FBS) and 100 unit/ml recombinant colony stimulating factor from PeproTech, Rocky Hill, NJ). After 7 d in culture at 37 °C with 5% CO_2, the adherent cells (> 95% are expected to be macrophages) were harvested for assays (Link, Park et al. 2010).

Mammalian whole-cell electrophysiology. HEK293T, Cos-1, and CHO cells were used for the heterologous expression experiments and were transfected using Lipofectamine 2000 (Invitrogen). The pipette solution contained 147 mM Cs, 120 mM methane-sulfonate, 4 mM NaCl, 10 mM EGTA, 2 mM Na_2-ATP, 2 mM $MgCl_2$, and 20 mM HEPES (pH 7.2; free $[Ca^{2+}]_i$ < 10 nM). The standard extracellular bath solution (modified Tyrode's solution) contained 153 mM NaCl, 5 mM KCl, 2 mM $CaCl_2$, 1 mM $MgCl_2$, 20 mM HEPES, and 10 mM glucose (pH 7.4). The "Low pH Tyrode" solution contained 150 mM Na- Gluconate, 5 mM KCl, 2 mM $CaCl_2$, 1 mM $MgCl_2$, 10 mM glucose, 10 mM HEPES, and 10 mM MES (pH 4.6). All bath solutions were applied via a perfusion system to achieve a complete solution exchange within a few seconds. Data were collected using an Axopatch 2A patch clamp amplifier, Digidata 1440, and pClamp 10.0 software (Axon Instruments). Whole-cell currents were digitized at 10 kHz and filtered at 2 kHz. All experiments were conducted at room temperature (21-23 °C), and all recordings were analyzed with pClamp 10.0, and Origin 8.0 (OriginLab, Northampton, MA).

Endolysosomal electrophysiology. Endolysosomal electrophysiology was performed in isolated endolysosomes using a modified patch-clamp method (Dong, Cheng et al. 2008; Dong, Shen et al. 2010). Briefly, cells were treated with 1 µM vacuolin-1 for 2-5 h to increase the size of endosomes and lysosomes. Whole-endolysosome recordings were performed on isolated enlarged LELs. The

bath (internal/cytoplasmic) solution contained 140 mM K-Gluconate, 4 mM NaCl, 1 mM EGTA, 2

mM Na_2-ATP, 2 mM $MgCl_2$, 0.39 mM $CaCl_2$, 0.2 mM GTP, and 10 mM HEPES (pH adjusted

with KOH to 7.2; free $[Ca^{2+}]_i$ approximately 100 nM based on the Maxchelator software

(http://maxchelator.stanford.edu/)). The pipette (luminal) solution consisted of a "Low pH

Tyrode's solution" with 145 mM NaCl, 5 mM KCl, 2 mM $CaCl_2$, 1 mM $MgCl_2$, 10 mM HEPES,

10 mM MES, and 10 mM glucose (pH 4.6).

Fura-2 Ca^{2+} imaging. Cells were loaded with 5 μM Fura-2 AM in the culture medium at 37 °C

for 60 min. Fluorescence was recorded at different excitation wavelengths using an EasyRatioPro

system (PTI). Fura-2 ratios (F_{340}/F_{380}) were used to monitor changes in intracellular $[Ca^{2+}]$ upon

stimulation. GPN (Glycyl-L-phenylalanine 2-naphthylamide; 200-400 μM, a lysosome-disrupting

agent) and Bafilomycin A1 (500 nM, a V-ATPase inhibitor) were used as positive controls to

induce Ca^{2+} release from lysosome and acidic stores, respectively (Calcraft, Ruas et al. 2009).

Ionomycin (1 μM) was added at the conclusion of all experiments to induce a maximal response

for comparison. For endogenous lysosomal Ca^{2+} release measurement, Ca^{2+} imaging was carried

out within 0.5-3 h after plating and when cells still exhibited a round morphology.

GCaMP3 Ca^{2+} imaging. 18-24 h after transfection with GCaMP3-ML1, CHO or human

fibroblast cells were trypsinized and plated onto glass coverslips. Most experiments were carried

out within 0.5-3 h after plating when cells still exhibited a round morphology. The fluorescence

intensity at 470 nm (F_{470}) was monitored using the EasyRatioPro system. Lysosomal Ca^{2+} release

was measured under a "low" external Ca^{2+} solution, which contained 145mM NaCl, 5 mM KCl, 3 mM $MgCl_2$, 10 mM Glucose, 1mM EGTA, and 20 mM HEPES (pH7.4). Ca^{2+} concentration in the nominally-free Ca^{2+} solution is estimated to be 1-10 μM. With 1 mM EGTA, the free Ca^{2+} concentration is estimated to be < 10 nM based on the Maxchelator software (http://maxchelator.stanford.edu/).

Data analysis. Data are presented as the mean ± standard error of the mean (SEM). Statistical comparisons were made using analysis of variance (ANOVA). A *P* value < 0.05 was considered statistically significant.

Results

Identification of several weak TRPML1 activators

15 small-molecule chemical compounds (SF compounds) that can activate recombinant surface-expressed TRPML3 were identified by a recent high-throughput screen (Grimm, Jors et al. 2010). Since TRPML1 is primarily localized on the membranes of LELs (Cheng, Shen et al. 2010), this screen, which is based on whole-cell patch clamp and calcium imaging assay, is unable to test the effect of these compounds on wild-type TRPML1 channel. Using whole-endolysosome patch-clamp recordings (Dong, Cheng et al. 2008; Dong, Shen et al. 2010), we found that several SF compounds also weakly activated whole-endolysosome TRPML1-mediated currents (I_{TRPML1} or I_{ML1}), such as SF22 and SF51 (**Fig 3.1**). In HEK293T cells transfected with surface-expressed mutant TRPML1 channels (TRPML1-L^{15}L/AA-L^{577}L/AA, abbreviated as ML1-4A (Vergarajauregui and Puertollano 2006; Grimm, Jors et al. 2010)), one of the SF compounds, SF-51 (Grimm, Jors et al. 2010), induced small cytosolic [Ca^{2+}] ([Ca^{2+}]$_{cyt}$) increases (measured with Fura-2 ratios; **Fig 3.2a, b**), and activated small but significant inwardly-rectifying whole-cell currents (I_{ML1-4A}; **Fig 3.2d**).

Identification of a potent synthetic agonist for TRPML1

By conducting a Fura-2-based low-throughput-screen for more potent TRPML1 agonists (see **Table 3.1**), we identified a SF-51-related compound (see **Fig 3.2c** for the chemical structures; Mucolipin Synthetic Agonist 1 or ML-SA1) that could induce significant $[Ca^{2+}]_{cyt}$ increases in HEK293 cells stably- or transiently-expressing ML1-4A (**Fig 3.2a**). In electrophysiological assays, ML-SA1 robustly activated whole-cell I_{ML1-4A} (**Fig 3.2d**) and whole-endolysosome I_{ML1} (**Fig 3.2e**). ML-SA1 also activated whole-cell I_{TRPML2} and I_{TRPML3}, but not six other related channels (**Fig 3.4**). ML-SA1 (10 μM) activation of whole-endolysosome I_{ML1} was comparable to the effect of the endogenous TRPML agonist $PI(3,5)P_2$ (1 μM; **Fig 3.2e**), and these agonists were synergistic with each other (**Fig 3.2f**). ML-SA1 activated an endogenous whole-endolysosome TRPML-like current (I_{ML-L}) in all mammalian cell types that we investigated, including Chinese Hamster Ovary (CHO) (**Fig 3.3a**), Cos-1, HEK293, skeletal muscle, pancreatic β, and macrophage cells (**Fig 3.3b**). ML-SA1 activated whole-endolysosome I_{ML-L} in wild-type (WT; $ML1^{+/+}$), but not ML4 ($ML1^{-/-}$) human fibroblasts (**Fig 3.3c**), suggesting that although ML-SA1 targets all three TRPMLs, the expression levels of TRPML2 and TRPML3 are very low, and TRPML1 is the predominant lysosomal TRPML channel in this cell type. Thus, we have identified a reasonably specific and potent agonist that can be a useful chemical tool for studying the functions of TRPMLs, especially TRPML1.

A lysosome-targeted genetically-encoded Ca^{2+} indicator

To measure lysosomal Ca^{2+} release in intact cells, GCaMP3, a single-wavelength genetically-encoded Ca^{2+} indicator (Tian, Hires et al. 2009), was engineered to the cytoplasmic N-terminus of TRPML1 (**Fig 3.5a**). When transfected into HEK293T, CHO, or Cos-1 cell lines, GCaMP3-TRPML1 (GCaMP3-ML1) was mainly localized in the Lamp-1 and LysoTracker-positive compartments, i.e., LEL (**Fig 3.5b,c**). To determine the specificity of the GCaMP3-ML1 fluorescence signal, I tested a variety of Ca^{2+} release reagents and found that GCaMP3 fluorescence (F_{470}) responded preferentially and reliably to lysosome-acting Ca^{2+}-mobilization reagents ($\Delta F/F_0 = 0.2-1$), including Glycyl-L-phenylalanine 2-naphthylamide (GPN, a Cathepsin C

substrate that induces osmotic lysis of lysosomes; **Fig 3.5d**) and bafilomycin A1 (Baf-A, a V-ATPase inhibitor) (Lloyd-Evans, Morgan et al. 2008). In a subset of cells, GCaMP3 also responded to large ($\Delta F/F_0 > 2$) Ca^{2+} increases triggered by thapsigargin (TG, targeting the ER Ca^{2+} store; **Fig 3.5d**), which may presumably spread to close proximity of lysosomes. In the majority of the cells, however, TG failed to significantly increase GCaMP3 fluorescence (**Fig 3.5d**), suggesting that small ER Ca^{2+} release was not detected by GCaMP3-ML1. Taken together, GCaMP3-ML1 readily and preferentially detects juxta-lysosomal Ca^{2+} increases.

ML-SA1 induces TRPML1-mediated Ca^{2+} release from lysosomes

In GCaMP3-ML1-transfected CHO (**Fig 3.6a, 3.6b**), HEK293T, and Cos-1 cell lines, application of ML-A1 (20 μM) induced rapid increases in GCaMP3 fluorescence ($\Delta F/F_0 = 0.45 \pm 0.05$, n = 77 cells; **Fig 3.6a, 3.7f**) in the presence of low external Ca^{2+} (nominally-free Ca^{2+} + 1 mM EGTA; free Ca^{2+} estimated to be < 10 nM). In contrast, no significant increase in GCaMP3 fluorescence ($\Delta F/F_0 = 0.03 \pm 0.01$, n = 32 cells; **Fig 3.6c, 3.6d, 3.7f**) was observed in cells transfected with a plasmid carrying GCaMP3 fused to a non-conducting pore mutant of TRPML1 (Pryor, Reimann et al. 2006; Dong, Shen et al. 2010) (GCaMP3-ML1-KK). Both GPN and Baf-A1 largely abolished ML-SA1-induced Ca^{2+} responses (**Fig 3.7a-f**). In contrast, ML-SA1-induced Ca^{2+} response was mostly intact in TG-treated cells (**Fig 3.7f**). Collectively, these results suggest that ML-SA1 activated endolysosomal TRPML1 to induce Ca^{2+} release from lysosomes. Thus I have established a robust Ca^{2+} imaging assay to measure TRPML1-mediated lysosomal Ca^{2+} release.

ML-SA1 activates endogenous TRPMLs in intact cells.

To investigate whether ML-SA1 can activate endogenous TRPMLs in intact cells, fura-2 based calcium imaging assay were carried out in WT CHO and macrophages cells. In WT CHO cells, small but significant Ca^{2+} increases were seen upon application of 100 μM ML-SA1 in low external Ca^{2+} (**Fig 3.8a**). Similarly, 100 μM ML-SA1 also evoked small Ca^{2+} increases in wild type macrophage cells (**Fig 3.8b**). The ML-SA1-induced lysosomal Ca^{2+} responses are most likely

mediated by TRPML1, since NPC1$^{-/-}$ mouse macrophages exhibited a significant reduction in ML-SA1-induced lysosomal Ca^{2+} release compared to WT cells (**Fig 3.8c**). These results suggest that high concentration of ML-SA1 can activate endogenous TRPMLs in intact cells.

Discussion

In this study, I reported the discovery of a potent small molecular agonist for TRPML1. Under lysosomal patch clamp configuration, the agonist (ML-SA1) can potently activate recombinant TRPML channels, but not other related channels on the endolysosomal membranes. The agonist also activates endogenous TRPML1 channel in various cell types. By using Gcamp3-based Ca^{2+} sensors localized on late endosome and lysosomes, I found the agonist could evoke Ca^{2+} release from endolysosomes in intact cells by activating intracellular TRPML1 channels. These results revealed that ML-SA1 is a potent and specific synthetic chemical activator for TRPMLs.

The activation site of ML-SA1 on TRPML1 is yet unknown. Given that ML-SA1 is membrane permeable, it is difficult to test which side of the channel ML-SA1 binds to by using the electrophysiology method. Our results showed that ML-SA1 was able to activate TRPML1 from both the luminal side (whole cell configuration) and cytosolic side (whole lysosomal configuration) of the channel. Under both configurations, the activation is very rapid, and the time course is similar, which suggests that either ML-SA1 can activate the channel on both sides, or the translocation of ML-SA1 across the membrane is very fast. Further mutagenesis assays on the TRPML1 channel are required to map out the activation site of ML-SA1.

Although ML-SA1 is able to evoke Ca^{2+} release in intact cells through endogenous

TRPML1 (**Fig 3.8**), such Ca^{2+} release was only observed when using high concentration of ML-SA1 (>50μM). It is possible that with low concentration of ML-SA1 (<50 μM), the fura-2 based assay may not be sensitive enough to catch the Ca^{2+} release events through TRPMLs. Alternatively, ML-SA1 might just sensitize the endogenous TRPML1s, but is not potent enough to activate them at the low concentration. One interesting observation is that upon agonist application, the endogenous Ca^{2+} response is usually bigger for newly-plated cells with round morphology, compared to long-time cultured cells with extensive morphology. The major difference between these two conditions is that the former cells just went through the trypsinization and pipetting processes, which may introduce physical damages to cell membranes, while the latter cells did not. It would be interesting to test whether such a difference will cause the change of lysosomal calcium store, or even the sensitization of TRPMLs, since certain stress conditions are indeed associated with lysosomal biogenesis and increased expression levels of lysosomal genes (Karageorgos, Isaac et al. 1997; Helip-Wooley and Thoene 2004).

Another interesting observation is that high concentrations of ML-SA1 leads to robust calcium oscillations in fura-2 loaded CHO cells. The oscillation was not caused by the Ca^{2+} channels on plasma membrane, since the experiments were carried out under 0 Ca^{2+} external solution conditions. But thapsigagin pretreatment abolished the oscillation (data not shown). A possible explanation is that ML-SA1 induces the Ca^{2+} release from lysosomes that are in close proximity to ER. This Ca^{2+} release activates the ryanodine receptor on ER (Hamilton and Serysheva 2009) and causes massive ER Ca^{2+} efflux , giving rise to the large Ca^{2+} spike. However, increased Ca^{2+} level subsequently inactivates the ryanodine receptor, and cytosolic Ca^{2+} concentration is quickly reduced due to PM Ca^{2+} pumps. Yet, due to the continuous presence of

ML-SA1, Ca^{2+} release from lysosomes will trigger the repetition of the aforementioned process.

This study introduced a genetically encoded calcium indicator – GCaMP3-TRPML1 for calcium imaging assay. The calcium detection range for GCaMP3 is from 100nM to 2μM, which is suitable for monitoring most of the cytosolic $[Ca^{2+}]$ change events (Tian, Hires et al. 2009). Compared to conventional synthetic calcium indicator (e.g. Fura-2), our GCaMP3-TRPML1 indicator has at least two advantages. Firstly, it specifically targets to late endosome/lysosome compartments, and is more sensitive to local $[Ca^{2+}]$ change. Secondly, this indicator can be engineered into model organisms, and therefore allows long-term, repeated *in vivo* measurements, while most synthetic calcium indicators cannot. One caveat, however, is that TRPML1 is overexpressed when using this indicator, which may affect the intracellular trafficking, and makes it impossible to study the endogenous TRPML1 function. This problem, however, can be circumvented by tagging GCaMP3 to different lysosomal protein (e.g.Lamp1 or Vamp7). Special care will still need to be taken of the overexpression of that specific lysosomal protein.

Overall, the identification of ML-SA1 and GCaMP3 based indicator provides valuable tools to study the multiple cellular processes that TRPMLs are involved in, such as exocytosis and endolysosomal fusion/fission. For example, the activation of TRPML1 and its coincidence with fusion/fission processes may be captured by using high-resolution, live imaging techniques with the help of the ML-SA1 agonist and our GCaMP3 based Ca^{2+} sensor. As TRPMLs do not exhibit significant voltage-dependent inactivation, even a small TRPML current may lead to substantial Ca^{2+} release(Cheng, Shen et al. 2010). Therefore, pretests need to be carried out to determine the proper concentration of ML-SA1 for such in vivo assays. Another important direction is further characterization of ML-SA1. As many ML4 patients still have residual TRPML1 channel activity

71

even though the channel is mutated (Altarescu, Sun et al. 2002; Bargal, Goebel et al. 2002; Goldin, Stahl et al. 2004), it is important to study the effect of ML-SA1 on these mutated channels. These studies, together with mice model work and clinical trials, may eventually lead to a novel therapeutic approach for treating ML4 disease.
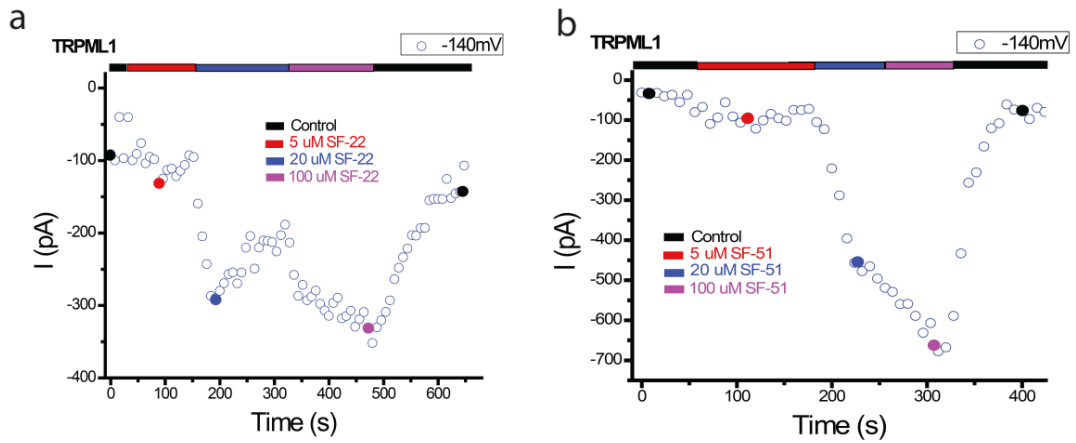
Fig 3.1. Identification of SF-22 and SF51 as weak activators for TRPML1.

Bath application of different concentrations of SF-22 (**a**) and SF51(**b**) activated inwardly rectifying whole-endolysosome TRPML1-mediated current (I_{TRPML1}) in enlarged endolysosome/vacuoles from a TRPML1-EGFP-expressing Cos-1 cell that was pre-treated with vacuolin-1. $I_{TRPML1}$was elicited by repeated voltage ramps (-140 to +140 mV; 400 ms) with a 4-s interval between ramps. I_{TRPML1} is small even with very high concentration of agonist (measured at -140 mV)
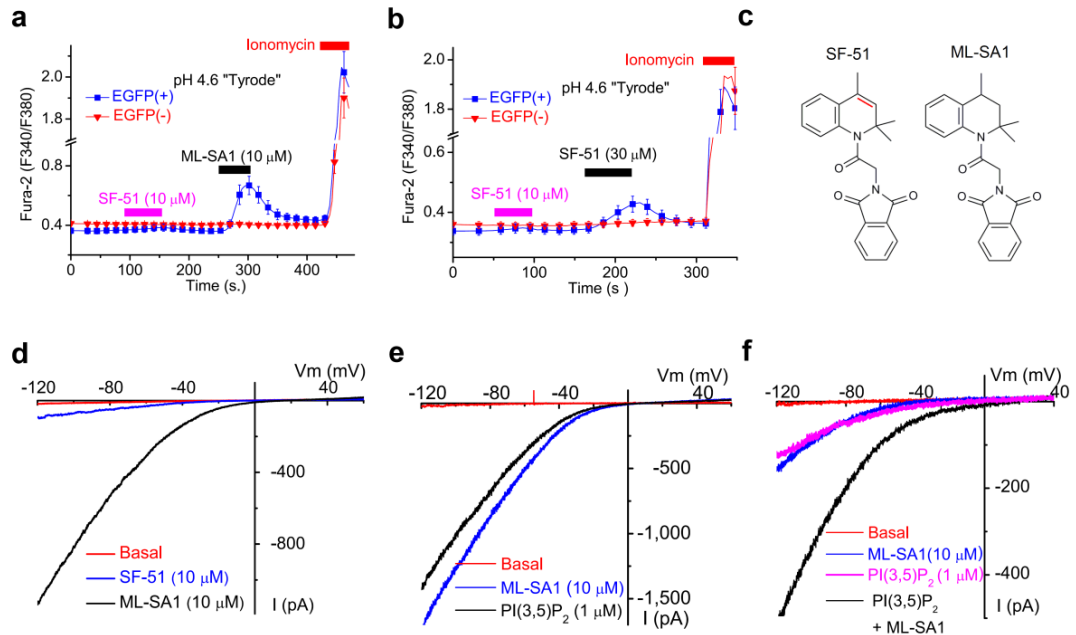
**Fig 3.2. Identification of ML-SA1 as a potent small molecular agonist for TRPML1. (a)** ML-SA1 induced increases in cytosolic [Ca^{2+}], as measured by the Fura-2 ratio (F$_{340}$/F$_{380}$) in HEK293T cells expressing TRPML1-L^{15}L/AA-L^{577}L/AA (ML1-4A) at low pH (pH 4.6) external solution. SF-51 (10 μM) induced much smaller responses in the same cells. **(b)** SF-51 (30 μM) induced increases in cytosolic [Ca^{2+}] in ML1-4A-expressing HEK293T cells at low pH external solution. **(c)** Chemical structures of SF-51 and ML-SA1. The difference between SF-51 and ML-SA1 is highlighted in red. **(d)** Activation of whole-cell currents by SF-51 and ML-SA1 in ML1-4A-expressing HEK293T cells. ML1-4A-mediated current (I_{ML1-4A}) was elicited by repeated voltage ramps (-140 to +140 mV; 400 ms) with a 4-s interval between ramps. Only a portion of the voltage protocol is shown; holding potential = 0 mV. **(e)** Activation of whole-endolysosome I_{ML1} by ML-SA1 and PI(3,5)P$_2$. Enlarged vacuoles/endolysosomes were isolated from vacuolin-treated HEK293 cells stably-expressing ML1-4A. ML-SA1 and PI(3,5)P$_2$ were applied to the cytosolic sides of the isolated vacuoles. The pipette (luminal) solution was a standard external (Tyrode's) solution adjusted to pH 4.6; the bath (internal/cytoplasmic) solution was a K$^+$-based solution (140 mM K$^+$-gluconate). Note that the inward current indicates cations flowing out of the endolysosome. **(f)** Synergistic activation of whole-endolysosome I_{ML1} by ML-SA1 and PI(3,5)P$_2$ in human fibroblasts. I_{ML1} was activated by PI(3,5)P$_2$ (1 μM) and ML-SA1 (10 μM); co-application of PI(3,5)P$_2$ and ML-SA1 further increased I_{ML1}. (Fig 3.2 e,f were prepared by Xiang Wang and Xiaoli Zhang)
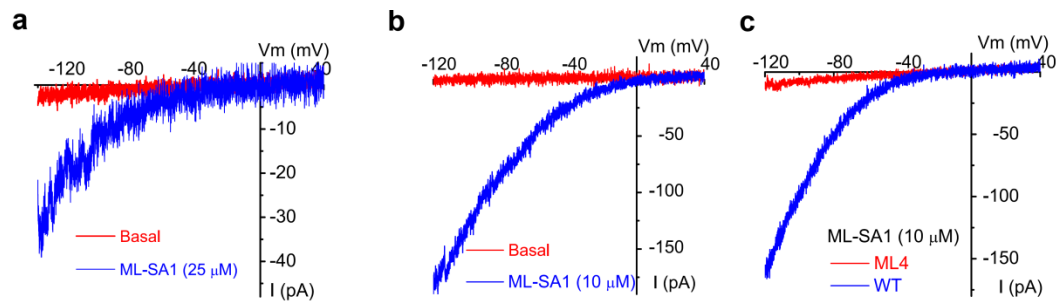
Fig 3.3. ML-SA1 activates endogenous TRPM-like currents in the endolysosomal membranes. **a)** ML-SA1 activated endogenous whole-endolysosome ML-like currents (I_{ML-L}) in CHO cells. (**b**) ML-SA1 activated whole-endolysosome I_{ML-L} in mouse primary macrophages. (**c**) ML-SA1 activated whole-endolysosome I_{ML1} in WT (ML1$^{+/+}$), but not ML4 (ML1$^{-/-}$) human fibroblasts. (Prepared by Xiang Wang and Xiaoli Zhang)
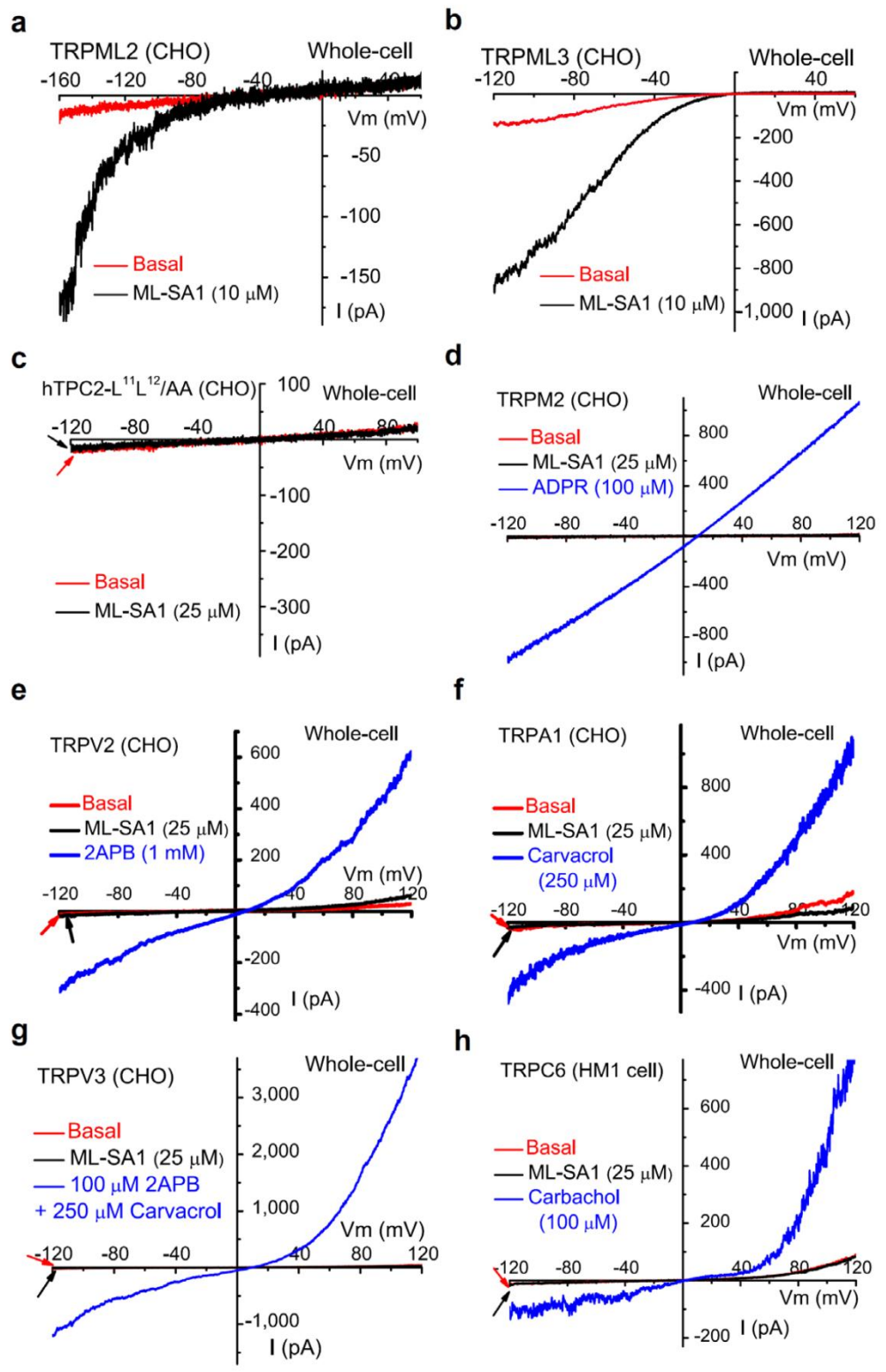
Figure 3.4. ML-SA1 activates TRPMLs, but not other related channels.

(a) Activation of small inwardly rectifying whole-cell currents by ML-SA1 (10 uM) in TRPML2-expressing CHO cells. **(b)** Activation of whole-cell I_{TRPML3} by ML-SA1 (10 uM) in TRPML3-expressing CHO cells. **(c)** ML-SA1 (25 uM) failed to activate whole-cell currents in CHO cells transfected with surface-expressing human TPC2 mutant (hTPC2-L11L12/AA-EGFP) channels. **(d)** ML-SA1 (25 uM) failed to activate whole-cell currents in TRPM2-expressing cells. In contrast, pipette dialysis of ADPR (100 uM) elicited whole-cell I_{TRPM2}. **(e)** I_{TRPV2} was not activated by ML-SA1. 2APB(1 mM) activated I_{TRPV2} in the same cell. **(f)** I_{TRPA1} was not activated by ML-SA1. Carvacrol (250 uM) activated I_{TRPA1} in the same cell. **(g)** I_{TRPV3} was not activated by ML-SA1. Co-application of 2APB(100 uM) and Carvacrol (250 uM) activated I in the same cell. **(h)** I_{TRPC6} was not activated by ML-SA1 in TRPC6-expressing HEK cells stably-expressing Muscarinic receptor 1 (HM1). Carbachol activated I_{TRPC6} in the same cell.
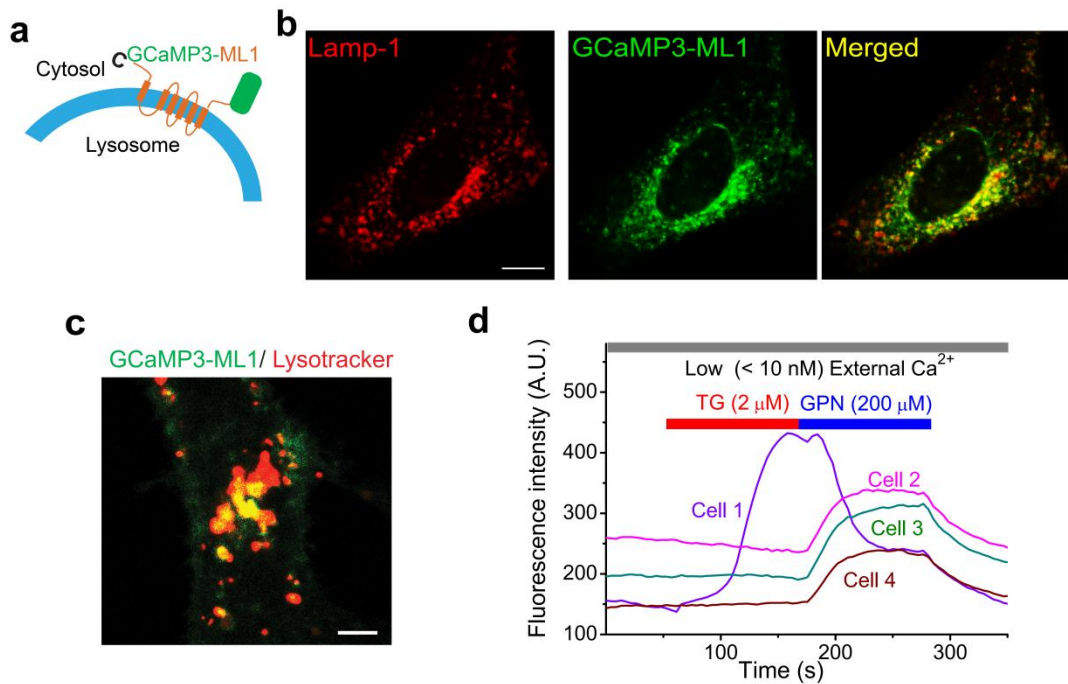
Figure 3.5. A lysosome-targeted genetically-encoded Ca^{2+} indicator.

(a) GCaMP3-TRPML1 (GCaMP3-ML1) fusion strategy. GCaMP3 is fused to the N- terminus of TRPML1. **(b)** Co-localization of GCaMP3-ML1 fluorescence with Lamp-1 in HEK293T cells expressing both GCaMP3-ML1 and Lamp-1-mCherry. Scale bar = 5 μm. **(c)** Co-localization of GCaMP3-ML1 fluorescence with LysoTracker in GCaMP3-ML1-expressing HEK293T cells. Scale bar = 2 μm. **(d)** Preferential detection of Ca^{2+} release from lysosome stores by GCaMP3-ML1 in GCaMP3-ML1-transfected Cos-1 cells. ER and lysosome Ca^{2+} releases were triggered by thapsigargin (TG, 2 μM) and Glycyl-L-phenylalanine 2-naphthylamide (GPN, 200 μM), respectively, in low (nominally-free Ca^{2+} + 1 mM EGTA; free [Ca^{2+}] estimated to be < 10 nM) external [Ca^{2+}]. All cells responded to GPN; only 1 out 4 cells responded to TG. (Fig 3.5b was prepared by Xinran Li)
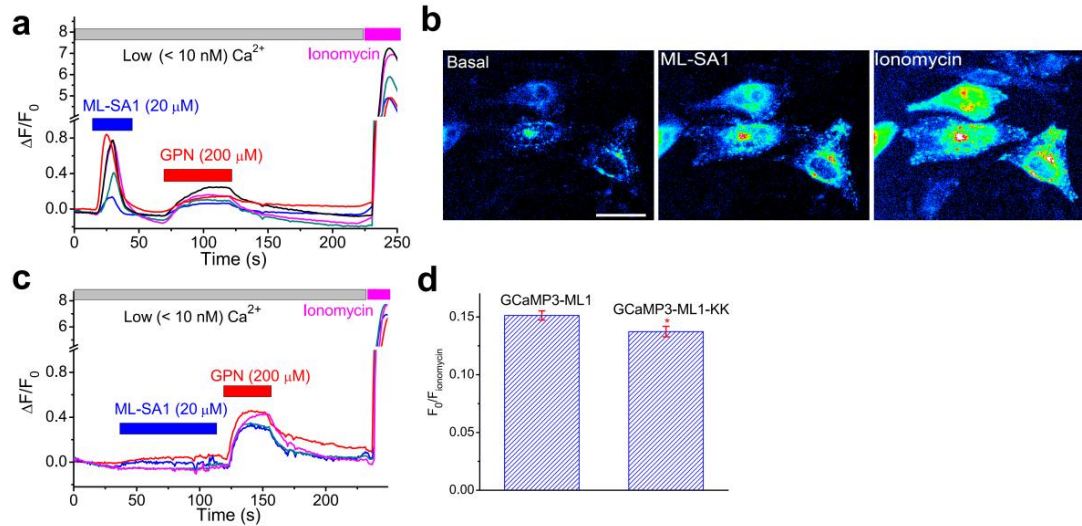
**Figure 3.6. ML-SA1 induces TRPML1-dependent intracellular Ca^{2+} release.**

(a) ML-SA1 (20 μM) induced rapid increases in GCaMP3 fluorescence (measured as change of GCaMP3 fluorescence ΔF over basal fluorescence F_0; $\Delta F/F_0$) under low (< 10 nM) external Ca^{2+} in CHO cells transfected with GCaMP3-ML1. Subsequent application of GPN (200 μM) induced smaller responses. Maximal responses were induced by ionomycin (1 μM) application.(b) Representative micrographs from panel (a) to show the changes of GCaMP3 fluorescence upon bath application of ML-SA1 and ionomycin to GCaMP3-ML1-transfected CHO cells. Scale bar = 5 μm. (c) ML-SA1 failed to induce significant Ca^{2+} increases in CHO cells transfected with GCaMP3-ML1-KK (non-conducting pore mutation). (d) Basal GCaMP3 fluorescence (normalized to the maximal ionomycin-induced fluorescence) of GCaMP3-ML1-KK and GCaMP3-ML1. For panels d, the responses were averaged for 40-100 transfected cells from at least 3 independent experiments; data are presented as the mean ± SEM. Statistical comparisons were made using analysis of variance: * P <0.05.
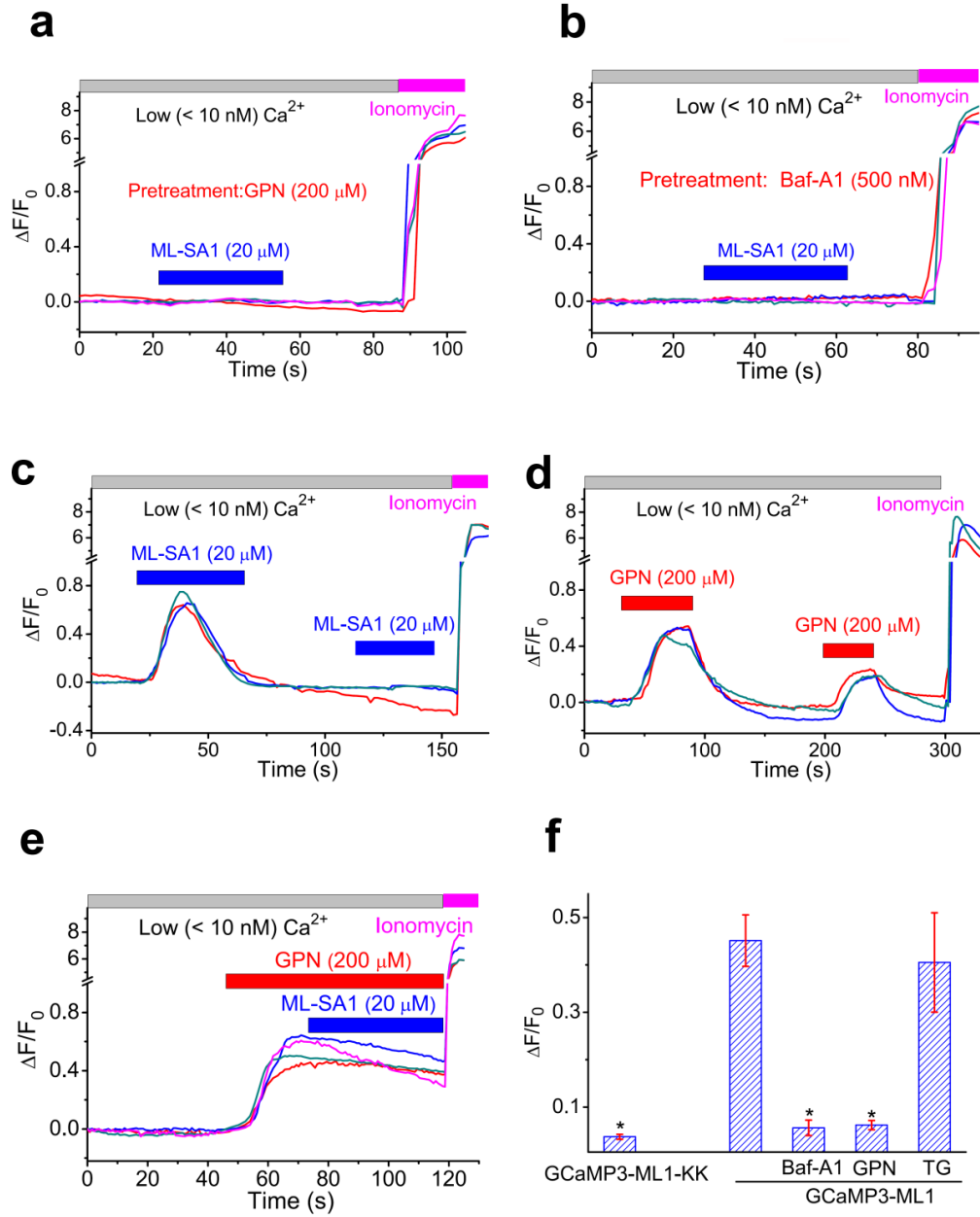
Figure 3.7. ML-SA1 induced Ca^{2+} release is from lysosomes.

(a) GPN (200 µM) pretreatment abolished ML-SA1-induced responses in GCaMP3-ML1-expressing CHO cells. (b) Bafilomycin A1 (Baf-A1, 500 nM) pretreatment abolished ML-SA1-induced Ca^{2+} response in GCaMP3-ML1-expressing CHO cells. (c) Repetitive applications of ML-SA1 (20 µM) induced little or no responses in GCaMP3-ML1-expressing CHO cells. (d) Repetitive applications of GPN (200 µM) induced smaller GCaMP3 responses in GCaMP3-ML1-expressing CHO cells. (e) ML-SA1 failed to further increase GCaMP3 fluorescence in GCaMP3-ML1-expressing CHO cells in the presence of GPN (200 µM). (f) ML-SA1-induced responses in CHO cells transfected with GCaMP3-ML1-KK (non-conducting pore mutation), and GCaMP3-ML1-transfected cells pretreated with Baf-A1, GPN, or TG. For panels f, the responses were averaged for 40-100 transfected cells from at least 3 independent experiments; data are presented as the mean ± SEM. Statistical comparisons were made using analysis of variance: * P <0.05.
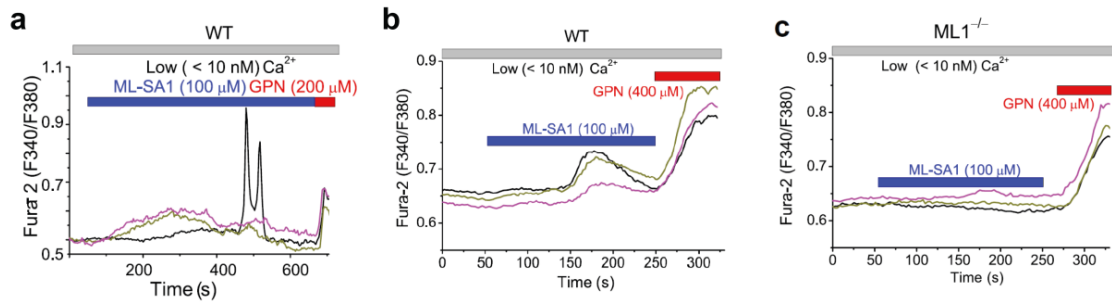
Figure 3.8. High concentration of ML-SA1 activates endogenous TRPMLs in intact cells. (a) Endogenous TRPML1-mediated lysosomal Ca^{2+} release (measured with Fura-2 ratios) in WT CHO cells. **(b,c)** Endogenous TRPML1-mediated lysosomal Ca^{2+} release (measured with Fura-2 ratios) in WT (b), and ML1-/- (c) mouse macrophages.

Table 3.1. List of small molecules tested for TRPML1 agonist.

CAS #	Structure	Effect of 10uM chemical on TRPML1[4A] in pH4.6 Tyrode $(\Delta F_{340/380})$Mean $\pm$SEM
332382-54-4		0.31 $\pm$0.082 (10uM)
352660-31-2		0.15 $\pm$0.045 (10uM)
SF51 (Prototype)		0.033 $\pm$0.008 (10uM) 0.084 $\pm$0.016 (30uM)
300701-43-3		0.053 $\pm$0.007 (10uM)
351498-57-2		0.045 $\pm$0.009 (10uM)
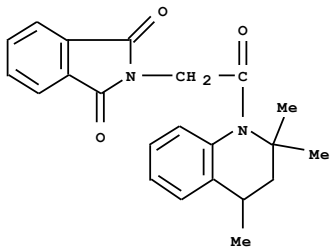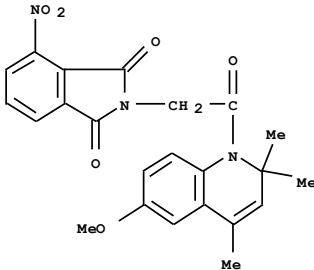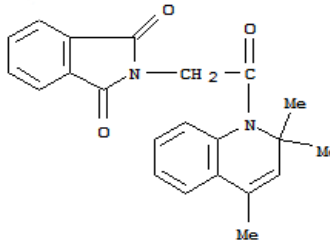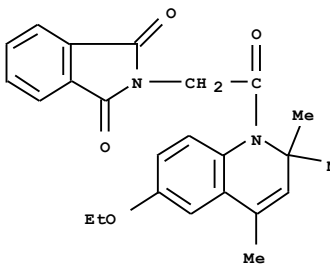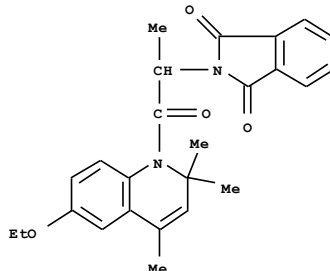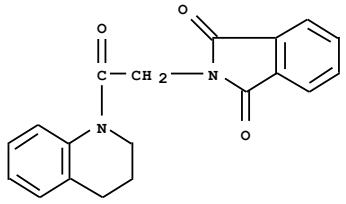
328282-81-1		**0.072 ±0.011 (10uM)**
16875-66-4		**0.041 ±0.009 (10uM)**
300731-02-6		**0.062 ±0.012 (10uM)**
302344-61-2		**0.042 ±0.007 (10uM)**
349610-85-1		No effect
332043-79-5		No effect
351498-60-7		No effect
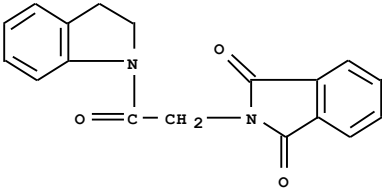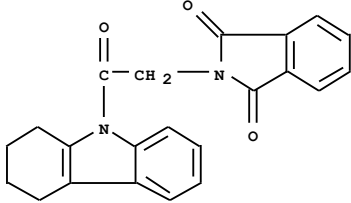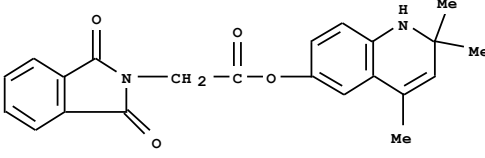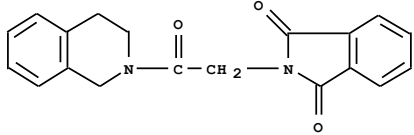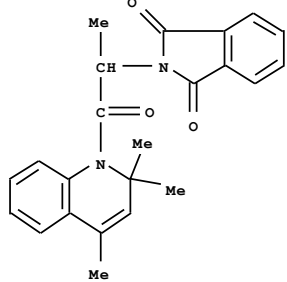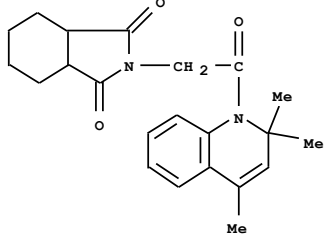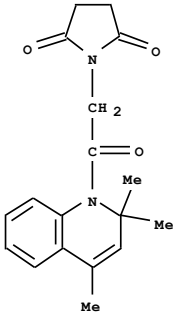
304868-03-9		No effect
300805-48-5		No effect
371201-01-3		No effect
292143-45-4		No effect
348131-40-8		No effect
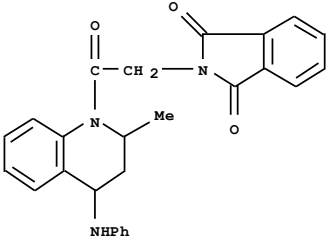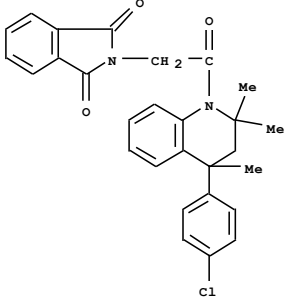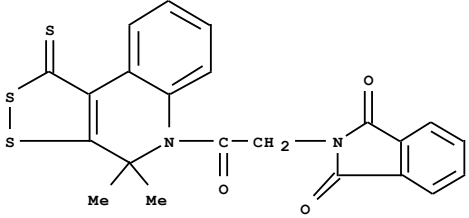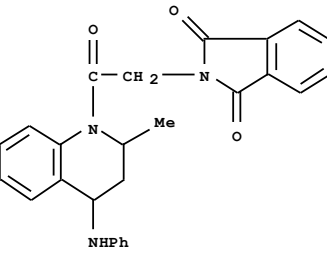
CHAPTER 4

LIPID STORAGE DISORDERS BLOCK LYSOSOMAL TRAFFICKING BY INHIBITING TRP CHANNEL AND CALCIUM RELEASE

Abstract

Lysosomal lipid accumulation, defects in membrane trafficking, and altered Ca^{2+} homeostasis are common features in many lysosomal storage diseases. Mucolipin TRP channel 1 (TRPML1) is the principle Ca^{2+} channel in the lysosome. Here we show that TRPML1-mediated lysosomal Ca^{2+} release, measured using a genetically encoded Ca^{2+} indicator (GCaMP3) attached directly to TRPML1 and elicited by a potent membrane-permeable synthetic agonist, is dramatically reduced in Niemann-Pick (NP) disease cells. Sphingomyelins (SMs) are plasma membrane lipids that undergo Sphingomyelinase (SMase)-mediated hydrolysis in the lysosomes of normal cells, but accumulate distinctively in NP cell lysosomes. Patch-clamp analyses revealed that TRPML1 channel activity is inhibited by SMs, but potentiated by SMases. In NP type C (NPC) cells, increasing TRPML1's expression/activity was sufficient to correct the trafficking defects and reduce lysosome storage and cholesterol accumulation. We propose that abnormal accumulation of luminal lipids causes secondary lysosome storage by blocking TRPML1- and Ca^{2+}-dependent lysosomal trafficking.

Introduction

The lysosome, which serves as the cell's recycling center, can mediate the hydrolase-based degradation of a variety of biomaterials, including proteins, lipids, and membranes (de Duve 2005). Most Lysosomal Storage Diseases (LSDs), of which more than 50 are known, are due to the defective activities of specific lysosomal enzymes, which result in lysosomal accumulation of specific substrates (Parkinson-Lawrence, Shandala et al. 2010). For instance, in Niemann-Pick (NP) type A and B diseases (NPA and NPB), sphingomyelins (SMs) accumulate in lysosomes due to insufficient activity of acid SMase (aSMase) (Schuchman 2010); similarly, insufficient aSMase activity and SM accumulation occur in Niemann-Pick type C (NPC), where the genetic defect occurs in components of an intracellular cholesterol/lipid trafficking pathway (Schuchman 2010; Rosenbaum and Maxfield 2011). Interestingly, regardless of the nature of the primary undigested metabolites, common cellular defects are seen in a spectrum of LSDs (Vitner, Platt et al. 2010). For example, defects in lipid trafficking (the exit of lipids from the late endosome and lysosome) and autophagome-lysosome fusion are commonly observed in almost all sphingolipidoses, including NPA, NPB, and NPC (Puri, Watanabe et al. 1999; Parkinson-Lawrence, Shandala et al. 2010). In addition, altered Ca^{2+} and Fe^{2+} homeostasis are also common factors in these LSDs (Kiselyov, Yamaguchi et al. 2010; Parkinson-Lawrence, Shandala et al. 2010; Vitner, Platt et al. 2010). Thus, it is likely that the common trafficking machinery is impaired in LSDs with unrelated origins or primary defects. One intriguing hypothesis is that the primary accumulated materials cause a sort of "lysosome stress," which impairs common biochemical and/or signaling pathways in the lysosome, similar to the way unfolded proteins cause "ER stress" to trigger an "unfolded protein response" (Parkinson-Lawrence, Shandala et al. 2010; Vitner, Platt et al. 2010).

Cells that lack mucolipin transient receptor potential (TRP) channel 1 (TRPML1) exhibit lysosomal defects similar to those seen in NP cells: defective autophagosome-lysosome fusion or lysosome reformation, abnormal lipid trafficking, and altered Ca^{2+} and Fe^{2+} homeostasis (Pryor, Reimann et al. 2006; Vergarajauregui and Puertollano 2006; Thompson, Schaheen et al. 2007; Dong,

Cheng et al. 2008; Venkatachalam, Long et al. 2008; Cheng, Shen et al. 2010; Dong, Shen et al. 2010; Shen, Wang et al. 2011). Furthermore, mutations in the human *Trpml1* gene cause mucolipidosis type IV (ML4) LSD, which exhibits membrane trafficking defects and excessive lysosomal storage (Bargal, Avidan et al. 2000; Bassi, Manzoni et al. 2000; Sun, Goldin et al. 2000). TRPML1 is a ubiquitously-expressed Fe^{2+}- and Ca^{2+}-dually permeable channel predominantly localized in late endosomes and lysosomes (LELs) (Grimm, Cuajungco et al. 2007; Xu, Delling et al. 2007; Dong, Cheng et al. 2008; Cheng, Shen et al. 2010; Grimm, Jors et al. 2010). TRPML1 is specifically activated by phosphatidylinositol 3,5-bisphosphate ($PI(3,5)P_2$), an LEL-localized low-abundance phosphoinositide (Dong, Shen et al. 2010). In addition, both TRPML1-lacking and $PI(3,5)P_2$-deficient cells exhibit defects in LEL-to-Golgi retrograde trafficking and autophagosome-lysosome fusion (Pryor, Reimann et al. 2006; Zhang, Zolov et al. 2007; Abe and Puertollano 2011; Shen, Wang et al. 2011), suggesting that the TRPML1-$PI(3,5)P_2$ system represents a common signaling pathway essential for late endocytic trafficking.

Because of the high degree of similarity in lysosomal defects, we hypothesize that TRPML1-$PI(3,5)P_2$ signaling is compromised in NPs and many other LSDs. In this study, by measuring lysosomal Ca^{2+} release using lysosome-targeted, genetically-encoded Ca^{2+} indicators, we found that TRPML1-mediated lysosomal Ca^{2+} release was compromised in NPC and NPA cells. Patch-clamp analyses demonstrated that TRPML1's channel activity was inhibited by micromolar concentrations of SMs, but potentiated by SM-hydrolyzing enzyme SMases. In type C NP (NPC) cells, increasing TRPML1's expression/activity was found to be capable of correcting the trafficking defects and decrease cholesterol accumulation. We conclude that SMs are negative regulators of TRPML1 channels under physiological conditions, and that abnormal accumulations of SMs in the lysosome lumen block Ca^{2+}-dependent membrane trafficking by directly inhibiting TRPML1.

Methods

Molecular biology and biochemistry. The GCaMP3-ML1 construct was made by inserting the full length GCaMP3 sequence (Tian, Hires et al. 2009) between the HindIII and BamHI sites of a pcDNA6 plasmid that contains the mouse TRPML1 cDNA at the XhoI site. TRPML1-L^{15}L/AA-L577L/AA (abbreviated as ML1-4A) and the TRPML1 non-conducting pore mutant (D471K/D472K; abbreviated ML1-KK) were constructed using a site-directed mutagenesis kit (Qiagen). All constructs were confirmed by sequencing, and protein expression was verified by western blot. CHO, HEK293T, Cos-1, and human fibroblast cells were transiently transfected with GCaMP3-ML1 for electrophysiology, Ca^{2+} imaging, and confocal imaging.

PCR primers used for real-time qPCR analysis of *TRPML* expression in human fibroblasts and mouse macrophages are as follows:

Human *TRPML1*: F, CGGATGACACCTTCGCAGCCTAC; R, ACGCATACCGGCCCAGTGACAC

Human *TRPML2*: F, GGTCACCACACAGCTTGTTCGT; R, TGATGATACTGATTAATAGCA

Human *TRPML3*: F, CCAGAAATTGAAACTGAGTGTT; R, ATGTTATAGTCAGAGTAAAGTC

Mouse *TRPML1*: F, AAACACCCCAGTGTCTCCAG; R, GAATGACACCGACCCAGACT

ML4 and NPC cell lines. NPC (CT43; NPC1$^{-/-}$) and WT control (RA25) CHO cells were a gift from Dr. Chang TY (Dartmouth Medical School). Human skin fibroblast cells from an ML4 patient (ML1$^{-/-}$, clone GM02048), an NPC patient (NPC1$^{-/-}$, clone GM03123), an NPA patient (clone GM00112), and non-disease control cells (ML1$^{+/+}$/ NPC1$^{-/-}$, clone GM00969) were obtained from the Coriell Institute for Medical Research (NJ, U.S.A). Human fibroblasts were transiently transfected by electroporation (260 V, 950 μF) with 100 μg of GCaMP3-ML1 plasmid, and then used for Ca^{2+} imaging experiments 24 h after electroporation.

Mouse lines. NPC1 KO mice (BALB/cNctr-*Npc1m1N*/J) and WT littermates were ordered from the Jackson Laboratories. TRPML1 KO mice were kindly provided by Dr. Susan Slaugenhaupt (Harvard Medical School) and Dr. Jim Pickel (NIH) (Venugopal, Browning et al. 2007). Animals were used under approved animal protocols and University of Michigan Institutional Animal Care Guidelines.

Preparation and culture of mouse macrophages. Bone marrow cells from femurs and tibias were harvested and cultured in macrophage differentiation medium (RPMI-1640 medium with 10% fetal bovine serum (FBS) and 100 unit/ml recombinant colony stimulating factor from PeproTech, Rocky Hill, NJ). After 7 d in culture at 37 °C with 5% CO_2, the adherent cells (> 95% are expected to be macrophages) were harvested for assays (Link, Park et al. 2010).

Mammalian whole-cell electrophysiology. HEK293T, Cos-1, and CHO cells were used for the heterologous expression experiments and were transfected using Lipofectamine 2000 (Invitrogen). The pipette solution contained 147 mM Cs, 120 mM methane-sulfonate, 4 mM NaCl, 10 mM EGTA, 2 mM Na_2-ATP, 2 mM $MgCl_2$, and 20 mM HEPES (pH 7.2; free $[Ca^{2+}]_i$ < 10 nM). The standard extracellular bath solution (modified Tyrode's solution) contained 153 mM NaCl, 5 mM KCl, 2 mM $CaCl_2$, 1 mM $MgCl_2$, 20 mM HEPES, and 10 mM glucose (pH 7.4). The "Low pH Tyrode" solution contained 150 mM Na- Gluconate, 5 mM KCl, 2 mM $CaCl_2$, 1 mM $MgCl_2$, 10 mM glucose, 10 mM HEPES, and 10 mM MES (pH 4.6). All bath solutions were applied via a perfusion system to achieve a complete solution exchange within a few seconds. Data were collected using an Axopatch 2A patch clamp amplifier, Digidata 1440, and pClamp 10.0 software (Axon Instruments). Whole-cell currents were digitized at 10 kHz and filtered at 2 kHz. All experiments were conducted at room temperature (21-23 ºC), and all recordings were analyzed with pClamp 10.0, and Origin 8.0 (OriginLab, Northampton, MA).

Endolysosomal electrophysiology. Endolysosomal electrophysiology was performed in isolated endolysosomes using a modified patch-clamp method (Dong, Cheng et al. 2008; Dong, Shen et al.

2010). Briefly, cells were treated with 1 μM vacuolin-1 for 2-5 h to increase the size of endosomes and lysosomes. Whole-endolysosome recordings were performed on isolated enlarged LELs. The bath (internal/cytoplasmic) solution contained 140 mM K-Gluconate, 4 mM NaCl, 1 mM EGTA, 2 mM Na_2-ATP, 2 mM $MgCl_2$, 0.39 mM $CaCl_2$, 0.2 mM GTP, and 10 mM HEPES (pH adjusted with KOH to 7.2; free $[Ca^{2+}]_i$ approximately 100 nM based on the Maxchelator software (http://maxchelator.stanford.edu/)). The pipette (luminal) solution consisted of a "Low pH Tyrode's solution" with 145 mM NaCl, 5 mM KCl, 2 mM $CaCl_2$, 1 mM $MgCl_2$, 10 mM HEPES, 10 mM MES, and 10 mM glucose (pH 4.6).

Fura-2 Ca^{2+} imaging. Cells were loaded with 5 μM Fura-2 AM in the culture medium at 37 °C for 60 min. Fluorescence was recorded at different excitation wavelengths using an EasyRatioPro system (PTI). Fura-2 ratios (F_{340}/F_{380}) were used to monitor changes in intracellular $[Ca^{2+}]$ upon stimulation. GPN (Glycyl-L-phenylalanine 2-naphthylamide; 200-400 μM, a lysosome-disrupting agent) and Bafilomycin A1 (500 nM, a V-ATPase inhibitor) were used as positive controls to induce Ca^{2+} release from lysosome and acidic stores, respectively (Calcraft, Ruas et al. 2009). Ionomycin (1 μM) was added at the conclusion of all experiments to induce a maximal response for comparison. For endogenous lysosomal Ca^{2+} release measurement, Ca^{2+} imaging was carried out within 0.5-3 h after plating and when cells still exhibited a round morphology.

GCaMP3 Ca^{2+} imaging. 18-24 h after transfection with GCaMP3-ML1, CHO or human fibroblast cells were trypsinized and plated onto glass coverslips. Most experiments were carried out within 0.5-3 h after plating when cells still exhibited a round morphology. The fluorescence intensity at 470 nm (F_{470}) was monitored using the EasyRatioPro system. Lysosomal Ca^{2+} release was measured under a "low" external Ca^{2+} solution, which contained 145mM NaCl, 5 mM KCl, 3 mM $MgCl_2$, 10 mM Glucose, 1mM EGTA, and 20 mM HEPES (pH7.4). Ca^{2+} concentration in the nominally-free Ca^{2+} solution is estimated to be 1-10 μM. With 1 mM EGTA, the free Ca^{2+} concentration is estimated to be < 10 nM based on the Maxchelator software (http://maxchelator.stanford.edu/).

LacCer-BODIPY trafficking. Cells for the Lactosylceramide (LacCer)-BODIPY uptake experiment were grown on glass coverslips and incubated with 5 µM BSA-complexed LacCer in "Tyrode" solution for 45 min at room temperature. Cells were then washed twice with PBS and incubated with normal DMEM/F12 medium containing 10% FBS at 37 °C for 1h. For the correction experiments, NPC1$^{-/-}$ macrophages were pre-treated with ML-SA1 (10 µM) for 12 hrs, and chased in the presence of ML-SA1 (10 µM). Images were taken using a Leica (TCS SP5) confocal microscope.

Filipin Staining. Cells were fixed in 3% paraformaldehyde for 1 h, washed twice with PBS, and then incubated with 1.5 mg/ml glycine in PBS for 10 min. Cells were then stained for 2 h with 0.05 mg/ml filipin (Lloyd-Evans, Morgan et al. 2008) in PBS supplemented with 10% FBS. All procedures were conducted at room temperature. Images were taken using a fluorescence microscope with a UV filter. The lysosome-like storage organelle filipin intensity was calculated based on low- and high-threshold intensities in the image (Devlin, Pipalia et al. 2010).

Lysenin Staining. Cells were fixed with 4% PFA for 20 min, blocked with 1% BSA in PBST for 2h, and then incubated with lysenin (0.1 µg/ml, Peptides International) for 20 h at 4 ˚C. The cells were then incubated with anti-lysenin antibody (Peptides International) for 1h, followed by Alexa Fluor 488 anti-rabbit (Invitrogen) for 45 min. Images were taken using a Leica confocal microscope.

Reagents. Sphingomyelins (Sigma) were dissolved in "Tyrode" or "Low pH Tyrode" solutions by sonication. Beta-cyclodextrin, filipin, and fluoxetine were obtained from Sigma; desipramine was purchased from Santa Cruz; C6-ceramide was obtained from Matreya, LLC; sphingomyelinase was obtained from MP Biomedicals; SF-51 and ML-SA1 were purchased from Princeton BioMolecular Research Inc; PI(3,5)P$_2$ was purchased from Echelon; U18666A was purchased from Enzo; LacCer-BODIPY was purchased from Invitrogen, and lysenin and anti-lysenin antibody were purchased from Peptides International.

Data analysis. Data are presented as the mean ± standard error of the mean (SEM). Statistical comparisons were made using analysis of variance (ANOVA). A *P* value < 0.05 was considered statistically significant.

Results

Reduced TRPML1-mediated lysosomal Ca^{2+} release in NPC cells

Whether TRPML1-mediated lysosomal Ca^{2+} release is altered in NP cells was first investigated. I chose an easy-to-transfect NPC cellular model, i.e, NPC (NPC1$^{-/-}$) CHO cells, which exhibit all the hallmark features of NPC disease (Cadigan, Spillane et al. 1990; Cruz, Sugii et al. 2000). WT CHO cells transfected with GCaMP3-ML1 exhibited large TRPML1-mediated lysosomal Ca^{2+} release (**Fig. 4.1a, c**). In contrast, NPC CHO cells exhibited much smaller TRPML1-mediated Ca^{2+} release with a ~ 75% reduction compared to WT controls (**Fig 4.1b, c**). GCaMP3-ML1 was still mainly co-localized with Lamp-1 in NPC cells (**Fig 4.2a**). In addition, the expression levels of GCaMP3-ML1, as estimated from the maximal fluorescence intensity induced by ionomycin, were comparable for WT and NPC cells (**Fig 4.2b**). A previous study reported that lysosomal Ca^{2+} stores are compromised in NPC cells (Lloyd-Evans, Morgan et al. 2008). However, we found that GPN- (a cell-permeable cathepsin C peptide substrate that, when cleaved, causes osmotic lysis of lysosomes) induced GCaMP3-ML1 increases were comparable for WT and NPC cells (**Fig 4.3a**). Likewise, GPN-induced and NH$_4$Cl-induced Fura-2 responses were also comparable in non-transfected WT and NPC cells (**Fig 4.3b, 4.4a**). Furthermore, TRPML1-mediated, but not GPN-induced lysosomal Ca^{2+} release, was also reduced in GCaMP3-transfected NPC human fibroblasts compared to WT cells (**Fig 4.4b**). Collectively, these results suggest that TRPML1-mediated lysosomal Ca^{2+} release is selectively reduced in NPC cells.

NPC-like cellular phenotypes can be pharmacologically induced with a small-molecule drug U18666A (Liscum and Faust 1989). After incubating GCaMP3-ML1-transfected WT CHO cells with

U18666A (2 μg/ml) for 16-20 h, cells exhibited significant increases in cholesterol level as detected by filipin staining (Rosenbaum and Maxfield 2011) (**Fig 4.5a**), and sphingomyelin (SM) level as detected by lysenin staining (**Fig 4.5b**). U18666A-treated cells exhibited a ~ 70% reduction in TRPML1-mediated lysosomal Ca^{2+} release (**Fig 4.6a, b**). Conversely, drug treatment failed to result in noticeable changes in GPN-induced GCaMP3 responses (**Fig 4.3a**) or Fura-2 Ca^{2+} responses (**Fig 4.3b**). Taken together, these results suggest a specific reduction of TRPML1-mediated lysosomal Ca^{2+} release in pharmacologically-induced NPC cells.

We next investigated the effect of NPC on endogenous Ca^{2+} release using Fura-2 Ca^{2+} imaging. In WT CHO cells, small but significant Ca^{2+} increases were seen upon application of 100 μM ML-SA1 in low external Ca^{2+} (ΔFura-2 = 0.08 ± 0.01, n = 89; **Fig 4.7d, f**). In contrast, in NPC CHO cells, ML-SA1 failed to induce significant Ca^{2+} responses (ΔFura-2 = 0.01 ± 0.002, n = 61; **Fig 4.7e,f**). Cyclodextrin, a polysaccharide that reportedly alleviates NPC cellular phenotypes (Rosenbaum and Maxfield 2011), was found to partially restore ML-SA1-induced lysosomal Ca^{2+} release (**Fig 4.8**). Finally, NPC1^{-/-} mouse macrophages, one of the major cell types affected in NPC (Schuchman 2010), also exhibited a significant reduction in ML-SA1-induced lysosomal Ca^{2+} release compared to WT cells (**Fig 4.7a,b, f**). The ML-SA1-induced lysosomal Ca^{2+} responses are most likely mediated by TRPML1, as demonstrated by the lack of response in ML1^{-/-} macrophages (**Fig 4.7c, f**). Collectively, the reduction in TRPML1-mediated lysosomal Ca^{2+} release may be a general feature of most NPC cell types.

Reduced TRPML1-mediated currents in NPC cell lysosomes

We next investigated the effect of NPC on whole-endolysosome I_{ML1} in human fibroblasts. Compared to WT fibroblasts (**Fig 4.9a, c**), much smaller ML-SA1-activated I_{ML1} was seen in NPC fibroblasts at three different concentrations of ML-SA1 (**Fig 4.9b, c**). On average, whole-endolysosome I_{ML1} activated by 25 μM ML-SA1 was 75 ± 25 (n = 8) pA/pF for NPC cells, a ~ 70% reduction from the values observed for WT cells (442 ± 150 pA/pF; n = 6). Notably, the mRNA expression levels of *TRPML1-3* were not decreased in NPC cells (**Fig 4.10**). These results suggest that a reduction of

whole-endolysosome I_{ML1} accounts for the reduced TRPML1-mediated Ca^{2+} release observed in NPC cells.

Inhibition of TRPML1 by SMs

The reduced TRPML1-mediated lysosomal Ca^{2+} release and I_{ML1} in the presence of normal *TRPML1* expression in NPC cells suggest tonic inhibition of TRPML1 by cytoplasmic and/or luminal factors. One possibility is that lipids accumulated in NPC lysosomes, such as cholesterol, SM, sphingosine (Sph), and glycosphingolipids (GSLs) (Lloyd-Evans and Platt 2010; Rosenbaum and Maxfield 2011), might directly inhibit TRPML1. To test this possibility, we performed whole-cell recordings in ML1-4A-expressing HEK293T cells. Under this configuration, the extracellular side is analogous to the luminal side (see **Fig 4.11**), making it possible to study the effects of luminal lipids on I_{ML1-4A}. SMs, but not cholesterol or GSLs (data not shown), acutely inhibited SF-51- (**Fig 4.12a, d**) or ML-SA1-activated I_{ML1-4A}. In contrast, SMs failed to inhibit $I_{ML1- Va}$, a gain-of-function mutation that locks TRPML1 in the open state (Cheng, Shen et al. 2010) (**Fig 4.12b, d**). SMs can be hydrolyzed into ceramide and phosphocholine via SMase. No significant inhibition was seen with ceramide (**Fig. 12c, d**) or phosphocholine (**Fig 4.12d**). Sphingosine, a hydrolyzed product of ceramide, potentiated I_{ML1-4A} (**Fig 4.12e**).

The robust inhibition of I_{ML1-4A} by SMs, but not ceramide or phosphocholine, suggests that the activity of SMase may regulate I_{ML1-4A}. Indeed, bath application of SMases, but not heat-inactivated enzymes, significantly potentiated SF-51-activated I_{ML1-4A} (**Fig 4.13a-f**), with the potentiation being more dramatic at acidic extracellular (luminal) pH than at neutral pH (**Fig 4.13f**).

SM accumulation reduces TRPML1-mediated Ca^{2+} release

The results presented above suggest that SM-mediated inhibition underlies NPC-mediated reduction in TRPML1-mediated lysosomal Ca^{2+} release. Consistent with this, in fibroblasts derived from NPA patients, which completely lack the activity of acid SMase (Schuchman 2010), TRPML1-mediated , but not GPN-induced lysosomal Ca^{2+} release (**Fig 4.14a-c**), was significantly reduced. To further test

this hypothesis, we induced lysosomal SM accumulation by incubating cells with desipramine and fluoxetine for 2-4 hrs, which cause proteolytic degradation of acid SMase (Hurwitz, Ferlinz et al. 1994; Kornhuber, Tripal et al. 2008). Compared to non-treated cells, TRPML1-mediated lysosomal Ca^{2+} release was dramatically reduced in desipramine/fluoxetine -treated CHO cells, and the reduction was abolished in the presence of a protease inhibitor leupeptin (Hurwitz, Ferlinz et al. 1994; Kornhuber, Tripal et al. 2008) (**Fig 4.15a-d**). Taken together, these results suggest that SM inhibition of TRPML1 underlies NPA or NPC-mediated attenuation of TRPML1-mediated lysosomal Ca^{2+} release.

TRPML1 regulates lysosomal lipid and cholesterol trafficking

Human NPC, NPA, and NPB fibroblasts exhibit defects in LEL-to-Golgi trafficking of lipids and proteins (Puri, Watanabe et al. 1999; Cruz, Sugii et al. 2000). Consistent with this, BODIPY-LacCer, a fluorescent analogue of lactosylceramide that is localized in the Golgi apparatus of WT cells after a pulse-chase period (Pagano and Chen 1998), was predominantly localized in the LEL-like compartments of NPC1^{-/-} mouse macrophages (**Fig 4.16a**). Because of the established roles of $PI(3,5)P_2$/TRPML1/Ca^{2+} in LEL-to-Golgi lipid trafficking (Shen, Wang et al. 2011), it is possible that the trafficking defects seen in NP cells are due to the aforementioned attenuated TRPML1-mediated lysosomal Ca^{2+} release. If so, one would expect that boosting TRPML1 activity may correct the trafficking defects. Indeed, more than 60% of ML-SA1-treated NPC macrophages exhibited a Golgi-like pattern of LacCer staining, suggestive of a significant restoration in LEL-to-Golgi transport (**Fig 4.16a**). In NPC1^{-/-} mouse macrophages and TRPML1-transfected NPC CHO cells, the puncta number of LacCer staining that reflects the function of LEL-to-Golgi transport, was significantly reduced in the presence of ML-SA1 (**Fig 4.16b-d**). Collectively, these results suggest that increasing TRPML1's channel activity may restore the trafficking defects in NPC cells, and that TRPML1 deregulation is a pathogenic mechanism underlying lipid trafficking defects in NP cells.

NPC cells accumulate cholesterol, as demonstrated by elevated filipin staining (Lloyd-Evans, Morgan et al. 2008). However, in U18666A-treated CHO cells, ML-SA1 induced a significant

reduction in filipin staining in TRPML1, but not TRPML1-KK-transfected cells (**Fig 4.17a, b**). Reduction of filipin staining was also seen in aSMase- (**Fig 4.17c, d**) and TRPML1^{Va}- transfected NPC CHO cells (**Fig 4.17e, f**). These results suggest that increased TRPML1 activity may reduce cholesterol accumulation in NPC cells.

Discussion

We used a lysosome-targeted GCaMP3-based Ca^{2+} imaging method to demonstrate that TRPML1-mediated lysosomal Ca^{2+} release, but not the lysosomal Ca^{2+} store as has been previously reported (Lloyd-Evans, Morgan et al. 2008), is selectively compromised in NPC and NPA cells. SM, a sphingolipid that is known to accumulate in all three types of NP cells (Rosenbaum and Maxfield 2011), inhibits TRPML1. Pharmacologically-induced SM accumulation significantly reduces TRPML1-mediated lysosomal Ca^{2+} release. Conversely, increasing TRPML1's expression/activity is sufficient to correct the trafficking defects and reduce cholesterol accumulation in NPC cells. Collectively, our work has provided a feedback mechanism for luminal lipids to control lipid efflux from the lysosome, as well as a pathogenic cause for the secondary lysosome storage present in many LSDs.

Sphingomyelin is the first negative regulator for TRPML1 that has been identified so far. In normal cells, SMs in the late endosome/lysosome would be rapidly degraded by acid SMase activity (Kolter and Sandhoff 2010). However, in NP type A and B cells, due to the defective aSMase enzyme activity, SMs accumulate in the lumen and limited lysosomal membranes (**Fig 4.11**). In NP type C cells, although the primary storage is likely to be cholesterol, they are found to have a much lower level of aSMase activity, which also leads to SMs accumulation. A restoration of aSMase activity has been reported to be able to revert cholesterol accumulation (Devlin, Pipalia et al. 2010). It is not known whether the level of SM is perturbed in other sphingodoses. However, rather than absolute SM levels, the relative localization (plasma membrane versus lysosome) is the critical factor for lysosomal

Ca^{2+} release. Although TRPML1 is the dominant lysosomal TRPML channel in most cell types, in other cell types where TRPML2 and TRPML3 are more abundantly expressed (Cheng, Shen et al. 2010), our proposed SM-mediated inhibitory mechanism may also be applied to TRPML2/3, causing lysosomal trafficking defects. Finally, SM and cholesterol accumulation might also contribute to NP phenotypes via mechanisms unrelated to lysosomal trafficking and TRPMLs (Schuchman 2010).

LEL-to-Golgi trafficking defects are seen in $PI(3,5)P_2$-deficient cells (Zhang, Zolov et al. 2007), ML4 fibroblasts (Chen, Bach et al. 1998; Shen, Wang et al. 2011), and NP fibroblasts, as well as fibroblasts from several other sphingolipid LSDs (Chen, Patterson et al. 1999; Puri, Watanabe et al. 1999). Our results suggest that reduced TRPML1-mediated lysosomal Ca^{2+} release directly causes trafficking defects, and boosting TRPML1 activity by a small molecular activator can largely rescue the trafficking defects. The compromised TRPML1 activity is likely to slow down the trafficking process, but not totally block the trafficking. Indeed, while most NPC-/- macrophage cells exhibit a puncta pattern of LacCer staining after 1 hour chasing (when most WT macrophage cells have a Golgi-like pattern), 4 hours later, 30%-40% of NPC-/- macrophage cells start to exhibit a Golgi-like pattern of LacCer (data not shown). Future studies will need to include more chasing timelines for lacCer staining in order to fully explore the effect of TRPML1 activity on LEL-to-Golgi trafficking.

For most LSDs, impaired lysosomal degradation due to a lack of hydrolytic enzymes leads to trafficking defects and lysosome storage. On the other hand, lysosome storage can further affect lysosomal degradation and membrane trafficking, which results in a positive feedback loop and a vicious cycle (Parkinson-Lawrence, Shandala et al. 2010). We previously reported that impaired Fe^{2+} homeostasis facilitates the formation of autofluorescent lipofuscin in ML4 cells (Dong, Cheng et al. 2008). Interestingly, lipofuscin formation is also increased in NPC cells (**Fig 4.18**). Although there is no study of TRPML1 activity in other LSDs, the impaired Ca^{2+} release we observed in NP cells might be a common pathogenic mechanism for many LSDs. Our work suggests a novel concept that lysosome enhancement by the manipulation of TRPML1 to speed membrane trafficking may break the vicious cycle, providing a novel therapeutic approach for NPs and many other LSDs.
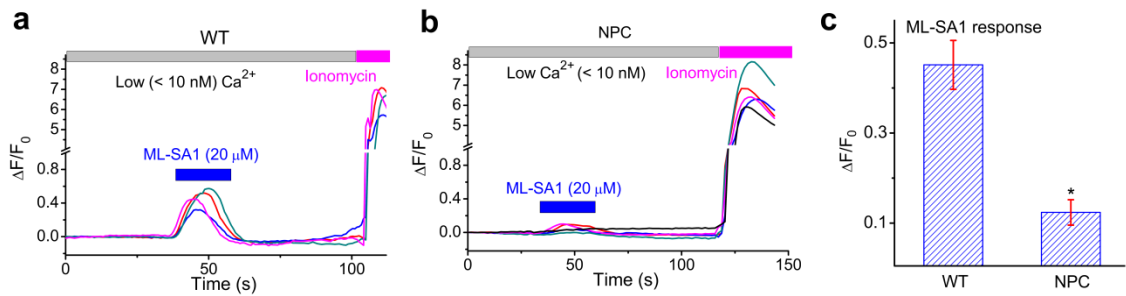
Figure 4.1. TRPML1-mediated lysosomal Ca^{2+} release is reduced in NPC cells. (a, b) ML-SA1-induced lysosomal Ca^{2+} release in GCaMP3-ML1-transfected WT (a) and NPC (b) CHO cells. (c) ML-SA1-induced peak GCaMP3 responses were reduced in GCaMP3-ML1-transfected NPC cells. The results were averaged for 40-100 cells from at least 3 independent experiments; data are presented as the mean ± SEM. Statistical comparisons were made using analysis of variance: * P <0.05.
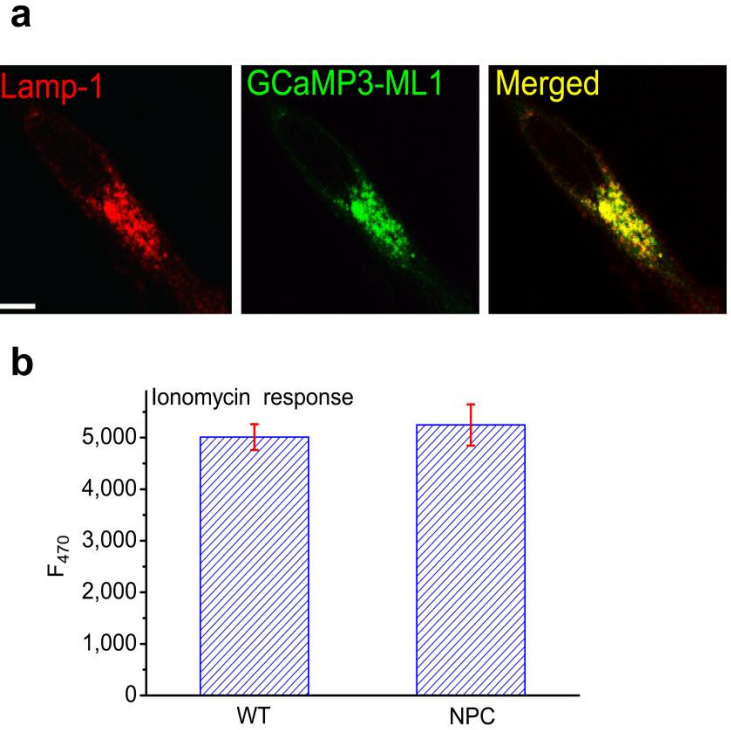
Figure 4.2. Reduced Ca^{2+} response in NPC-/- CHO cells is not due to the localization or expression level changes of GCaMP3-ML1. a) Co-localization of GCaMP3-ML1 fluorescence with Lamp-1 in NPC CHO cells doubly-transfected with GCaMP3-ML1 and Lamp-1-mCherry. Scale bar = 5 μm. (b) Comparable expression levels of GCaMP3-ML1 in WT and NPC CHO cells. Expression level of GCaMP3-ML1 was estimated by the maximal GCaMP3 fluorescence signal induced by ionomycin (1 μM). (Fig 4.2b was prepared by Xinran Li)
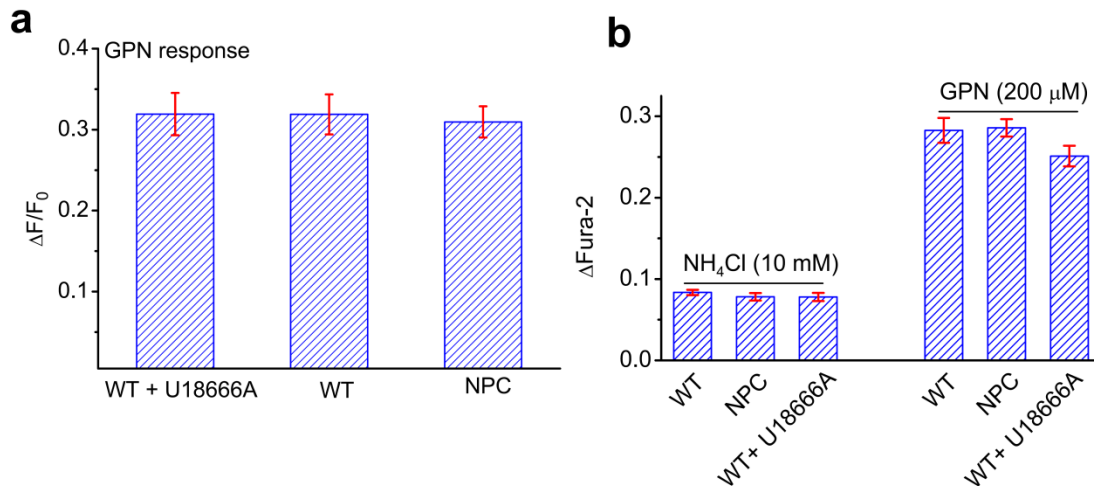
Figure 4.3. Reduced Ca^{2+} response in NPC-/- CHO cells is not due to reduced lysosome Ca^{2+} store. (a) Comparable GPN-induced GCaMP3 responses in WT, NPC, or U18666A-treated GCaMP3-ML1-transfected CHO cells. (b) NH$_4$Cl (10 mM) and GPN (200 µM) induced comparable levels of Ca^{2+} increases (measured with Fura-2 ratios) in WT, NPC, and U18666A-treated CHO cells. The results were averaged for 40-100 cells from at least 3 independent experiments; data are presented as the mean ± SEM. Statistical comparisons were made using analysis of variance: * P <0.05.
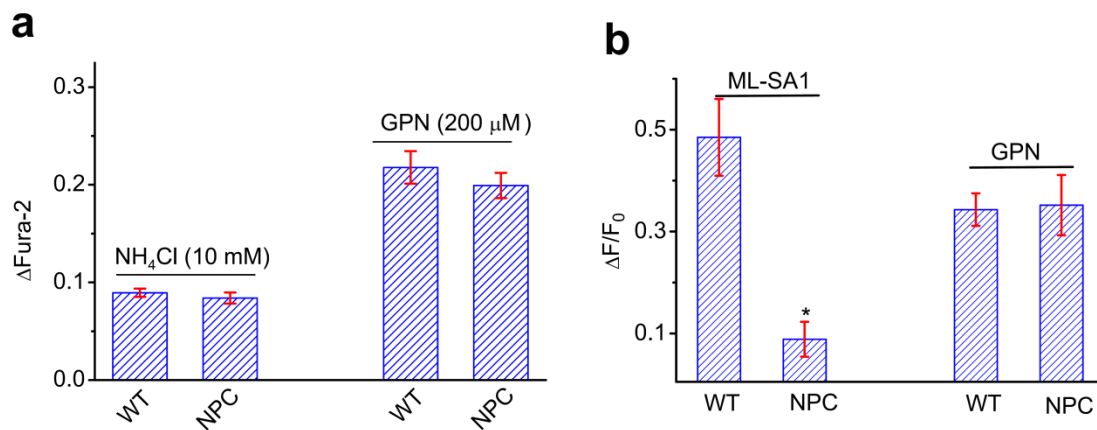
Figure 4.4. TRPML1-mediated lysosomal Ca^{2+} release, not lysosomal Ca^{2+} store, is reduced in NPC cells. (a) NH$_4$Cl (10 mM) and GPN (200 µM) induced comparable levels of Fura-2 Ca^{2+} responses in WT and NPC human fibroblasts. (b) TRPML1-mediated, but not GPN-induced lysosomal Ca^{2+} release, was reduced in GCaMP3-ML1-transfected NPC human fibroblasts compared to WT cells. The results were averaged for 40-100 cells from at least 3 independent experiments; data are presented as the mean ± SEM. Statistical comparisons were made using analysis of variance: * P <0.05.
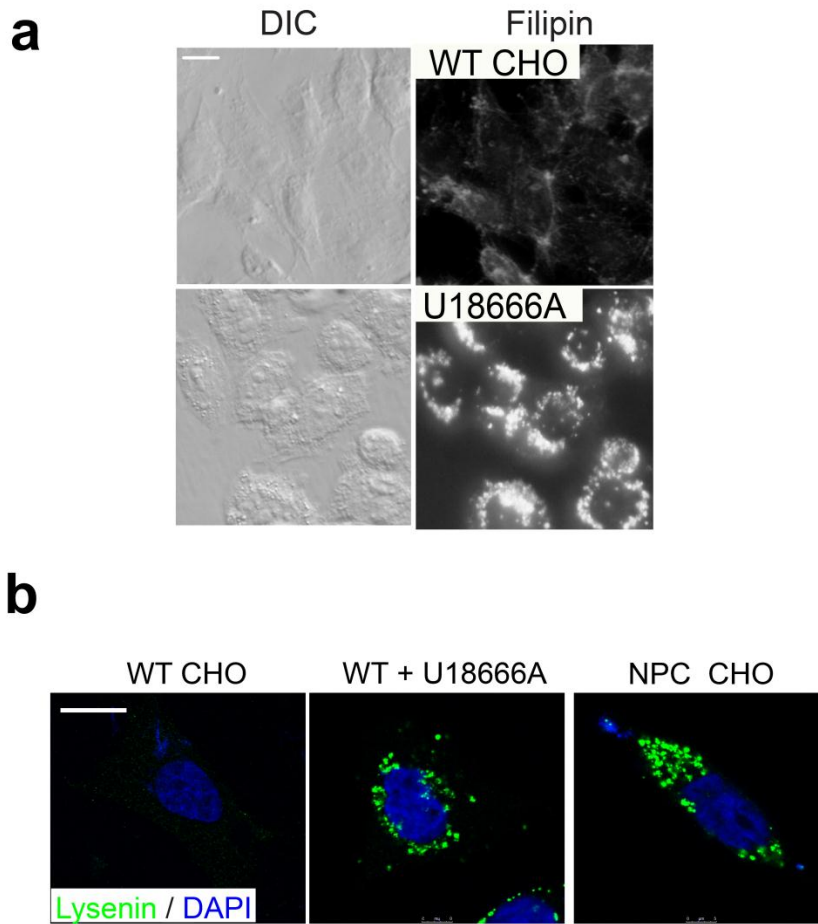
Figure 4.5. U18666A treatment induces cholesterol and sphingomyelin accumulations in WT cells. (a) WT CHO cells were treated with U18666A (2 µg/ml) for 16 h, and then subjected to filipin staining. Scale bar = 10 µm. (b) Sphingomyelins were stained with Lysenin (0.1 µg/ml) in WT CHO cells, WT CHO cells treated with U18666A (2 µg /ml) for 16 h, and NPC CHO cells. Scale bar = 10 µm. (Fig 4.5b was prepared by Xinran Li)
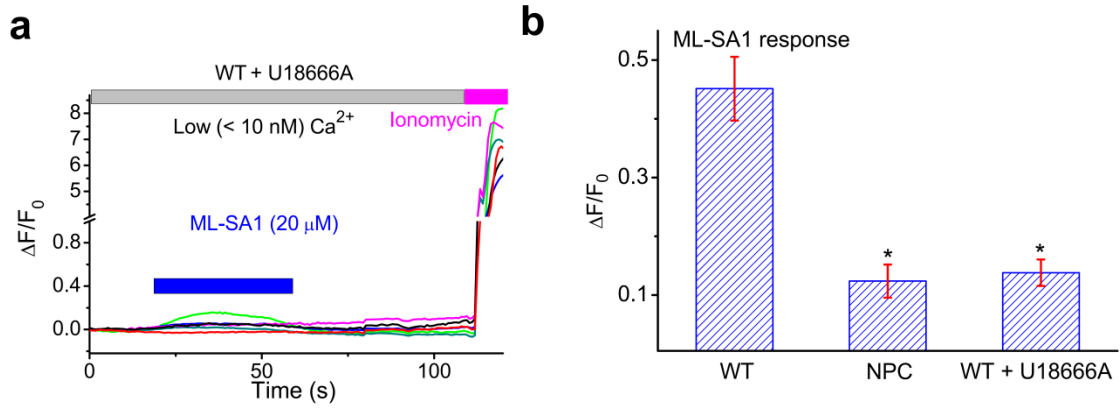
Figure 4.6. TRPML1-mediated lysosomal Ca^{2+} release is reduced in pharmacologically indued NPC-/- cells. (a) Ca^{2+} responses in GCaMP3-ML1-transfected WT CHO cells treated with U18666A (2 µg /ml) for 16-20 h. (b) ML-SA1-induced peak GCaMP3 responses were reduced in GCaMP3-ML1-transfected NPC or U18666A-treated WT CHO cells. The results were averaged for 40-100 cells from at least 3 independent experiments; data are presented as the mean ± SEM. Statistical comparisons were made using analysis of variance: * P <0.05.
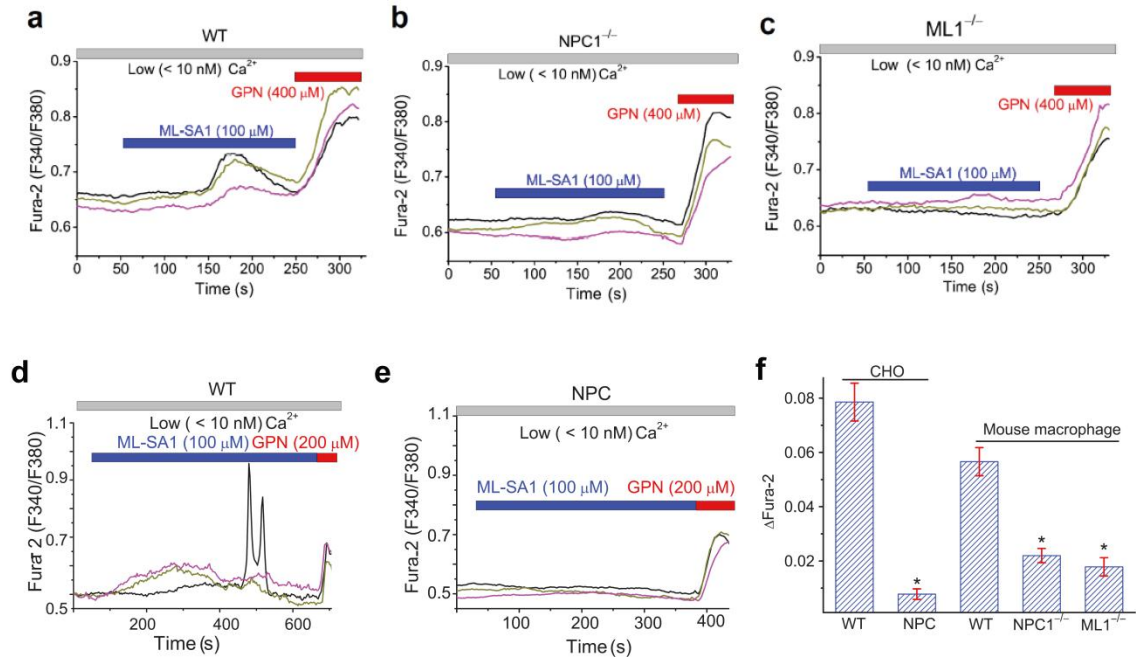
Figure 4.7. Endogenous TRPML1-mediated lysosomal Ca^{2+} release is compromised in NPC cells. (a-c). Endogenous TRPML1-mediated lysosomal Ca^{2+} release (measured with Fura-2 ratios) in WT (a), NPC1-/- (b), and ML1-/- (c) mouse macrophages. (d, e) Endogenous TRPML1-mediated lysosomal Ca^{2+} release (measured with Fura-2 ratios) in WT (d) and NPC (e) CHO cells. (f) Average endogenous ML-SA1-induced lysosomal Ca^{2+} responses in WT and NPC CHO cells, and WT, NPC1$^{-/-}$, and ML1$^{-/-}$ mouse macrophages. The results were averaged for 40-100 cells from at least 3 independent experiments; data are presented as the mean ± SEM. Statistical comparisons were made using analysis of variance: * P <0.05.
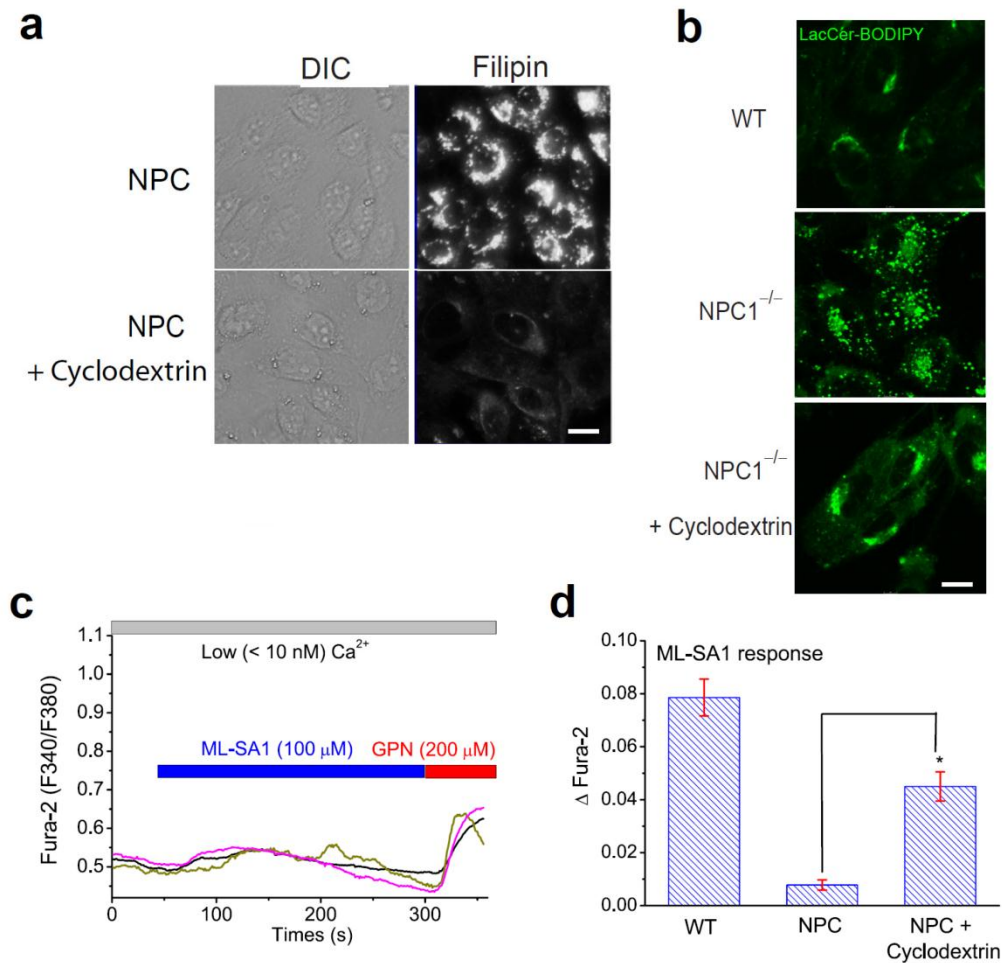
Figure 4.8. Cyclodextrin significantly reduces filipin staining and corrects trafficking defects in NPC CHO cells.
(**a**) Filipin staining in NPC CHO cells that were treated with cyclodextrin (300 μM) for 24 h. Scale bar = 10 μm. (**b**) LacCer staining in cyclodextrin-treated NPC CHO cells. Scale bar = 5 μm. (**c**) Endogenous TRPML1-mediated lysosomal Ca^{2+} release (measured with Fura-2 ratios) in NPC CHO cells that were treated with cyclodextrin (300 μM) for 24 h. (**d**) Endogenous TRPML1-mediated lysosomal Ca^{2+} release is partially restored by cyclodextrin treatment. The results were averaged for 40- 100 cells from at least 3 independent experiments; data are presented as the mean ± SEM. Statistical comparisons were made using analysis of variance: * $P < 0.05$. Results for WT and NPC cells are replotted from Fig. 6.
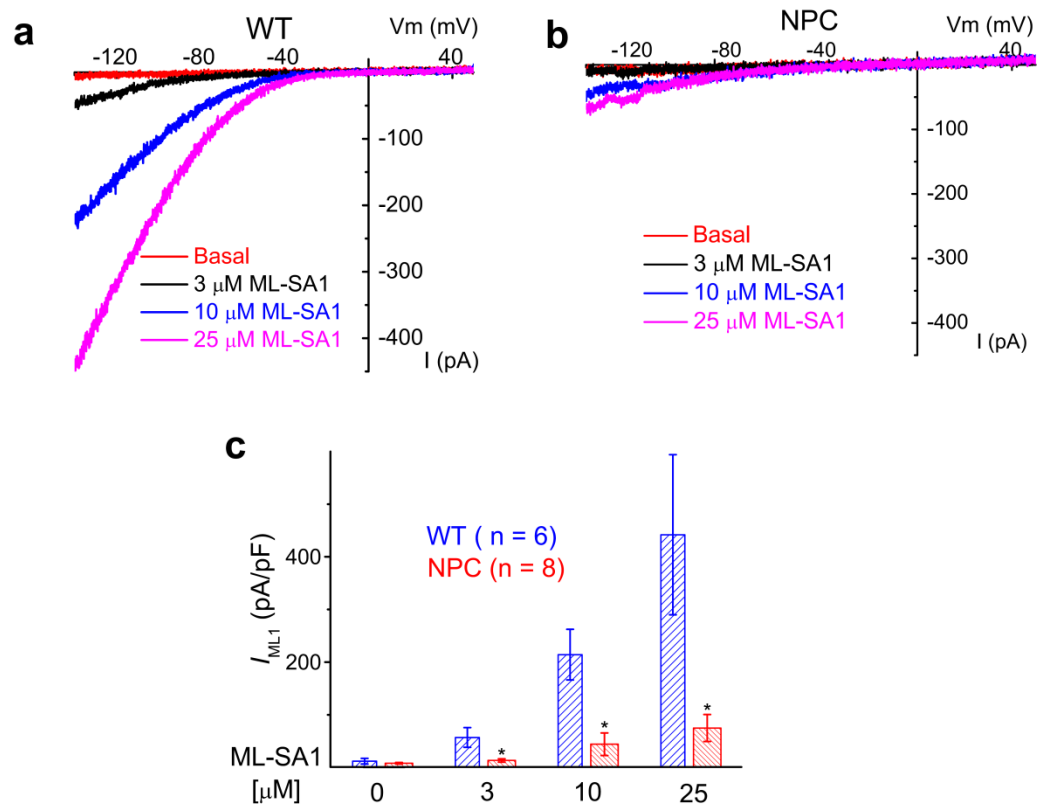
Figure 4.9. TRPML-mediated currents are reduced in the lysosomes of NPC cells.
(a, b) Concentration-dependent activation of whole-endolysosome I_{ML-L} in WT (a) and NPC (b) human fibroblasts. ML-SA1 (3, 10, 25 µM) was applied to the cytosolic sides of the vacuoles isolated from human fibroblasts. (c) Average current densities (pA/pF) of I_{ML-L} were reduced in NPC fibroblasts compared to WT cells. The current density was calculated from the current size (pA) normalized with the capacitance of the vacuole (pF). For panels c, data are presented as the mean ± SEM; the n numbers are in parentheses. Statistical comparisons were made using analysis of variance: * P <0.05. (Prepared by Xiang Wang)
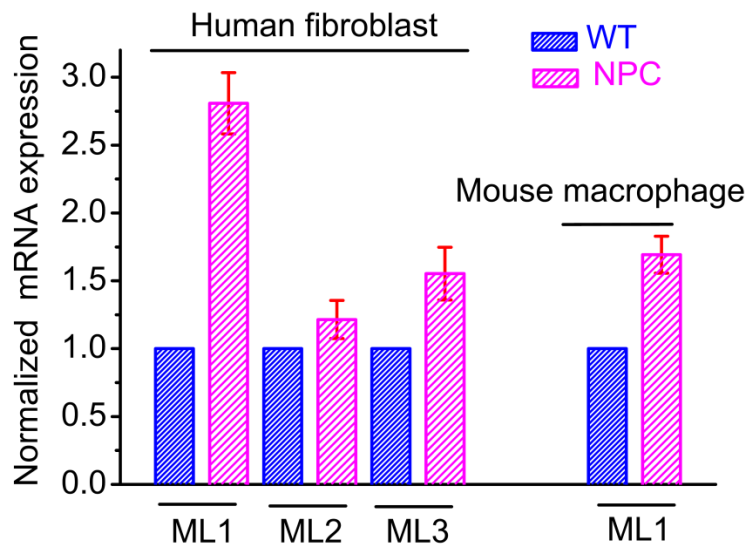
Figure 4.10. The mRNA level of TRPMLs is not reduced in NPC cells. RT-PCR analysis of *TRPML1-3* mRNA expression in WT and NPC human fibroblasts, and NPC1 $^{-/-}$ mouse macrophages. Expression levels were normalized to that of GAPDH (human fibroblast) and L32 (mouse macrophage). Data are presented as the mean ± SEM; the n numbers are in parentheses. Statistical comparisons were made using analysis of variance: * P <0.05.
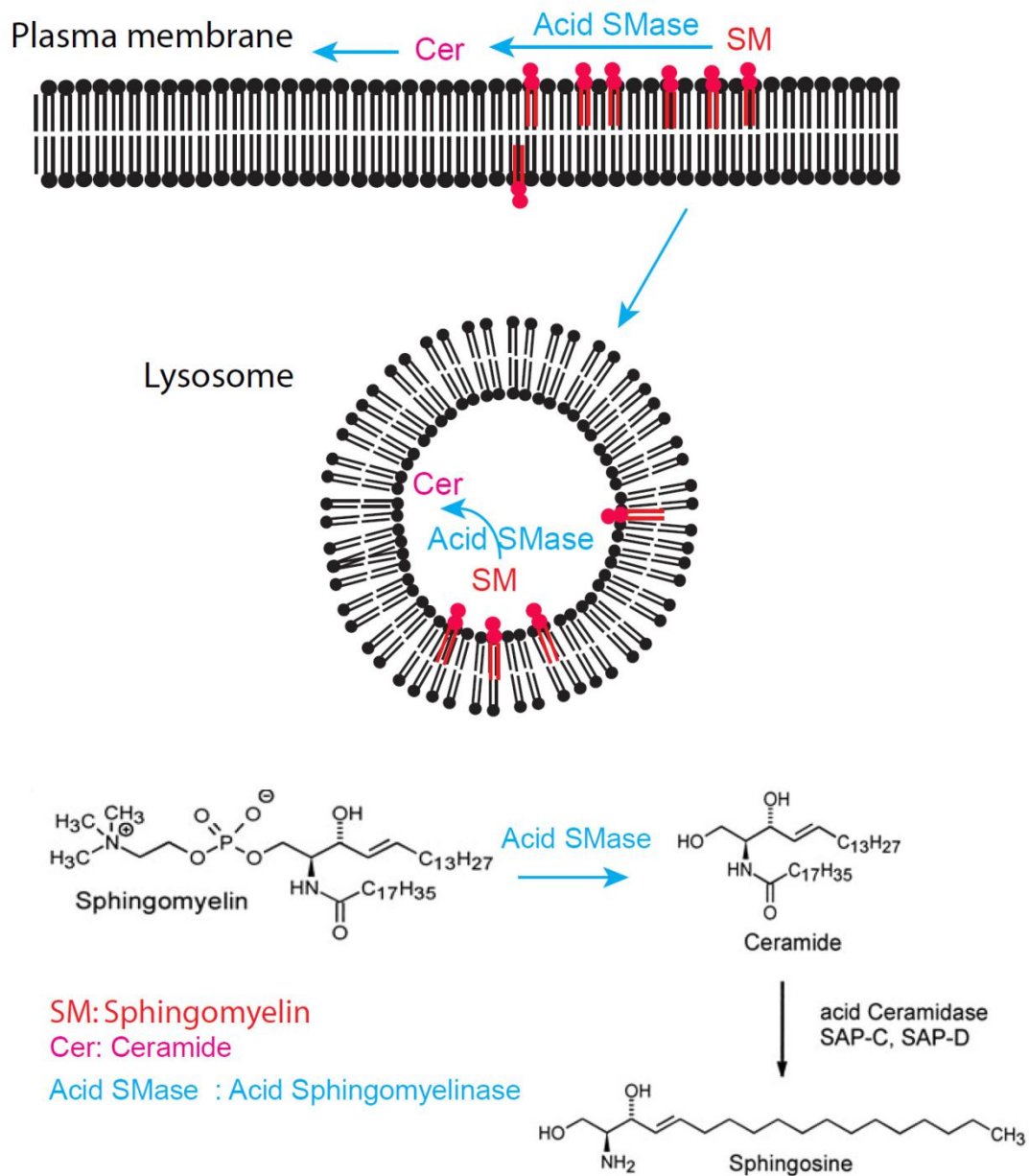
Figure 4.11. Sphingomyelin localization and turnover at the plasma membrane and in the lysosome.
At the plasma membrane, SMs are mainly localized at the outer leaflet. Upon endocytosis, SMs are localized in the luminal leaflet of limited membranes and internal vesicles. Acid SMases (aSMase) hydrolyze SMs into ceramide (Cer) and phosphocholine (PC). Ceramide can be further converted into sphingosine (Sph) via acid ceramidases. In NPs, SMs accumulate in the lysosome due to insufficient aSMase activity.
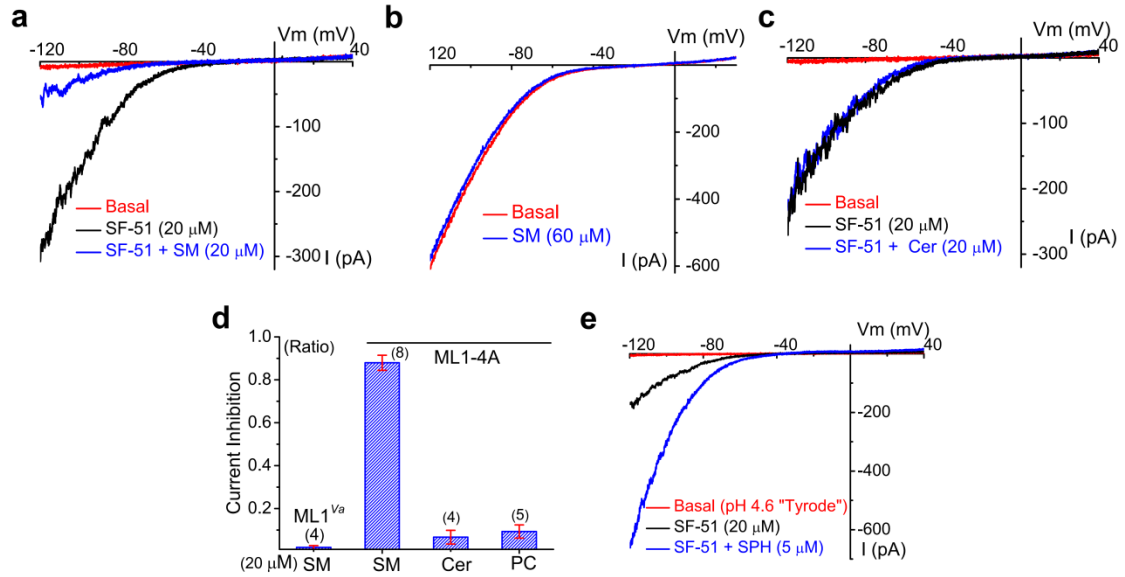
Figure 4.12. Regulation of TRPML1 by SMs.

(a) SF-51-activated whole-cell I_{ML1-4A} was inhibited by sphingomyelins (SMs; 20 µM) at low extracellular pH in ML1-4A-expressing HEK293T cells. (b) Insensitivity of whole-cell I_{ML1-Va} to SMs (60 µM). (c) Lack of effect of ceramide (Cer, 20 µM) on whole-cell I_{ML1-4A}. (d) Summary of the effects of various sphingolipids on whole-cell I_{ML1-4A} in ML1-4A-expressing HEK293T cells. PC: phosphocholine. (e) SF-51-activated whole-cell I_{ML1-4A} was potentiated by sphingosine (Sph; 5 µM) at low external pH in ML1-4A-expressing HEK293T cells. For panels d, data are presented as the mean ± SEM; the n numbers are in parentheses. Statistical comparisons were made using analysis of variance: * P <0.05.
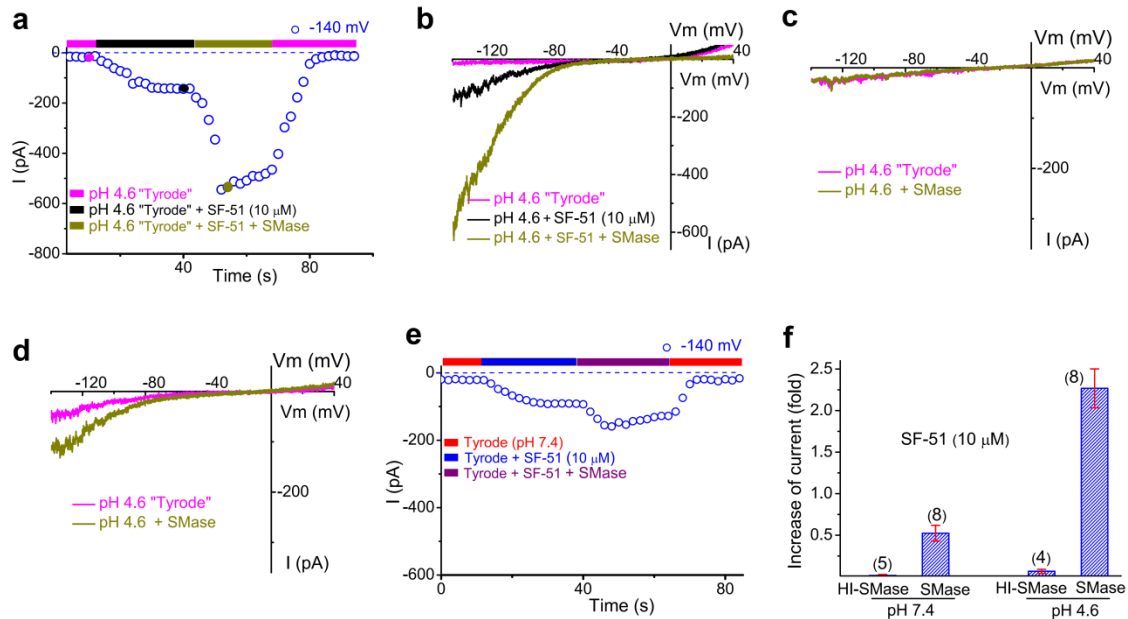
Figure 4.13. Regulation of TRPML1 by sphingomyelinase.
(a) The effects of SMase (50 ng/ml) treatment on I_{ML1-4A} at low external pH. I_{ML1-4A} was elicited by repeated voltage ramps ($-$ 140 to $+$ 140 mV; 400 ms) with a 4-s interval between ramps. Current amplitudes at -140 mV were used to plot the time dependence. **(b)** Representative traces of I_{ML1-4A} before (black) and after (dark yellow) SMase treatment at two different time points, as shown in **f**. (**c, d**) SMase (50 ng/ml) treatment alone had no (6 out of 7 cells; see **c** for an example) or small (1 out of 7 cells; **d**) activation effect on basal whole-cell I_{ML1-4A} in ML1-4A-expressing HEK293T cells. **(e)** The effects of SMase (50 ng/ml) treatment on SF-51-activated I_{ML1-4A} at neutral external pH (pH 7.4). **(f)** The potentiation effect of SMase was more dramatic at pH 4.6, but abolished by heat inactivation of the enzyme activity. HI-SMase: heat-inactivated SMase. For panels **f**, data are presented as the mean $\pm$ SEM; the n numbers are in parentheses. Statistical comparisons were made using analysis of variance: * P <0.05.
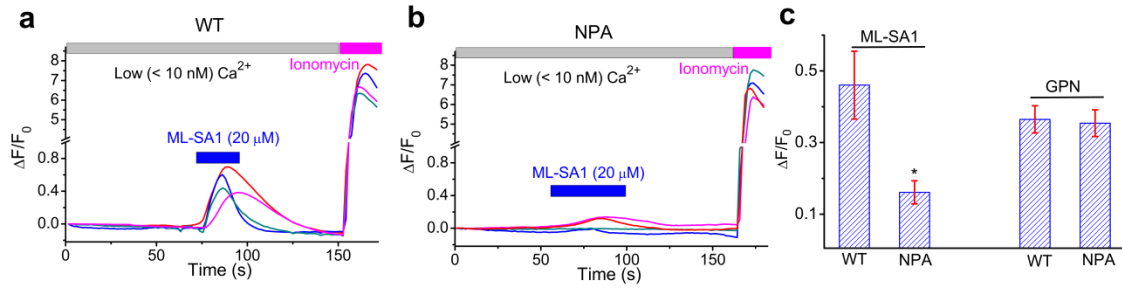
Figure 4.14. NPA fibroblasts have reduced TRPML1-mediated Ca^{2+} release.
(a,b) ML-SA1-induced lysosomal Ca^{2+} release was reduced in GCaMP3-ML1-transfected NPA fibroblasts (b) compared to WT fibroblasts (a). (c) Average ML-SA1 (20 µM) and GPN (200 µM)-induced responses in GCaMP3-ML1-transfected WT and NPA fibroblasts. For panels c, the results were averaged for 40-100 cells from at least 3 independent experiments; data are presented as the mean ± SEM. Statistical comparisons were made using analysis of variance: * P <0.05.
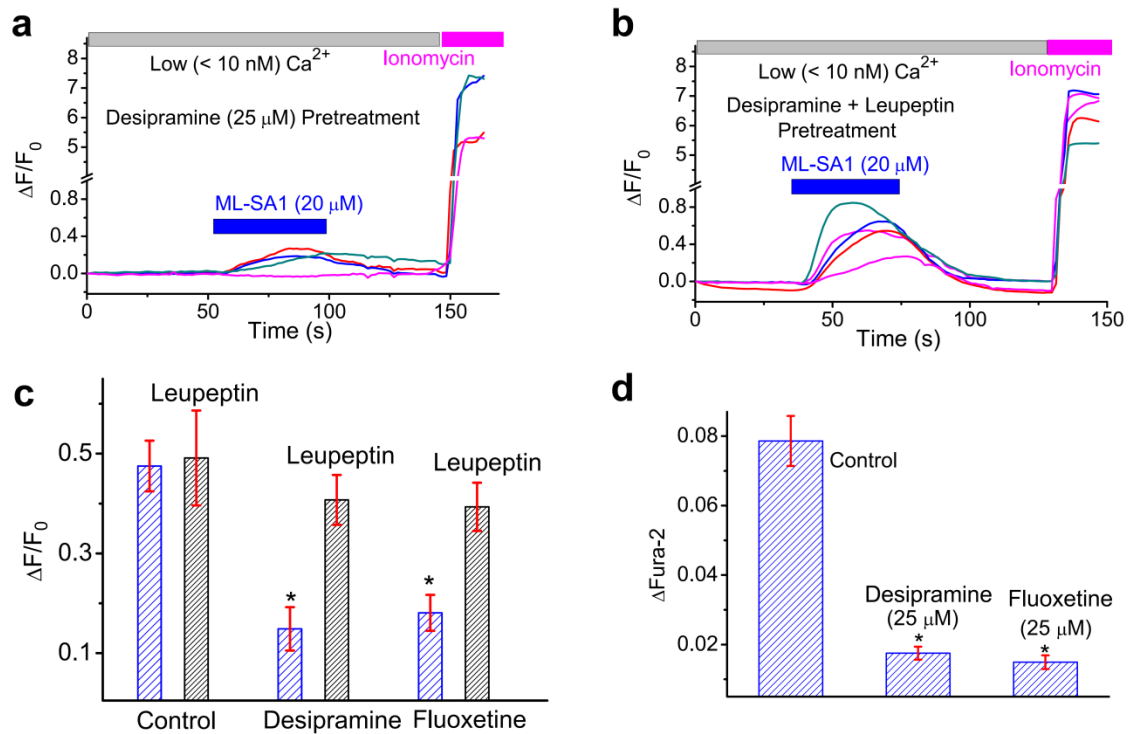
Figure 4.15. Phamacutically inducing SM accumulation in lysosomes reduces TRPML1-mediated Ca^{2+} release. a) Desipramine (25 μM) treatment for 2-4 hrs reduced TRPML1-mediated lysosomal Ca^{2+} release responses (20 μM ML-SA1) in GCaMP3-ML1-transfected CHO cells. (**b**) Pretreatment of a protease inhibitor Leupeptin (25 μM) abolished the effects of Desipramine in ML-SA1-induced GCaMP3 responses. (**c**) Summary of the effects of Desipramine (25 μM) and Fluoxetine (25 μM) treatment for 2-4 hrs on TRPML1-mediated lysosomal Ca^{2+} release responses (20 μM ML-SA1) in GCaMP3-ML1-transfected CHO cells. (**d**) Desipramine and fluoxetine treatment for 2-4 hrs reduced endogenous lysosomal Ca^{2+} release responses (measured with Fura-2 ratios; 100 μM ML-SA1) in CHO cells. For panels **c**, **d**, the results were averaged for 40-100 cells from at least 3 independent experiments; data are presented as the mean ± SEM. Statistical comparisons were made using analysis of variance: * P <0.05.
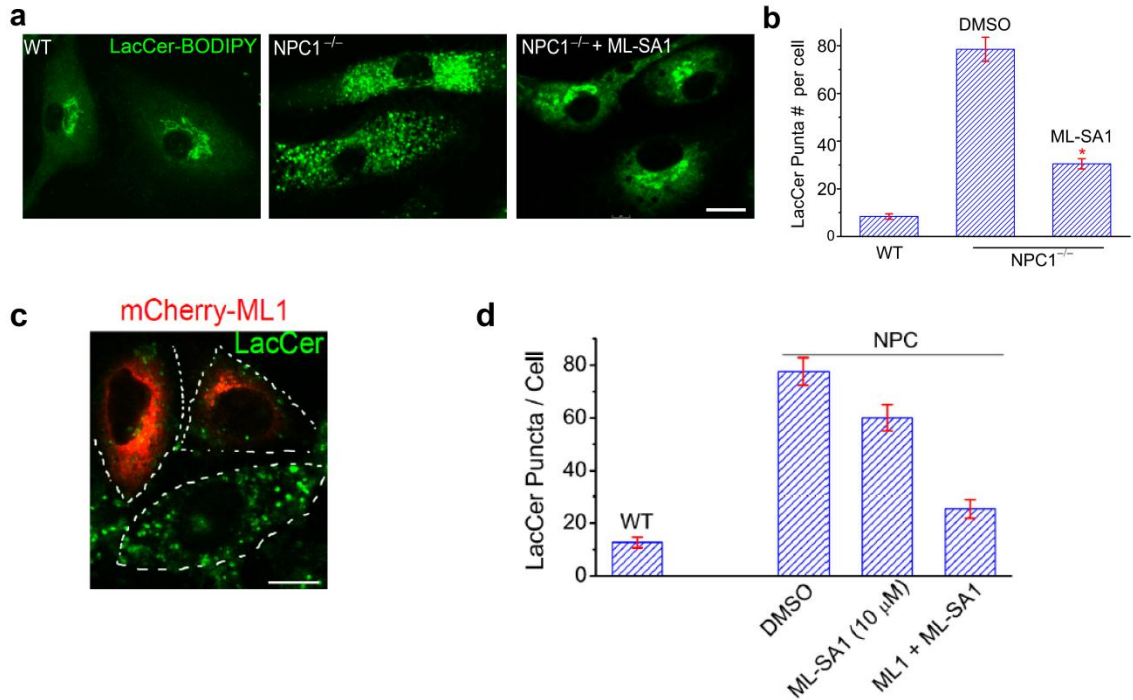
Figure 4.16. ML-SA1 together with TRPML1 overexpression rescues the trafficking defects in NPC cells.

(a) A fluorescent analogue of lactosylceramide, BODIPY-LacCer, was mainly localized in the Golgi-like structures of WT macrophages after a pulse-chase for 1 h, but accumulated in the LEL-like vesicles of NPC macrophages. ML-SA1 (10 μM) treatment of NPC1$^{-/-}$ macrophages for 12 h resulted in a primary Golgi-like localization for LacCer. Scale bar = 10 μm. (b) ML-SA1 reduced the number of LacCer puncta in NPC1$^{-/-}$ macrophages. (c) NPC CHO cells were transfected with TRPML1-mCherry, treated with ML-SA1 (10 μM) for 24 h and stained with LacCer. Scale bar = 5 μm. (d) Number of LacCer puncta in WT and NPC cells that were treated with ML-SA1. For panels b, d, the results were averaged for multiple randomly-taken micrographs from at least 3 independent experiments. Data are presented as the mean ± SEM. Statistical comparisons were made using analysis of variance: * P <0.05.
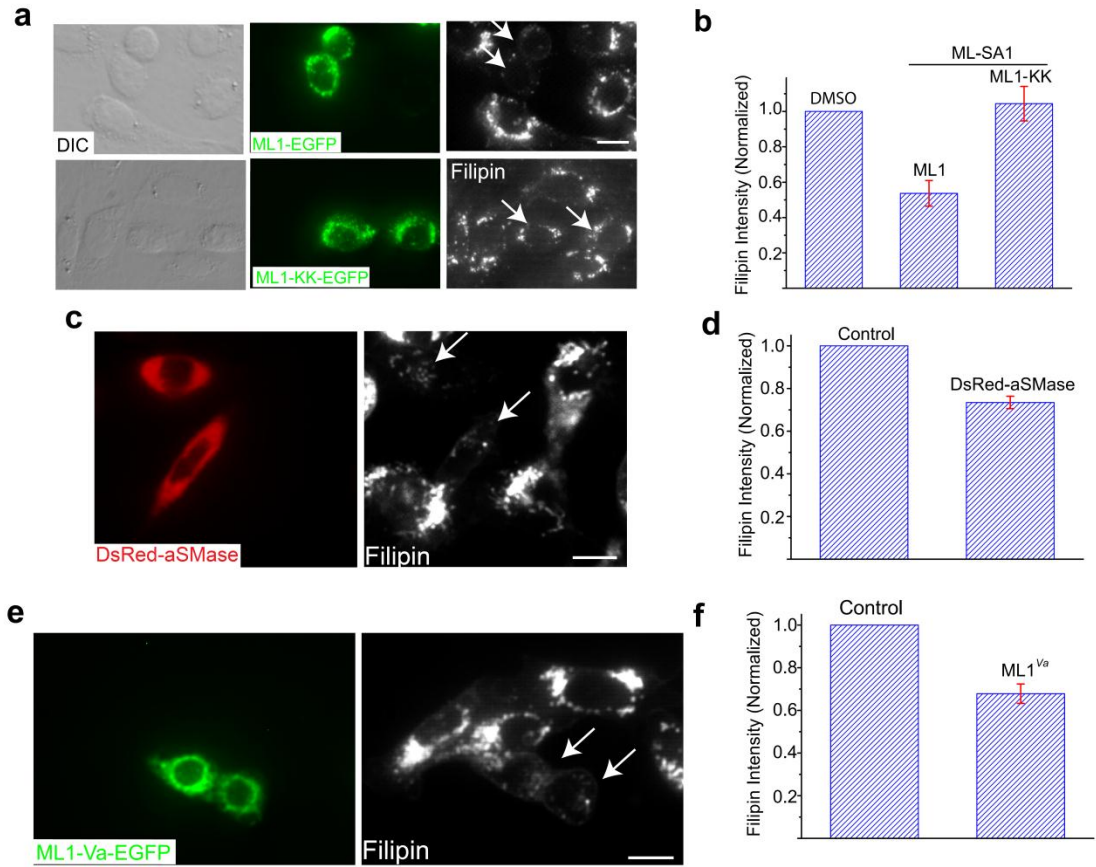
Figure 4.17. ML-SA1 together with TRPML1 overexpression reduces cholesterol accumulation in NPC cells.

(a, b) ML-SA1 reduced unesterified cholesterol (filipin) staining in ML1, but not ML1-KK-expressing U18666A-treated WT CHO cells. Differential interference contrast (DIC) images are shown for comparison. Scale bar = 10 µm. (c) Unesterified cholesterol (filipin) staining in NPC CHO cells was partially reduced in cells expressing DsRed-aSMase. Scale bar = 10 µm. (d) Average filipin staining (intensity normalized to non-transfected control cells) in DsRed-aSMase-transfected cells. (g) Unesterified cholesterol (filipin) staining in NPC CHO cells was partially reduced in cells expressing ML1-Va-EGFP (ML1^{Va}). Scale bar = 10 µm. (h) Average filipin staining (intensity normalized to non-transfected control cells) in ML1^{Va}-transfected cells. For panels b, d, f, the results were averaged for multiple randomly-taken micrographs from at least 3 independent experiments. Data are presented as the mean ± SEM. Statistical comparisons were made using analysis of variance: * P <0.05.
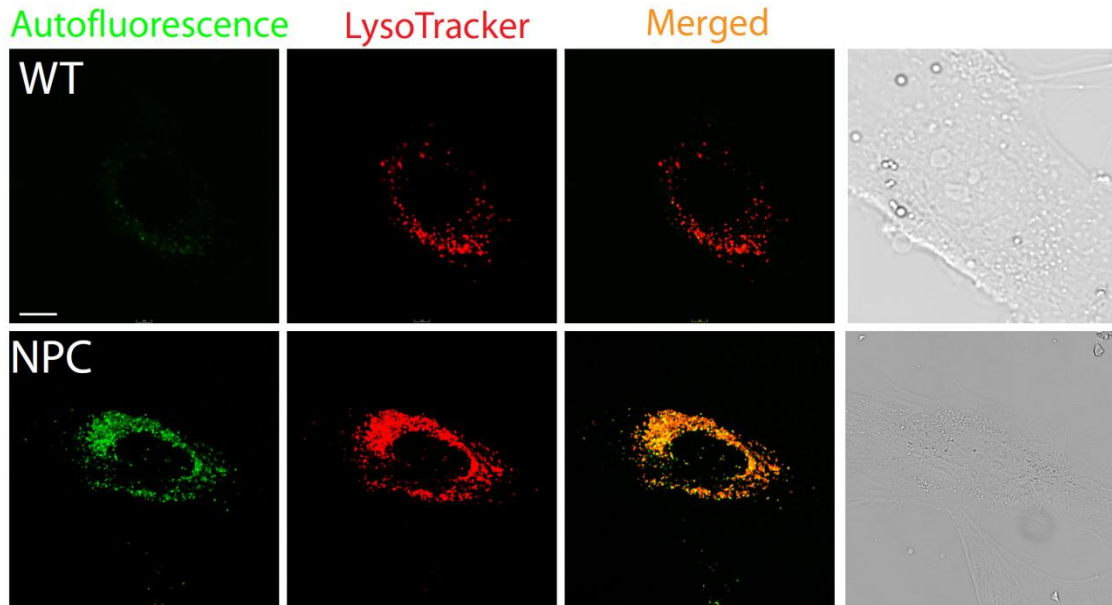
Figure 4.18. Lipofuscin-like autofluorescent materials accumulate in the lysosomes of NPC fibroblasts.

An NPC fibroblast showed autofluorescence (green) in LysoTracker-positive compartments. Autofluorescence was detected within a range of excitation wavelengths (shown with excitation at 480 nm). No significant autofluorescence was observed for WT cells. Differential interference contrast (DIC) images are shown for comparison. Scale bar = 5 μm.

CHAPTER 5

DISCUSSION

Summary of results

TRPML1 is an inwardly-rectifying Ca^{2+}-permeable channel in late endosomes and lysosomes. Loss-of-function mutations in the human *TRPML1* gene cause a devastating pediatric neurodegenerative disease called type IV Mucolipidosis (ML4). The aim of this thesis was to explore the intracellular regulatory mechanisms of TRPML1, and how the channel activity affects endolysosomal dynamics.

In chapter 2 an endogenous TRPML1 agonist - $PI(3,5)P_2$ was identified. $PI(3,5)P_2$ potently and specifically activates TRPML1 in both heterologous and endogenous systems. Biochemical binding assays show that $PI(3,5)P_2$ directly binds to the multiple positively-charged amino acid residues on the N terminus of TRPML1. Using a spectrum of yeast mutant strains with variable degrees of $PI(3,5)P_2$ deficiency, a high-degree of correlation between the levels of $PI(3,5)_2$ and the activity of a yeast functional TRPML homologue has been established. Notably, overexpression of TRPML1 was sufficient to rescue the trafficking defects in $PI(3,5)P_2$-deficient mammalian cells. These results demonstrate that TRPML1, an endolysosome-localized Ca^{2+} channel, is activated by the endolysosome-specific $PI(3,5)P_2$, providing a previously unknown link between these two important regulators of intracellular membrane trafficking.

In Chapter 3, a membrane-permeable small-molecule synthetic agonist for TRPMLs, Mucolipin-Synthetic Agonist 1 (ML-SA1), was identified. Electrophysiological results showed that ML-SA1 potently and specifically activates recombinant TRPMLs, as well as endogenous TRPML-like currents in the lysosomes of many cell types. In addition, ML-SA1 evoked TRPML1-dependent Ca^{2+} release

from endolysosomes in intact cells. ML-SA1 has therefore served as a valuable tool for studying intracellular functions of TRPMLs.

By taking advantage of ML-SA1, the activity of TRPML1 was examined under a pathological context (Chapter 4). I found that TRPML1-mediated lysosomal Ca^{2+} release, measured using a genetically-encoded Ca^{2+} indicator (GCaMP3) attached directly to TRPML1, was dramatically reduced in Niemann-Pick (NP) disease cells. Patch-clamp analyses revealed that TRPML1 channel activity was inhibited by sphingomyelin (SM), but potentiated by spingomyelinase. Importantly, increasing the expression/activity of TRPML1 was able to alleviate the lipid accumulation and trafficking defects in NPC cells. Our findings suggest that compromised channel activity of TRPML1 is the pathogenic cause for secondary lysosomal storage seen in many lysosomal storage disorders (LSDs). Thus manipulating TRPML1 channel activity by chemical agonists may provide therapeutic approaches not only for ML4, but also for other LSDs.

Taken together, the studies in this thesis investigated the regulatory mechanisms of TRPML1 under both physiological and pathological conditions. Two endogenous regulators and a synthetic agonist for TRPML1 have been identified. These findings add new perspectives to the roles of TRPML1 in the endolysosomal dynamics, yet many issues remain unsolved and new questions have been raised. In the following part of the thesis, the significance of the findings will be elaborated and unresolved questions will be discussed.

How TRPML1 is regulated by PI(3,5)P₂ under physiological conditions

My study revealed that lysosomal PI(3,5)P$_2$ is a physiological regulator of TRPML1. However, the exact concentration of local PI(3,5)P$_2$ in the LEL under basal conditions, or upon cellular stimulation, is not known. Therefore, the mechanisms by which PI(3,5)P$_2$ modulates TRPMLs under physiological

conditions remain unclear. A key question is whether $PI(3,5)P_2$ is the sole activator of TRPML1, or there are additional factors involved.

It is likely that constitutive trafficking signals, or acute stimuli, recruit/activate PIKfyve present in microdomains, thereby resulting in a rapid and transient increase in $PI(3,5)P_2$ and TRPML1-mediated Ca^{2+} release (Activation model, **Fig. 5.1A**). However, although the EC_{50} for recombinant TRPML1 is only ~50 nM (Dong, Shen et al. 2010), higher concentrations of $PI(3,5)P_2$ are required to activate endogenous TRPML1 (Wang, Dong, and Xu; unpublished data). Thus, it remains unclear whether physiological levels of $PI(3,5)P_2$, which are presumably in the low nanomolar range, are sufficient to activate endogenous TRPML1 in endolysosomes.

It is also possible that, *in vivo*, additional regulatory mechanisms for TRPML1 include factors other than $PI(3,5)P_2$. For example, $PI(4,5)P_2$ has been shown to be a "permissive" factor in the activation of voltage gated Ca^{2+} channels in response to depolarization (Wu, Bauer et al. 2002). Similarly, $PI(3,5)P_2$ may "sensitize", yet not fully "activate" TRPML1. Increases in levels of $PI(3,5)P_2$ may also promote Ca^{2+} channels to be maintained in a "willing state", thereby facilitating channel activation in the absence of secondary activation factors (Sensitization model, see **Fig. 5.1B**). Conversely, in the absence of $PI(3,5)P_2$, activation of Ca^{2+} channels may require much higher concentrations or stronger binding interactions by activation factors that exceed the physiologically permitted range. One activation factor to consider is that of mechanical force, which may be generated by the membrane curvature achieved prior to fusion(Martens and McMahon 2008). Since the Ca^{2+} release site is hypothesized to be in close proximity to the fusion/fission sites (Pryor, Mullock et al. 2000; Chen, Ahluwalia et al. 2002; Hay 2007), such mechanical force is likely to be sensed by Ca^{2+} release channels. Indeed, YVC1/TRPY1, the TRPML homolog in yeast, has been shown to be directly gated by mechanical force (Su, Zhou et al. 2009). Further studies will be needed to test whether TRPML1 is synergistically gated by $PI(3,5)P_2$ and mechanical force. However, other activation factors should be evaluated as well, including proteins that are recruited to interact with TRPML1 following transient elevations in levels of $PI(3,5)P_2$. These studies would test the

sensitization model that PI(3,5)P$_2$, in coordination with these 'cofactors', can achieve specific activation of endolysosomal Ca^{2+} release channels.

In either model, since TRPMLs are specifically modulated by PI(3,5)P$_2$ but not by other PIPs, it is possible to regulate Ca^{2+} release via TRPMLs by regulating PI-metabolizing enzymes, such as PIKfyve or Fig4 and MTM/MTMR phosphatases. To avoid excessive Ca^{2+} efflux from endolysosomes, the activation of TRPML1 needs to be transient, which can be achieved by tight coupling of the synthesis and turnover of PI(3,5)P$_2$ (Botelho, Efe et al. 2008). This has been shown to be the case in yeast where Fab1 (the PI 5-kinase) physically associates with Fig4 (PI 5-phosphatase) and Vac14 (a regulator of Fab1) (Sbrissa, Ikonomov et al. 2007; Botelho, Efe et al. 2008; Jin, Chow et al. 2008). The formation of the Fab1-Vac14-Fig4 complex allows rapid synthesis and turnover of PI(3,5)P$_2$ in response to hyperosmotic stress (Duex, Tang et al. 2006). In mammalian cells, although the PI-metabolizing enzymes are usually localized to the cytosol (Botelho, Efe et al. 2008), they can be recruited to endolysosomal membranes based on the binding of phosphoinositides to their PI-binding domains (Kutateladze 2010), or by interacting with key components of the trafficking pathways (Botelho, Efe et al. 2008). For example, PI(3)P can recruit Rab5, and activation of Rab5 can further stimulate the activity of Vps34 PI-3 kinase (Shin, Hayashi et al. 2005). Similar mechanisms may also be employed by PI(3,5)P$_2$, Rab7, and PI(3,5)P$_2$-metabolising enzymes (Duex, Tang et al. 2006; Botelho, Efe et al. 2008). Therefore, rapid switch on-and-off of PI kinase and phosphatase activity may occur near the membrane fusion/fission site, so as to tightly control the extent of Ca^{2+} release from endolysosomes (see **Fig 5.2**).

How TRPML1 is regulated by SM in a compartment-specific manner

Similar to PI(3,5)P$_2$, the exact concentrations of SM in late endosomes/lysosomes or other membranes that TRPML1 may temporarily reside on (e.g. the plasma membrane) remain unknown. To help the reader get a quick idea, we could make an estimate by comparing SM with PI(4,5)P$_2$, a relatively well-

studied lipid. It is estimated that $PI(4,5)P_2$ could make up 1.5% of plasma membrane lipids (in molar terms) and its concentration at PM can reach ~10 μM range (Ferrell and Huestis 1984; Roth 2004; Suh and Hille 2008). Since sphingomyelin comprises of ~15% of PM lipids (in molar terms) (van Meer, Voelker et al. 2008), the concentration of SM at PM could be estimated at ~100 μM range. In late endosomes/lysosomes, the concentration of SM drops by more than 3-fold (van Meer, Voelker et al. 2008; Sztolsztener, Dobrzyn et al. 2012), thus the SM concentration there could be at ~30 μM range. However, this estimate (~30 μM) is the average SM concentration of both the limiting and luminal membranes in lysosomes. Given that SM/cholesterol are more than 5 times as concentrated in the luminal membranes (Mobius, van Donselaar et al. 2003), SM concentration at the limiting membrane where TRPML1 resides on would be less than ~6 μM, one order of magnitude less than that on PM. However, in pathological conditions, such as Niemann Pick disease, SM concentration at the limiting lysosomal membrane could be much higher than ~6 μM (Sztolsztener, Dobrzyn et al. 2012), or even reaches the level at PM (~100 μM) due to the defective aSMase activity. It is worth noting that the abovementioned estimates are the overall concentration of SM on the specific membranes, its local concentration is likely to vary in different microdomains.

Based on the above estimates and my work that high concentration of SMs in TRPML1-residing membranes (>20μM) can negatively regulate TRPML1, the modulation of TRPML1 by SMs appears to be both physiologically and pathologically significant. Under normal conditions, late endosomes/lysosomes have relatively low level of sphingomylin/cholesterol, rendering TRPML1 sensitive to cytosolic activating signals. This is consistent with the fact that TRPML1 is actively involved in various membrane trafficking processes that late endosomes/lysosomes are associated with (Cheng, Shen et al. 2010). However, when TRPML1 transiently appear on the plasma membrane during lysosome exocytosis (Dong, Wang et al. 2009; Medina, Fraldi et al. 2011), mechanisms must exist to rapidly turn off TRPML1 activity so as to prevent the excessive Ca^{2+} influx from the extracellular space. While the quick synthesis and turnover of activation signals (such as $PI(3,5)P_2$) may be an efficient way as mentioned in the previous section, the massive sphingomyelins on plasma

membrane (~100 μM) represent another defense mechanism to prevent Ca^{2+} overload. Such mechanism is especially important for TRPML1 since TRPML is not inactivated by voltage or desensitized by Ca^{2+} (Dong, Shen et al. 2010). On the other hand, under NP disease conditions, the SM concentration in the limiting lysosomal membrane could be as high as that in the PM, therefore inhibiting TRPML1. In sum, SM may play an important role in balancing TRPML1's channel activity in different cellular compartments, the disturbance of which may underlie the pathological cause of many lysosomal storage disorders.

The identification of SM as a negative regulator of TRPML1 also suggests that the breakdown of SM has two distinct yet interconnected effects on membrane trafficking processes. On one hand, as mentioned in the introduction, the conversion from SM to ceramide can induce local membrane curvature, thus increasing the fusogenic potential of the membrane. On the other hand, such conversion may also sensitize TRPML1 or even induce Ca^{2+} release from TRPML1 on endolysosomes. Both membrane curvature and Ca^{2+} signaling are key components for efficient membrane fusion/fission process. Therefore, the activity of ASMase in the lumen of late endosomes/lysosomes or during its transient appearance on the outer leaflet of PM upon lysosomal exocytosis may represent an economical and efficient means to control the membrane fusion/fission processes.

The advantage of regulating TRPML1 from both cytosolic and luminal sides

The fact that both a cytosol-localized lipid ($PI(3,5)P_2$) and a luminal localized lipid (SM) regulate TRPML1 may allow TRPML1 to integrate signals from both sides to orchestrate the Ca^{2+} release events. After two endolysosomal membranes are brought into close proximity, increases in levels of $PI(3,5)P_2$ may lead to the direct activation of TRPML1 to elevate levels of juxtaorganellar Ca^{2+}, and thereby triggering fusion events (**Fig 5.2**). Alternatively, regarding the hypothesis that $PI(3,5)P_2$ configures TRPML1 in a "willing" state, the assembly of SNARE complexes and the membrane curvature involved in this process, may provide a necessary "activation factor" for TRPML1-mediated

Ca^{2+} release (**Fig 5.1B**), as in the case for yeast where trans-SNARE complex formation has been shown to promote Ca^{2+} release from yeast vacuoles (Merz and Wickner 2004). Moreover, as mentioned in the preceding paragraph, the conversion from SM to ceramide at the luminal side can further induce the local membrane curvature to promote fusion or fission events. In this sense, the PI(3,5)P$_2$-TRPML1-sphingomyelin signaling pathway add a fine layer of regulation to the late endocytic trafficking system, and the balance of PI(3,5)P$_2$ or SM level in the endolysosomal membrane need to carefully maintained. Indeed, when SMs are abnormally accumulated in late endosomes and lysosomes in NP disease, the inhibitory effect of SMs could be potent enough to render TRPML1 insensitive to cytosolic activation signals (**Fig 5.3**).

Other factors regulated by PI(3,5)P$_2$ / SM or regulating lysosomal Ca^{2+} channels

In this thesis, TRPML1 was discovered as a downstream effector of PI(3,5)P$_2$ and SM, but it is not their only effector. PI(3,5)P$_2$ -deficient cells have been observed to have more defects in their membrane trafficking processes than TRPML1$^{-/-}$ cells (Dong, Shen et al. 2010), suggesting that PI(3,5)P$_2$ regulates a number of other cellular events besides the modulation of Ca^{2+} signaling. Indeed, PI(3,5)P$_2$ has been shown to recruit the necessary cytosolic proteins for membrane fusion and fission, and may regulate the functions of other endolysosomal membrane proteins to determine the physical properties and fusogenic potential of endolysosomal membranes (Dove, Dong et al. 2009; Poccia and Larijani 2009; Dong, Shen et al. 2010). Similarly, SM is likely to have other effectors along the endolysosome trafficking pathway. It has been reported that increased cholesterol content in endolysosomal membranes can aberrantly sequester the soluble N-ethylmaleimide attachment protein (SNAP) receptor (SNARE) proteins, thereby blocking efficient endolysosomal fusion (Fraldi, Annunziata et al. 2010). Since SM is usually associated with cholesterol, it would be interesting to test whether the assembly and disassembly of endolysosomal SNARE complex is also defective in NP disease cells.

Likewise, It is possible that $PI(3,5)P_2$ and SM are not the only endogenous regulators of TRPML1. Future studies need to test for other possible modulators of TRPML1 at the cytosol side, such as various effectors of PIP or Rab proteins, phosphorylated derivatives of sphingolipids and mechanical force. At the lysosomal lumen side, other offending metabolites that inhibit TRPML1, and/or $PI(3,5)P_2$-metabolizing enzymes, may be identified when investigating TRPML1 activity in other LSDs. As many TRP channels function as polymodal receptors (Clapham 2003; Wu, Sweet et al. 2010), it is not surprising to expect more endogenous regulators of TRPML1 to be discovered in the near future.

The link between lysosomal lipids and TRPMLs also brings us new insights into the gating mechanisms of the Ca^{2+} channels along the endolysosomal pathway. Like various channels on the plasma membrane whose function is usually phospholipid-dependent, endolysosomal Ca^{2+} channels are likely to be modulated by the lipids mainly enriched in endolysosomes. We speculate that lysosomal specific phosphoinositides or sphingolipids may also modulate other Ca^{2+} channels such as TPCs and TRPM2 in the endolysosomal system.

Downstream events after Ca^{2+} release.

My thesis work mainly focused on the upstream events of Ca^{2+} release from endolysosmes (how they are regulated), the downstream events following Ca^{2+} release are largely unknown. There are at least two outstanding questions remain unanswered. First of all, the Ca^{2+} sensors are yet unidentified. Given the specificity of endolysosomal trafficking processes, compartment-specific Ca^{2+} sensors might be involved. The best candidate is ALG-2, a penta-EF-hand protein that physically associates with TRPML1 in a Ca^{2+}-dependent manner (Vergarajauregui, Martina et al. 2009). Calmodulin has also been implicated in endolysosomal trafficking processes (Peters and Mayer 1998; Pryor, Mullock et al. 2000; Burgoyne and Clague 2003), with vacuolar fusion being found to be defective in loss-of-function calmodulin mutants in yeast (Peters and Mayer 1998). Synaptotagmins are another type of

Ca^{2+} sensor that have been shown to be essential for exocytosis (Suh and Hille 2008). Since lysosomes also undergo Ca^{2+}-regulated exocytosis for plasma membrane repair (Reddy, Caler et al. 2001), synaptotagmins may play a role in the fusion of lysosomes with other membranes. In addition, recent studies have demonstrated that Doc2b, a high-affinity Ca^{2+} sensor, is important for the spontaneous release of neurotransmitters and may play a role in endolysosomal trafficking (Groffen, Martens et al.). Future studies promise exciting discoveries of compartment-specific Ca^{2+} sensors.

Another unanswered question is how Ca^{2+} sensors transduce the Ca^{2+} increase to fusion/fission events. One possibility is that upon binding of Ca^{2+}, a putative Ca^{2+} sensor may exhibit high-affinity associations with phospholipids such as PI(3,5)P$_2$, thus bringing two membranes into closer proximity. This has been observed during the release of neurotransmitters using functional assays of synaptotagmins and PI(4,5)P$_2$ (Arac, Chen et al. 2006). Another possibility is that a putative Ca^{2+} sensor may interact with SNARE proteins to facilitate the formation of a SNARE complex, and thereby promoting membrane fusion. Correspondingly, calmodulin has been shown to interact with SNAREs and promote intracellular membrane fusion (Burgoyne and Clague 2003). A third possibility is that Ca^{2+} signaling may regulate other trafficking factors including phosphoinositide effectors. For example, TRPML2 and Ca^{2+} have been shown to promote the activity of Arf6 GTPase and other ArfGAPs, respectively (Karacsonyi, Miguel et al. 2007). Ca^{2+}/calmodulin is shown to be a positive regulator of Vps34 in phagosomes (Vergne, Chua et al. 2004). Thus, functional cross-talk between endolysosomal Ca^{2+} channels, phosphoinositides, phosphoinositide effectors and other lipids may regulate the release of Ca^{2+} in a spatiotemporal manner, thus ensuring the specificity of endolysosomal membrane trafficking.

TRPML1 as a new therapeutic target

My thesis work highlights the significance of TRPML1 in the pathological causes of lipid storage disorders. Studies on Mucolipidosis type IV disease have revealed that total or partial loss of TRPML1 channel activity causes trafficking defects and lipid storage, leading to severe

neurodegenerative symptoms in MLIV patients. My work demonstrates that in several other LSDs, the comprised TRPML1 channel activity due to SM accumulation also impairs endolysosomal trafficking, causing secondary lipid storage and cell damage (**Fig 5.3**). Since I only examined the acute effect of lipids on TRPML1, future work should utilize a longer time scale (hours or days of lipid incubation) to see if other sphingolipids or cholesterol can also modulate TRPML1 activity. Many LSDs are characterized with progressive accumulation of mucopolysaccharides and oligosaccharides with defective membrane trafficking (Parkinson-Lawrence, Shandala et al.). Naturally, these accumulated lipids are also good candidates to be tested as potential regulators of TRPML1.

The importance of TRPML1 is further illustrated by a recent finding that TFEB, a transcription factor that regulates lysosomal genes, can reduce the pathologic storage in many LSDs except Mucolipidosis IV (Medina, Fraldi et al. 2011), suggesting that TRPML1 may represents a key entry point to reduce lysosomal storage. Consistent with this hypothesis, my work shows that increasing TRPML1's expression/activity was able to alleviate the lipid accumulation in NPC cells. Such rescue effects could be due to increased retrograde trafficking from the late endosome/lysosome to Golgi, or increased lysosomal exocytosis, or even enhanced activities of hydrolase upon ML-SA1 application. Further study is needed to distinguish these possibilities. But in either case, a novel concept is brought up that clearance of lysosome storage might be achieved by up-regulating membrane trafficking using chemical agonists of TRPML1. Thus, TRPML1 may represent a promising therapeutic target for the treatment of lysosomal storage disorders. Future investigation of the toxicity of ML-SA1 and its effectiveness in animal model is required. Given the fact that constitutively active TRPML1 channel may actually worsen cell condition in the long run (Dong, Wang et al. 2009) presumably due to the Ca^{2+} overload caused by the channel, great care needs to be taken to avoid over-activating the channel. An ideal scenario is to use low dose of the agonist to sensitize the channel while only removing the lipid inhibitory effect without over-activating it. Since lysosome storage is also observed in common neurodegenerative diseases such as Alzheimer's and Parkinson's (Bellettato and Scarpa 2010; Schneider and Zhang 2010), manipulating TRPML1's channel activity may provide therapeutic approaches not only for LSDs, but also for those common neurodegenerative diseases as well.
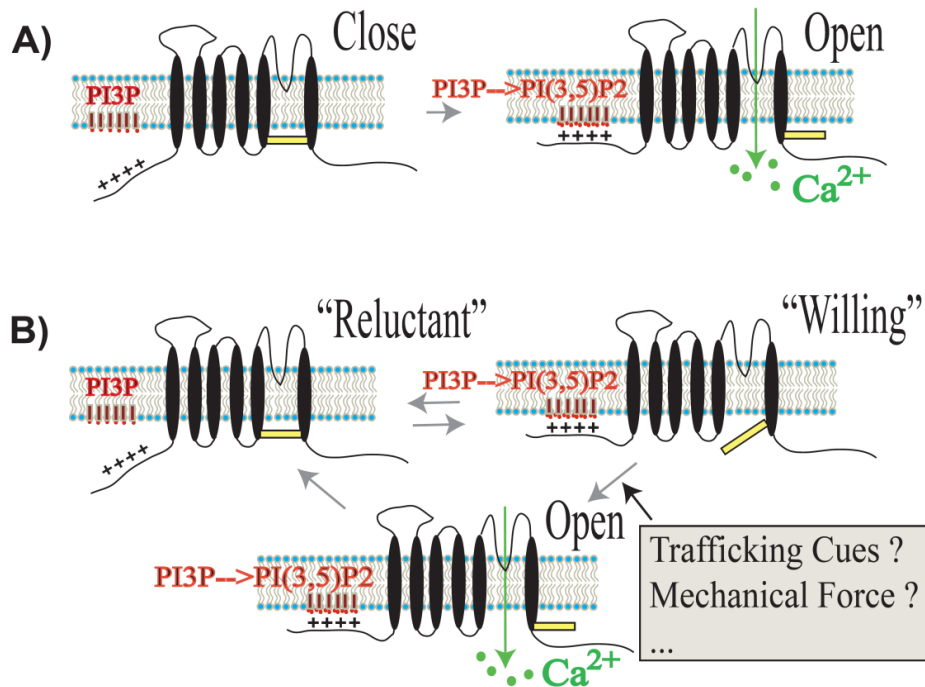
Fig 5.1. Two working models for PI(3,5)P$_2$-dependent TRPML1 activation in endolysosomes.

A: "Activation" model. Physiological levels of PI(3,5)P$_2$ activate TRPML1 by binding to the poly-basic domain in the N- terminus of TRPML1, leading to the release of Ca^{2+}.

B: "Sensitization" model. In this model, physiological levels of PI(3,5)P$_2$ are not sufficient to activate TRPML1. Instead, PI(3,5)P$_2$ is hypothesized to sensitize TRPML1 by converting the channel from a "reluctant" state to a "willing state" (see ref. (Wu, Bauer et al. 2002)). Channel opening/activation and Ca^{2+} release are then induced by unidentified trafficking cues, one of which may be the mechanical force generated during pre-fusion membrane curvature/bending. This model confers multiple layers of regulation upon TRPML1 activity. Under stress conditions that are analogous to hyper-osmotic shock in yeast, acute stimuli may induce high levels of PI(3,5)P$_2$ to sufficiently activate TRPML1 as shown in **A**.
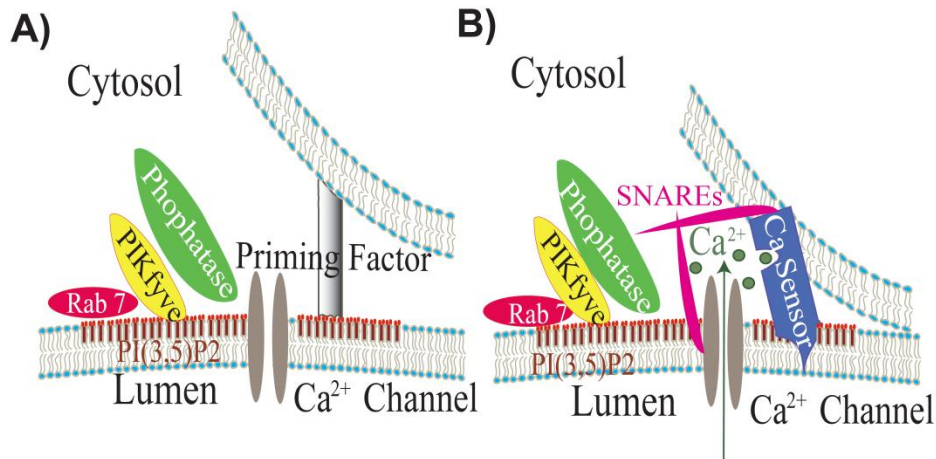
Fig 5.2. A proposed model for PI(3,5)P$_2$- and Ca^{2+}-dependent endolysosomal membrane fusion.

Microdomain specific recruitment of an array of tethering and priming factors has the potential to bring into close proximity two endolysosomal membranes (the upper membrane and lower membrane illustrated) .

A: Recruited proteins that may be involved include Rab GTPases (Rab7 for LEL), lipid kinases (PIKfyve for LEL), and several phosphatases (Fig4 and MTM/MTMRs). Activation of the assembled PI(3,5)P$_2$-metabolizing complex would ensure a transient and local increase in the level of PI(3,5)P$_2$. PI(3,5)P$_2$ effectors would also be subsequently recruited and/or activated.

B: The release of Ca^{2+} from the lumen of endolysosomes would transiently elevate the levels of juxtaorganellar Ca^{2+} to activate a putative Ca^{2+} sensor protein, such as ALG-2/Synaptotagmin/CaM, to promote the fusion of the lipid bilayers. Both SNARE complex formation and PI(3,5)P$_2$ may facilitate Ca^{2+} release. An increase in PI(3,5)P$_2$ levels could also alter the physical properties of the membranes involved, and regulate the interactions between SNARE complexes and Ca^{2+} sensor proteins.
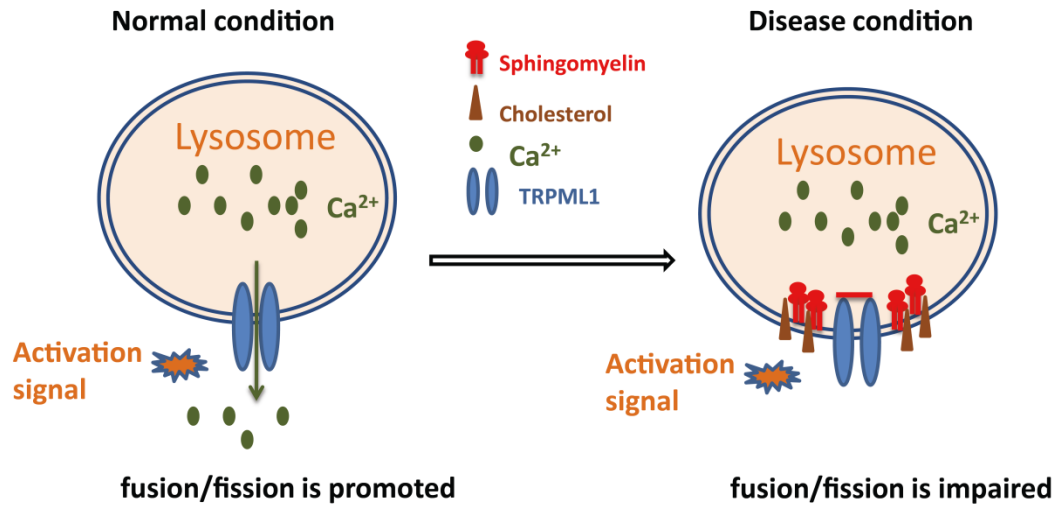
Fig 5.3. Sphingomyelin accumulation affects membrane trafficking by inhibiting TRPML1.

Under normal conditions, late endosome/lysosome has relatively low level of sphingomylin or cholesterol, rendering TRPML1 sensitive to cytosolic activating signals. The activation of TRPML1 leads to elevated levels of juxtaorganellar Ca^{2+}, thereby triggering fusion or fission events. Under Niemann Pick diseases condition, however, SM (and cholesterol) may accumulate at the limiting lysosomal membrane, subsequently inhibiting TRPML1 and making the channel insensitive to cytosolic activation signals.

References:

Abdul-Hammed, M., B. Breiden, et al. (2010). "Role of endosomal membrane lipids and NPC2 in cholesterol transfer and membrane fusion." J Lipid Res **51**(7): 1747-1760.

Abe, K. and R. Puertollano (2011). "Role of TRP channels in the regulation of the endosomal pathway." Physiology (Bethesda) **26**(1): 14-22.

Ahluwalia, J. P., J. D. Topp, et al. (2001). "A role for calcium in stabilizing transport vesicle coats." J Biol Chem **276**(36): 34148-34155.

Altarescu, G., M. Sun, et al. (2002). "The neurogenetics of mucolipidosis type IV." Neurology **59**(3): 306-313.

Anderson, R. A. and G. N. Sando (1991). "Cloning and expression of cDNA encoding human lysosomal acid lipase/cholesteryl ester hydrolase. Similarities to gastric and lingual lipases." J Biol Chem **266**(33): 22479-22484.

Andrade, L. O. and N. W. Andrews (2005). "The Trypanosoma cruzi-host-cell interplay: location, invasion, retention." Nat Rev Microbiol **3**(10): 819-823.

Anh, D. D., C. C. Carlos, et al. (2011). "Immunogenicity, reactogenicity and safety of the human rotavirus vaccine RIX4414 (Rotarix) oral suspension (liquid formulation) when co-administered with expanded program on immunization (EPI) vaccines in Vietnam and the Philippines in 2006-2007." Vaccine **29**(11): 2029-2036.

Arac, D., X. Chen, et al. (2006). "Close membrane-membrane proximity induced by Ca(2+)-dependent multivalent binding of synaptotagmin-1 to phospholipids." Nat Struct Mol Biol **13**(3): 209-217.

Axe, E. L., S. A. Walker, et al. (2008). "Autophagosome formation from membrane compartments enriched in phosphatidylinositol 3-phosphate and dynamically connected to the endoplasmic reticulum." J Cell Biol **182**(4): 685-701.

Azmitia, E. C. and R. Nixon (2008). "Dystrophic serotonergic axons in neurodegenerative diseases." Brain Res **1217**: 185-194.

Bai, J., W. C. Tucker, et al. (2004). "PIP2 increases the speed of response of synaptotagmin and steers its membrane-penetration activity toward the plasma membrane." Nat Struct Mol Biol **11**(1): 36-44.

Baldys, A. and J. R. Raymond (2009). "Critical role of ESCRT machinery in EGFR recycling." Biochemistry **48**(40): 9321-9323.

Bargal, R., N. Avidan, et al. (2000). "Identification of the gene causing mucolipidosis type IV." Nat Genet **26**(1): 118-123.

Bargal, R. and G. Bach (1988). "Phospholipids accumulation in mucolipidosis IV cultured fibroblasts." J Inherit Metab Dis **11**(2): 144-150.

Bargal, R., H. H. Goebel, et al. (2002). "Mucolipidosis IV: novel mutation and diverse ultrastructural spectrum in the skin." Neuropediatrics **33**(4): 199-202.

Bassi, M. T., M. Manzoni, et al. (2000). "Cloning of the gene encoding a novel integral membrane protein, mucolipidin-and identification of the two major founder mutations causing mucolipidosis type IV." Am J Hum Genet **67**(5): 1110-1120.

Beaule, P. E., D. B. Griffin, et al. (2004). "The Levine anterior approach for total hip replacement as the treatment for an acute acetabular fracture." J Orthop Trauma **18**(9): 623-629.

Bellettato, C. M. and M. Scarpa (2010). "Pathophysiology of neuropathic lysosomal storage disorders." J Inherit Metab Dis **33**(4): 347-362.

Berwick, D. C., G. C. Dell, et al. (2004). "Protein kinase B phosphorylation of PIKfyve regulates the trafficking of GLUT4 vesicles." J Cell Sci **117**(Pt 25): 5985-5993.

Bhattacharya, J., P. J. Peters, et al. (2003). "CD4-independent infection of HIV and SIV: implications for envelope conformation and cell tropism in vivo." AIDS **17 Suppl 4**: S35-43.

Bikman, B. T. and S. A. Summers (2011). "Ceramides as modulators of cellular and whole-body metabolism." J Clin Invest **121**(11): 4222-4230.

Binker, M. G., L. I. Cosen-Binker, et al. (2007). "Arrested maturation of Neisseria-containing phagosomes in the absence of the lysosome-associated membrane proteins, LAMP-1 and LAMP-2." Cell Microbiol **9**(9): 2153-2166.

Biswas, J., A. Bajaj, et al. (2011). "Membranes of cationic gemini lipids based on cholesterol with hydroxyl headgroups and their interactions with DNA and phospholipid." J Phys Chem B **115**(3): 478-486.

Blom, T., P. Somerharju, et al. (2011). "Synthesis and biosynthetic trafficking of membrane lipids." Cold Spring Harb Perspect Biol **3**(8): a004713.

Blott, E. J. and G. M. Griffiths (2002). "Secretory lysosomes." Nat Rev Mol Cell Biol **3**(2): 122-131.

Bonangelino, C. J., J. J. Nau, et al. (2002). "Osmotic stress-induced increase of phosphatidylinositol 3,5-bisphosphate requires Vac14p, an activator of the lipid kinase Fab1p." J Cell Biol **156**(6): 1015-1028.

Bonifacino, J. S. and R. Rojas (2006). "Retrograde transport from endosomes to the trans-Golgi network." Nat Rev Mol Cell Biol **7**(8): 568-579.

Botelho, R. J., J. A. Efe, et al. (2008). "Assembly of a Fab1 phosphoinositide kinase signaling complex requires the Fig4 phosphoinositide phosphatase." Mol Biol Cell **19**(10): 4273-4286.

Brady, R. O., J. N. Kanfer, et al. (1966). "The metabolism of sphingomyelin. II. Evidence of an enzymatic deficiency in Niemann-Pick diseae." Proc Natl Acad Sci U S A **55**(2): 366-369.

Brandt, A., F. Papagiannouli, et al. (2006). "Developmental control of nuclear size and shape by Kugelkern and Kurzkern." Curr Biol **16**(6): 543-552.

Breslow, D. K. and J. S. Weissman (2010). "Membranes in balance: mechanisms of sphingolipid homeostasis." Mol Cell **40**(2): 267-279.

Bright, N. A., M. J. Gratian, et al. (2005). "Endocytic delivery to lysosomes mediated by concurrent fusion and kissing events in living cells." Curr Biol **15**(4): 360-365.

Brown, G. K. (2000). "Glucose transporters: structure, function and consequences of deficiency." J Inherit Metab Dis **23**(3): 237-246.

Burgoyne, R. D. and M. J. Clague (2003). "Calcium and calmodulin in membrane fusion." Biochim Biophys Acta **1641**(2-3): 137-143.

Cadigan, K. M., J. G. Heider, et al. (1988). "Isolation and characterization of Chinese hamster ovary cell mutants deficient in acyl-coenzyme A:cholesterol acyltransferase activity." J Biol Chem **263**(1): 274-282.

Cadigan, K. M., D. M. Spillane, et al. (1990). "Isolation and characterization of Chinese hamster ovary cell mutants defective in intracellular low density lipoprotein-cholesterol trafficking." J Cell Biol **110**(2): 295-308.

Calcraft, P. J., M. Ruas, et al. (2009). "NAADP mobilizes calcium from acidic organelles through two-pore channels." Nature **459**(7246): 596-600.

Carlson, A. E., R. E. Westenbroek, et al. (2003). "CatSper1 required for evoked Ca2+ entry and control of flagellar function in sperm." Proc Natl Acad Sci U S A **100**(25): 14864-14868.

Carlton, J. G. and J. Martin-Serrano (2009). "The ESCRT machinery: new functions in viral and cellular biology." Biochem Soc Trans **37**(Pt 1): 195-199.

Carstea, E. D., J. A. Morris, et al. (1997). "Niemann-Pick C1 disease gene: homology to mediators of cholesterol homeostasis." Science **277**(5323): 228-231.

Casado-Terrones, S., J. F. Fernandez-Sanchez, et al. (2007). "Simple luminescence detectors using a light-emitting diode or a Xe lamp, optical fiber and charge-coupled device, or photomultiplier for determining proteins in capillary electrophoresis: a critical comparison." Anal Biochem **365**(1): 82-90.

Cerny, J., Y. Feng, et al. (2004). "The small chemical vacuolin-1 inhibits Ca(2+)-dependent lysosomal exocytosis but not cell resealing." EMBO reports **5**(9): 883-888.

Chang, H. M., R. Reitstetter, et al. (1995). "Attenuation of channel kinetics and conductance by cholesterol: an interpretation using structural stress as a unifying concept." J Membr Biol **143**(1): 51-63.

Changani, K. K., A. Nicholson, et al. (2003). "A longitudinal magnetic resonance imaging (MRI) study of differences in abdominal fat distribution between normal mice, and lean

overexpressers of mitochondrial uncoupling protein-3 (UCP-3)." <u>Diabetes Obes Metab</u> **5**(2): 99-105.

Chen, C. S., G. Bach, et al. (1998). "Abnormal transport along the lysosomal pathway in mucolipidosis, type IV disease." <u>Proc Natl Acad Sci U S A</u> **95**(11): 6373-6378.

Chen, C. S., M. C. Patterson, et al. (1999). "Broad screening test for sphingolipid-storage diseases." <u>Lancet</u> **354**(9182): 901-905.

Chen, J. L., J. P. Ahluwalia, et al. (2002). "Selective effects of calcium chelators on anterograde and retrograde protein transport in the cell." <u>J Biol Chem</u> **277**(38): 35682-35687.

Cheng, X., D. Shen, et al. (2010). "Mucolipins: Intracellular TRPML1-3 channels." <u>FEBS Lett</u> **584**(10): 2013-2021.

Chernomordik, L. V. and M. M. Kozlov (2003). "Protein-lipid interplay in fusion and fission of biological membranes." <u>Annu Rev Biochem</u> **72**: 175-207.

Cheruku, S. R., Z. Xu, et al. (2006). "Mechanism of cholesterol transfer from the Niemann-Pick type C2 protein to model membranes supports a role in lysosomal cholesterol transport." <u>J Biol Chem</u> **281**(42): 31594-31604.

Cho, H. S., J. L. Dominick, et al. (2010). "Lipid domains in bicelles containing unsaturated lipids and cholesterol." <u>J Phys Chem B</u> **114**(28): 9238-9245.

Choudhury, A., D. K. Sharma, et al. (2004). "Elevated endosomal cholesterol levels in Niemann-Pick cells inhibit rab4 and perturb membrane recycling." <u>Mol Biol Cell</u> **15**(10): 4500-4511.

Chow, A., D. Toomre, et al. (2002). "Dendritic cell maturation triggers retrograde MHC class II transport from lysosomes to the plasma membrane." <u>Nature</u> **418**(6901): 988-994.

Chow, C. Y., J. E. Landers, et al. (2009). "Deleterious variants of FIG4, a phosphoinositide phosphatase, in patients with ALS." <u>Am J Hum Genet</u> **84**(1): 85-88.

Chow, C. Y., Y. Zhang, et al. (2007). "Mutation of FIG4 causes neurodegeneration in the pale tremor mouse and patients with CMT4J." <u>Nature</u> **448**(7149): 68-72.

Church, L. D., G. Hessler, et al. (2005). "TNFR1-induced sphingomyelinase activation modulates TCR signaling by impairing store-operated Ca2+ influx." <u>J Leukoc Biol</u> **78**(1): 266-278.

Clapham, B. and A. J. Sutherland (2003). "Scintillation-based potassium signalling using 2,5-diphenyloxazole-tagged aza-18-crown-6." <u>Chem Commun (Camb)</u>(1): 84-85.

Clapham, D. E. (2003). "Symmetry, selectivity, and the 2003 Nobel Prize." <u>Cell</u> **115**(6): 641-646.

Clapham, D. E. (2003). "TRP channels as cellular sensors." <u>Nature</u> **426**(6966): 517-524.

Clapham, D. E., C. Montell, et al. (2003). "International Union of Pharmacology. XLIII. Compendium of voltage-gated ion channels: transient receptor potential channels." <u>Pharmacol Rev</u> **55**(4): 591-596.

Conus, S., C. Pop, et al. (2012). "Cathepsin D primes caspase-8 activation by multiple intra-chain proteolysis." <u>J Biol Chem</u>.

Cosner, C. C., J. T. Markiewicz, et al. (2009). "Investigation of N-aryl-3-alkylidenepyrrolinones as potential Niemann-Pick type C disease therapeutics." <u>J Med Chem</u> **52**(20): 6494-6498.

Cruz, J. C., S. Sugii, et al. (2000). "Role of Niemann-Pick type C1 protein in intracellular trafficking of low density lipoprotein-derived cholesterol." <u>J Biol Chem</u> **275**(6): 4013-4021.

Cuajungco, M. P. and M. A. Samie (2008). "The varitint-waddler mouse phenotypes and the TRPML3 ion channel mutation: cause and consequence." <u>Pflugers Arch</u> **457**(2): 463-473.

Curcio-Morelli, C., F. A. Charles, et al. (2010). "Macroautophagy is defective in mucolipin-1-deficient mouse neurons." <u>Neurobiol Dis</u> **40**(2): 370-377.

Czibener, C., N. M. Sherer, et al. (2006). "Ca2+ and synaptotagmin VII-dependent delivery of lysosomal membrane to nascent phagosomes." <u>J Cell Biol</u> **174**(7): 997-1007.

Davies, J. P. and Y. A. Ioannou (2000). "Topological analysis of Niemann-Pick C1 protein reveals that the membrane orientation of the putative sterol-sensing domain is identical to those of 3-hydroxy-3-methylglutaryl-CoA reductase and sterol regulatory element binding protein cleavage-activating protein." <u>J Biol Chem</u> **275**(32): 24367-24374.

de Duve, C. (2005). "The lysosome turns fifty." <u>Nat Cell Biol</u> **7**(9): 847-849.

Denis, V. and M. S. Cyert (2002). "Internal Ca(2+) release in yeast is triggered by hypertonic shock and mediated by a TRP channel homologue." <u>J Cell Biol</u> **156**(1): 29-34.

Desjardins, M. (1995). "Biogenesis of phagolysosomes: the 'kiss and run' hypothesis." Trends Cell Biol **5**(5): 183-186.

Devlin, C., N. H. Pipalia, et al. (2010). "Improvement in lipid and protein trafficking in Niemann-Pick C1 cells by correction of a secondary enzyme defect." Traffic **11**(5): 601-615.

Di Paolo, G. and P. De Camilli (2006). "Phosphoinositides in cell regulation and membrane dynamics." Nature **443**(7112): 651-657.

Domon, M., M. N. Nasir, et al. (2011). "Annexins as organizers of cholesterol- and sphingomyelin-enriched membrane microdomains in Niemann-Pick type C disease." Cell Mol Life Sci.

Dong, X. P., X. Cheng, et al. (2008). "The type IV mucolipidosis-associated protein TRPML1 is an endolysosomal iron release channel." Nature **455**(7215): 992-996.

Dong, X. P., D. Shen, et al. (2010). "PI(3,5)P(2) controls membrane trafficking by direct activation of mucolipin Ca(2+) release channels in the endolysosome." Nat Commun **1**: 38.

Dong, X. P., X. Wang, et al. (2009). "Activating mutations of the TRPML1 channel revealed by proline-scanning mutagenesis." J Biol Chem **284**(46): 32040-32052.

Dong, X. P., X. Wang, et al. (2010). "TRP channels of intracellular membranes." J Neurochem **113**(2): 313-328.

Dove, S. K., F. T. Cooke, et al. (1997). "Osmotic stress activates phosphatidylinositol-3,5-bisphosphate synthesis." Nature **390**(6656): 187-192.

Dove, S. K., K. Dong, et al. (2009). "Phosphatidylinositol 3,5-bisphosphate and Fab1p/PIKfyve underPPIn endo-lysosome function." Biochem J **419**(1): 1-13.

Dove, S. K., R. C. Piper, et al. (2004). "Svp1p defines a family of phosphatidylinositol 3,5-bisphosphate effectors." EMBO J **23**(9): 1922-1933.

Duan, R. D., E. Hertervig, et al. (1996). "Distribution of alkaline sphingomyelinase activity in human beings and animals. Tissue and species differences." Dig Dis Sci **41**(9): 1801-1806.

Duex, J. E., J. J. Nau, et al. (2006). "Phosphoinositide 5-phosphatase Fig 4p is required for both acute rise and subsequent fall in stress-induced phosphatidylinositol 3,5-bisphosphate levels." Eukaryot Cell **5**(4): 723-731.

Duex, J. E., F. Tang, et al. (2006). "The Vac14p-Fig4p complex acts independently of Vac7p and couples PI3,5P2 synthesis and turnover." J Cell Biol **172**(5): 693-704.

Ferguson, C. J., G. M. Lenk, et al. (2009). "Defective autophagy in neurons and astrocytes from mice deficient in PI(3,5)P2." Hum Mol Genet **18**(24): 4868-4878.

Fernandez-Borja, M., R. Wubbolts, et al. (1999). "Multivesicular body morphogenesis requires phosphatidyl-inositol 3-kinase activity." Curr Biol **9**(1): 55-58.

Ferrell, J. E., Jr. and W. H. Huestis (1984). "Phosphoinositide metabolism and the morphology of human erythrocytes." J Cell Biol **98**(6): 1992-1998.

Fili, N., V. Calleja, et al. (2006). "Compartmental signal modulation: Endosomal phosphatidylinositol 3-phosphate controls endosome morphology and selective cargo sorting." Proc Natl Acad Sci U S A **103**(42): 15473-15478.

Footitt, S., M. Ingouff, et al. (2003). "Expression of the viviparous 1 (Pavp1) and p34cdc2 protein kinase (cdc2Pa) genes during somatic embryogenesis in Norway spruce (Picea abies [L.] Karst)." J Exp Bot **54**(388): 1711-1719.

Fowler, S. (1969). "Lysosomal localization of sphingomyelinase in rat liver." Biochim Biophys Acta **191**(2): 481-484.

Fraldi, A., F. Annunziata, et al. (2010). "Lysosomal fusion and SNARE function are impaired by cholesterol accumulation in lysosomal storage disorders." EMBO J **29**(21): 3607-3620.

Fratti, R. A., J. M. Backer, et al. (2001). "Role of phosphatidylinositol 3-kinase and Rab5 effectors in phagosomal biogenesis and mycobacterial phagosome maturation arrest." J Cell Biol **154**(3): 631-644.

Fukuda, T., A. Roberts, et al. (2006). "Autophagy and lysosomes in Pompe disease." Autophagy **2**(4): 318-320.

Galione, A., A. J. Morgan, et al. (2010). "NAADP as an intracellular messenger regulating lysosomal calcium-release channels." Biochem Soc Trans **38**(6): 1424-1431.

Gallala, H. D., B. Breiden, et al. (2011). "Regulation of the NPC2 protein-mediated cholesterol trafficking by membrane lipids." J Neurochem **116**(5): 702-707.

Gao, M., M. Wang, et al. (2010). "Facile synthesis of carbon-11-labeled cholesterol-based cationic lipids as new potential PET probes for imaging of gene delivery in cancer." Steroids **75**(10): 715-720.

Garcia-Barros, M., F. Paris, et al. (2003). "Tumor response to radiotherapy regulated by endothelial cell apoptosis." Science **300**(5622): 1155-1159.

Gatt, S. (1963). "Enzymic Hydrolysis and Synthesis of Ceramides." J Biol Chem **238**: 3131-3133.

Gatt, S. (1976). "Magnesium-dependent sphingomyelinase." Biochem Biophys Res Commun **68**(1): 235-241.

Gault, C. R., L. M. Obeid, et al. (2010). "An overview of sphingolipid metabolism: from synthesis to breakdown." Adv Exp Med Biol **688**: 1-23.

Gerasimenko, J. V., A. V. Tepikin, et al. (1998). "Calcium uptake via endocytosis with rapid release from acidifying endosomes." Curr Biol **8**(24): 1335-1338.

Giacomello, M., R. Hudec, et al. (2011). "Huntington's disease, calcium, and mitochondria." Biofactors **37**(3): 206-218.

Ginzburg, L. and A. H. Futerman (2005). "Defective calcium homeostasis in the cerebellum in a mouse model of Niemann-Pick A disease." J Neurochem **95**(6): 1619-1628.

Ginzburg, L., S. C. Li, et al. (2008). "An exposed carboxyl group on sialic acid is essential for gangliosides to inhibit calcium uptake via the sarco/endoplasmic reticulum Ca2+-ATPase: relevance to gangliosidoses." J Neurochem **104**(1): 140-146.

Goldin, E., S. Stahl, et al. (2004). "Transfer of a mitochondrial DNA fragment to MCOLN1 causes an inherited case of mucolipidosis IV." Hum Mutat **24**(6): 460-465.

Graham, T. R. and M. M. Kozlov (2010). "Interplay of proteins and lipids in generating membrane curvature." Curr Opin Cell Biol **22**(4): 430-436.

Grassme, H., A. Cremesti, et al. (2003). "Ceramide-mediated clustering is required for CD95-DISC formation." Oncogene **22**(35): 5457-5470.

Greka, A., B. Navarro, et al. (2003). "TRPC5 is a regulator of hippocampal neurite length and growth cone morphology." Nat Neurosci **6**(8): 837-845.

Griffiths, G. (2002). "What's special about secretory lysosomes?" Semin Cell Dev Biol **13**(4): 279-284.

Grimm, C., M. P. Cuajungco, et al. (2007). "A helix-breaking mutation in TRPML3 leads to constitutive activity underlying deafness in the varitint-waddler mouse." Proc Natl Acad Sci U S A **104**(49): 19583-19588.

Grimm, C., S. Jors, et al. (2010). "Small molecule activators of TRPML3." Chem Biol **17**(2): 135-148.

Groffen, A. J., S. Martens, et al. "Doc2b is a high-affinity Ca2+ sensor for spontaneous neurotransmitter release." Science **327**(5973): 1614-1618.

Grosshans, B. L., A. Andreeva, et al. (2006). "The yeast lgl family member Sro7p is an effector of the secretory Rab GTPase Sec4p." J Cell Biol **172**(1): 55-66.

Grosshans, B. L., H. Grotsch, et al. (2006). "TEDS site phosphorylation of the yeast myosins I is required for ligand-induced but not for constitutive endocytosis of the G protein-coupled receptor Ste2p." J Biol Chem **281**(16): 11104-11114.

Grosshans, B. L., D. Ortiz, et al. (2006). "Rabs and their effectors: achieving specificity in membrane traffic." Proc Natl Acad Sci U S A **103**(32): 11821-11827.

Grosshans, E., J. Bourlond, et al. (2006). "[Nevocytic nevi associated elastic fibers hyperplasia: a type of "twin nevus"]." Ann Dermatol Venereol **133**(5 Pt 1): 435-438.

Gruenberg, J. and H. Stenmark (2004). "The biogenesis of multivesicular endosomes." Nat Rev Mol Cell Biol **5**(4): 317-323.

Guardamagna, O., F. Abello, et al. (2011). "Primary hyperlipidemias in children: effect of plant sterol supplementation on plasma lipids and markers of cholesterol synthesis and absorption." Acta Diabetol **48**(2): 127-133.

Guicciardi, M. E., M. Leist, et al. (2004). "Lysosomes in cell death." Oncogene **23**(16): 2881-2890.

Gutman, G. A., K. G. Chandy, et al. (2003). "International Union of Pharmacology. XLI. Compendium of voltage-gated ion channels: potassium channels." Pharmacol Rev **55**(4): 583-586.

Hamilton, S. L. and Serysheva, II (2009). "Ryanodine receptor structure: progress and challenges." J Biol Chem **284**(7): 4047-4051.

Hannun, Y. A. and L. M. Obeid (2008). "Principles of bioactive lipid signalling: lessons from sphingolipids." Nat Rev Mol Cell Biol **9**(2): 139-150.

Hanson, P. I., S. Shim, et al. (2009). "Cell biology of the ESCRT machinery." Curr Opin Cell Biol **21**(4): 568-574.

Harrison, R. E., C. Bucci, et al. (2003). "Phagosomes fuse with late endosomes and/or lysosomes by extension of membrane protrusions along microtubules: role of Rab7 and RILP." Mol Cell Biol **23**(18): 6494-6506.

Hay, J. C. (2007). "Calcium: a fundamental regulator of intracellular membrane fusion?" EMBO Rep **8**(3): 236-240.

He, C. and D. J. Klionsky (2009). "Regulation mechanisms and signaling pathways of autophagy." Annu Rev Genet **43**: 67-93.

Heinrich, M., M. Wickel, et al. (2000). "Ceramide as an activator lipid of cathepsin D." Adv Exp Med Biol **477**: 305-315.

Helip-Wooley, A. and J. G. Thoene (2004). "Sucrose-induced vacuolation results in increased expression of cholesterol biosynthesis and lysosomal genes." Exp Cell Res **292**(1): 89-100.

Hernandez, L. D., K. Hueffer, et al. (2004). "Salmonella modulates vesicular traffic by altering phosphoinositide metabolism." Science **304**(5678): 1805-1807.

Herrador, A., S. Herranz, et al. (2010). "Recruitment of the ESCRT machinery to a putative seven-transmembrane-domain receptor is mediated by an arrestin-related protein." Mol Cell Biol **30**(4): 897-907.

Hickey, C. M. and W. Wickner (2010). "HOPS initiates vacuole docking by tethering membranes before trans-SNARE complex assembly." Mol Biol Cell **21**(13): 2297-2305.

Higgins, M. E., J. P. Davies, et al. (1999). "Niemann-Pick C1 is a late endosome-resident protein that transiently associates with lysosomes and the trans-Golgi network." Mol Genet Metab **68**(1): 1-13.

Hill, E. V., C. A. Hudson, et al. (2010). "Regulation of PIKfyve phosphorylation by insulin and osmotic stress." Biochem Biophys Res Commun **397**(4): 650-655.

Horinouchi, K., S. Erlich, et al. (1995). "Acid sphingomyelinase deficient mice: a model of types A and B Niemann-Pick disease." Nat Genet **10**(3): 288-293.

Hurley, J. H. and S. D. Emr (2006). "The ESCRT complexes: structure and mechanism of a membrane-trafficking network." Annu Rev Biophys Biomol Struct **35**: 277-298.

Hurwitz, R., K. Ferlinz, et al. (1994). "The tricyclic antidepressant desipramine causes proteolytic degradation of lysosomal sphingomyelinase in human fibroblasts." Biol Chem Hoppe Seyler **375**(7): 447-450.

Hutagalung, A. H. and P. J. Novick (2011). "Role of Rab GTPases in membrane traffic and cell physiology." Physiol Rev **91**(1): 119-149.

Hutagalung, R., J. Marques, et al. (2011). "The obesity paradox in surgical intensive care unit patients." Intensive Care Med **37**(11): 1793-1799.

Huynh, K. K., E. L. Eskelinen, et al. (2007). "LAMP proteins are required for fusion of lysosomes with phagosomes." EMBO J **26**(2): 313-324.

Ikonomov, O. C., D. Sbrissa, et al. (2011). "The phosphoinositide kinase PIKfyve is vital in early embryonic development: Preimplantation lethality of PIKfyve-/- embryos but normality of PIKfyve+/- mice." J Biol Chem.

Ikonomov, O. C., D. Sbrissa, et al. (2009). "Sac3 is an insulin-regulated phosphatidylinositol 3,5-bisphosphate phosphatase: gain in insulin responsiveness through Sac3 down-regulation in adipocytes." J Biol Chem **284**(36): 23961-23971.

Infante, R. E., M. L. Wang, et al. (2008). "NPC2 facilitates bidirectional transfer of cholesterol between NPC1 and lipid bilayers, a step in cholesterol egress from lysosomes." Proc Natl Acad Sci U S A **105**(40): 15287-15292.

Isaev, N. P., V. N. Syryamina, et al. (2010). "Small-angle orientational motions of spin-labeled lipids in cholesterol-containing bilayers studied at low temperatures by electron spin echo spectroscopy." J Phys Chem B **114**(29): 9510-9515.

Jaiswal, J. K., N. W. Andrews, et al. (2002). "Membrane proximal lysosomes are the major vesicles responsible for calcium-dependent exocytosis in nonsecretory cells." J Cell Biol **159**(4): 625-635.

Jaiswal, J. K., S. Chakrabarti, et al. (2004). "Synaptotagmin VII restricts fusion pore expansion during lysosomal exocytosis." PLoS Biol **2**(8): E233.

James, D. J., C. Khodthong, et al. (2008). "Phosphatidylinositol 4,5-bisphosphate regulates SNARE-dependent membrane fusion." J Cell Biol **182**(2): 355-366.

Janvier, K. and J. S. Bonifacino (2005). "Role of the endocytic machinery in the sorting of lysosome-associated membrane proteins." Mol Biol Cell **16**(9): 4231-4242.

Jefferies, H. B., F. T. Cooke, et al. (2008). "A selective PIKfyve inhibitor blocks PtdIns(3,5)P(2) production and disrupts endomembrane transport and retroviral budding." EMBO Rep **9**(2): 164-170.

Jenkins, R. W., D. Canals, et al. (2010). "Regulated secretion of acid sphingomyelinase: implications for selectivity of ceramide formation." J Biol Chem **285**(46): 35706-35718.

Jennings, J. J., Jr., J. H. Zhu, et al. (2006). "Mitochondrial aberrations in mucolipidosis Type IV." J Biol Chem **281**(51): 39041-39050.

Jennings, L. J., Q. W. Xu, et al. (1999). "Cholesterol inhibits spontaneous action potentials and calcium currents in guinea pig gallbladder smooth muscle." Am J Physiol **277**(5 Pt 1): G1017-1026.

Jin, N., C. Y. Chow, et al. (2008). "VAC14 nucleates a protein complex essential for the acute interconversion of PI3P and PI(3,5)P(2) in yeast and mouse." EMBO J **27**(24): 3221-3234.

Jin, S., F. Yi, et al. (2008). "Lysosomal targeting and trafficking of acid sphingomyelinase to lipid raft platforms in coronary endothelial cells." Arterioscler Thromb Vasc Biol **28**(11): 2056-2062.

Jouaiti, A., M. W. Hosseini, et al. (2006). "Orthogonal packing of enantiomerically pure helical silver coordination networks." Chem Commun (Camb)(29): 3078-3080.

Karacsonyi, C., A. S. Miguel, et al. (2007). "Mucolipin-2 localizes to the Arf6-associated pathway and regulates recycling of GPI-APs." Traffic **8**(10): 1404-1414.

Karageorgos, L. E., E. L. Isaac, et al. (1997). "Lysosomal biogenesis in lysosomal storage disorders." Exp Cell Res **234**(1): 85-97.

Karten, B., K. B. Peake, et al. (2009). "Mechanisms and consequences of impaired lipid trafficking in Niemann-Pick type C1-deficient mammalian cells." Biochim Biophys Acta **1791**(7): 659-670.

Kaur, J. and D. F. Cutler (2002). "P-selectin targeting to secretory lysosomes of Rbl-2H3 cells." J Biol Chem **277**(12): 10498-10505.

Kerdpanich, A., K. Chokephaibulkit, et al. (2011). "Immunogenicity of a human rotavirus vaccine (RIX4414) after storage at 37 degrees C for seven days." Hum Vaccin **7**(1): 74-80.

Kim, H. J., Q. Li, et al. (2007). "Gain-of-function mutation in TRPML3 causes the mouse Varitint-Waddler phenotype." J Biol Chem **282**(50): 36138-36142.

Kim, H. J., A. A. Soyombo, et al. (2009). "The Ca(2+) channel TRPML3 regulates membrane trafficking and autophagy." Traffic **10**(8): 1157-1167.

Kirkegaard, T., A. G. Roth, et al. (2010). "Hsp70 stabilizes lysosomes and reverts Niemann-Pick disease-associated lysosomal pathology." Nature **463**(7280): 549-553.

Kiselyov, K., S. Yamaguchi, et al. (2010). "Aberrant Ca2+ handling in lysosomal storage disorders." Cell Calcium **47**(2): 103-111.

Kitatani, K., J. Idkowiak-Baldys, et al. (2008). "The sphingolipid salvage pathway in ceramide metabolism and signaling." Cell Signal **20**(6): 1010-1018.

Koishi, R., H. Xu, et al. (2004). "A superfamily of voltage-gated sodium channels in bacteria." J Biol Chem **279**(10): 9532-9538.

Kolter, T. and K. Sandhoff (2005). "Principles of lysosomal membrane digestion: stimulation of sphingolipid degradation by sphingolipid activator proteins and anionic lysosomal lipids." Annu Rev Cell Dev Biol **21**: 81-103.

Kolter, T. and K. Sandhoff (2010). "Lysosomal degradation of membrane lipids." FEBS Lett **584**(9): 1700-1712.

Korkotian, E., A. Schwarz, et al. (1999). "Elevation of intracellular glucosylceramide levels results in an increase in endoplasmic reticulum density and in functional calcium stores in cultured neurons." J Biol Chem **274**(31): 21673-21678.

Kornhuber, J., P. Tripal, et al. (2008). "Identification of new functional inhibitors of acid sphingomyelinase using a structure-property-activity relation model." J Med Chem **51**(2): 219-237.

Krapivinsky, G., L. Krapivinsky, et al. (2003). "The NMDA receptor is coupled to the ERK pathway by a direct interaction between NR2B and RasGRF1." Neuron **40**(4): 775-784.

Kutateladze, T. G. (2010). "Translation of the phosphoinositide code by PI effectors." Nat Chem Biol **6**(7): 507-513.

Lange, I., S. Yamamoto, et al. (2009). "TRPM2 functions as a lysosomal Ca2+-release channel in beta cells." Sci Signal **2**(71): ra23.

LaPlante, J. M., J. Falardeau, et al. (2002). "Identification and characterization of the single channel function of human mucolipin-1 implicated in mucolipidosis type IV, a disorder affecting the lysosomal pathway." FEBS Lett **532**(1-2): 183-187.

LaPlante, J. M., M. Sun, et al. (2006). "Lysosomal exocytosis is impaired in mucolipidosis type IV." Mol Genet Metab **89**(4): 339-348.

LaPlante, J. M., C. P. Ye, et al. (2004). "Functional links between mucolipin-1 and Ca2+-dependent membrane trafficking in mucolipidosis IV." Biochem Biophys Res Commun **322**(4): 1384-1391.

LaRocca, T. J., J. T. Crowley, et al. (2010). "Cholesterol lipids of Borrelia burgdorferi form lipid rafts and are required for the bactericidal activity of a complement-independent antibody." Cell Host Microbe **8**(4): 331-342.

Lee, S. H., B. Clapham, et al. (2003). "Rhodium carbenoid N-H insertion reactions of primary ureas: solution and solid-phase synthesis of imidazolones." Org Lett **5**(4): 511-514.

Lee, S. H., B. Clapham, et al. (2003). "Solid-phase rhodium carbenoid N-H insertion reactions: the synthesis of a diverse array of indoles." J Comb Chem **5**(2): 188-196.

Levine, B. (2004). "Autobiographical memory and the self in time: brain lesion effects, functional neuroanatomy, and lifespan development." Brain Cogn **55**(1): 54-68.

Levine, B. and D. J. Klionsky (2004). "Development by self-digestion: molecular mechanisms and biological functions of autophagy." Dev Cell **6**(4): 463-477.

Li, G., C. D'Souza-Schorey, et al. (1995). "Evidence for phosphatidylinositol 3-kinase as a regulator of endocytosis via activation of Rab5." Proc Natl Acad Sci U S A **92**(22): 10207-10211.

Liao, G., Y. Yao, et al. (2007). "Cholesterol accumulation is associated with lysosomal dysfunction and autophagic stress in Npc1 -/- mouse brain." Am J Pathol **171**(3): 962-975.

Lingwood, D. and K. Simons (2010). "Lipid rafts as a membrane-organizing principle." Science **327**(5961): 46-50.

Link, T. M., U. Park, et al. (2010). "TRPV2 has a pivotal role in macrophage particle binding and phagocytosis." Nat Immunol **11**(3): 232-239.

Lippincott-Schwartz, J. and R. D. Phair (2010). "Lipids and cholesterol as regulators of traffic in the endomembrane system." Annu Rev Biophys **39**: 559-578.

Lipsker, D., A. Mitschler, et al. (2006). "Could Jessner's lymphocytic infiltrate of the skin be a dermal variant of lupus erythematosus? An analysis of 210 cases." Dermatology **213**(1): 15-22.

Liscum, L. and J. R. Faust (1989). "The intracellular transport of low density lipoprotein-derived cholesterol is inhibited in Chinese hamster ovary cells cultured with 3-beta-[2-(diethylamino)ethoxy]androst-5-en-17-one." J Biol Chem **264**(20): 11796-11806.

Liu, J. P., Y. Tang, et al. "Cholesterol involvement in the pathogenesis of neurodegenerative diseases." Mol Cell Neurosci **43**(1): 33-42.

Lloyd-Evans, E., A. J. Morgan, et al. (2008). "Niemann-Pick disease type C1 is a sphingosine storage disease that causes deregulation of lysosomal calcium." Nat Med **14**(11): 1247-1255.

Lloyd-Evans, E., D. Pelled, et al. (2003). "Glucosylceramide and glucosylsphingosine modulate calcium mobilization from brain microsomes via different mechanisms." J Biol Chem **278**(26): 23594-23599.

Lloyd-Evans, E. and F. M. Platt (2010). "Lipids on trial: the search for the offending metabolite in Niemann-Pick type C disease." Traffic **11**(4): 419-428.

Lloyd-Evans, E., H. Waller-Evans, et al. (2010). "Endolysosomal calcium regulation and disease." Biochem Soc Trans **38**(6): 1458-1464.

Lozano, J., S. Menendez, et al. (2001). "Cell autonomous apoptosis defects in acid sphingomyelinase knockout fibroblasts." J Biol Chem **276**(1): 442-448.

Luzio, J. P., S. R. Gray, et al. (2010). "Endosome-lysosome fusion." Biochem Soc Trans **38**(6): 1413-1416.

Luzio, J. P., P. R. Pryor, et al. (2007). "Lysosomes: fusion and function." Nat Rev Mol Cell Biol **8**(8): 622-632.

Luzio, J. P., B. A. Rous, et al. (2000). "Lysosome-endosome fusion and lysosome biogenesis." J Cell Sci **113 (Pt 9)**: 1515-1524.

Mahalka, A. K., C. Code, et al. (2011). "Activation of phospholipase A2 by Hsp70 in vitro." Biochim Biophys Acta **1808**(10): 2569-2572.

Maki, K. C., M. R. Dicklin, et al. (2010). "Baseline lipoprotein lipids and low-density lipoprotein cholesterol response to prescription omega-3 acid ethyl ester added to Simvastatin therapy." Am J Cardiol **105**(10): 1409-1412.

Malerod, L. and H. Stenmark (2009). "ESCRTing membrane deformation." Cell **136**(1): 15-17.

Marathe, S., S. R. Miranda, et al. (2000). "Creation of a mouse model for non-neurological (type B) Niemann-Pick disease by stable, low level expression of lysosomal sphingomyelinase in the absence of secretory sphingomyelinase: relationship between brain intra-lysosomal enzyme activity and central nervous system function." Hum Mol Genet **9**(13): 1967-1976.

Marks, D. L. and R. E. Pagano (2002). "Endocytosis and sorting of glycosphingolipids in sphingolipid storage disease." Trends Cell Biol **12**(12): 605-613.

Martens, S. and H. T. McMahon (2008). "Mechanisms of membrane fusion: disparate players and common principles." Nat Rev Mol Cell Biol **9**(7): 543-556.

Martina, J. A., B. Lelouvier, et al. (2009). "The calcium channel mucolipin-3 is a novel regulator of trafficking along the endosomal pathway." Traffic **10**(8): 1143-1156.

Maxfield, F. R. and T. E. McGraw (2004). "Endocytic recycling." Nat Rev Mol Cell Biol **5**(2): 121-132.

Maxfield, F. R. and D. Wustner (2002). "Intracellular cholesterol transport." J Clin Invest **110**(7): 891-898.

McCrea, H. J. and P. De Camilli (2009). "Mutations in phosphoinositide metabolizing enzymes and human disease." Physiology (Bethesda) **24**: 8-16.

McDonald, B. and J. Martin-Serrano (2009). "No strings attached: the ESCRT machinery in viral budding and cytokinesis." J Cell Sci **122**(Pt 13): 2167-2177.

McNeil, P. L. and T. Kirchhausen (2005). "An emergency response team for membrane repair." Nat Rev Mol Cell Biol **6**(6): 499-505.

Medina, D. L., A. Fraldi, et al. (2011). "Transcriptional activation of lysosomal exocytosis promotes cellular clearance." Dev Cell **21**(3): 421-430.

Megha and E. London (2004). "Ceramide selectively displaces cholesterol from ordered lipid domains (rafts): implications for lipid raft structure and function." J Biol Chem **279**(11): 9997-10004.

Merz, A. J. and W. T. Wickner (2004). "Trans-SNARE interactions elicit Ca2+ efflux from the yeast vacuole lumen." J Cell Biol **164**(2): 195-206.

Mesmin, B. and F. R. Maxfield (2009). "Intracellular sterol dynamics." Biochim Biophys Acta **1791**(7): 636-645.

Milhas, D., C. J. Clarke, et al. (2010). "Sphingomyelin metabolism at the plasma membrane: implications for bioactive sphingolipids." FEBS Lett **584**(9): 1887-1894.

Mobius, W., E. van Donselaar, et al. (2003). "Recycling compartments and the internal vesicles of multivesicular bodies harbor most of the cholesterol found in the endocytic pathway." Traffic **4**(4): 222-231.

Mori, K., H. T. Lee, et al. (2005). "Endocytic delivery of lipocalin-siderophore-iron complex rescues the kidney from ischemia-reperfusion injury." J Clin Invest **115**(3): 610-621.

Mullock, B. M., N. A. Bright, et al. (1998). "Fusion of lysosomes with late endosomes produces a hybrid organelle of intermediate density and is NSF dependent." J Cell Biol **140**(3): 591-601.

Munafo, D. B. and M. I. Colombo (2001). "A novel assay to study autophagy: regulation of autophagosome vacuole size by amino acid deprivation." J Cell Sci **114**(Pt 20): 3619-3629.

Naureckiene, S., D. E. Sleat, et al. (2000). "Identification of HE1 as the second gene of Niemann-Pick C disease." Science **290**(5500): 2298-2301.

Navascues, M., F. Grosshans, et al. (2006). "Optimality of Gaussian attacks in continuous-variable quantum cryptography." Phys Rev Lett **97**(19): 190502.

Neufeld, E. B., M. Wastney, et al. (1999). "The Niemann-Pick C1 protein resides in a vesicular compartment linked to retrograde transport of multiple lysosomal cargo." J Biol Chem **274**(14): 9627-9635.

Ni, W., A. H. Hutagalung, et al. (2011). "The myosin-binding UCS domain but not the Hsp90-binding TPR domain of the UNC-45 chaperone is essential for function in Caenorhabditis elegans." J Cell Sci **124**(Pt 18): 3164-3173.

Nixon, R. A., D. S. Yang, et al. (2008). "Neurodegenerative lysosomal disorders: a continuum from development to late age." Autophagy **4**(5): 590-599.

Novick, P., M. Medkova, et al. (2006). "Interactions between Rabs, tethers, SNAREs and their regulators in exocytosis." Biochem Soc Trans **34**(Pt 5): 683-686.

Oancea, E., V. J. Bezzerides, et al. (2003). "Mechanism of persistent protein kinase D1 translocation and activation." Dev Cell **4**(4): 561-574.

Ozaki, S., D. B. DeWald, et al. (2000). "Intracellular delivery of phosphoinositides and inositol phosphates using polyamine carriers." Proc Natl Acad Sci U S A **97**(21): 11286-11291.

Pacheco, C. D., M. J. Elrick, et al. (2009). "Tau deletion exacerbates the phenotype of Niemann-Pick type C mice and implicates autophagy in pathogenesis." Hum Mol Genet **18**(5): 956-965.

Pacheco, C. D., R. Kunkel, et al. (2007). "Autophagy in Niemann-Pick C disease is dependent upon Beclin-1 and responsive to lipid trafficking defects." Hum Mol Genet **16**(12): 1495-1503.

Pagano, R. E. and C. S. Chen (1998). "Use of BODIPY-labeled sphingolipids to study membrane traffic along the endocytic pathway." Ann N Y Acad Sci **845**: 152-160.

Parkinson-Lawrence, E. J., T. Shandala, et al. (2010). "Lysosomal storage disease: revealing lysosomal function and physiology." Physiology (Bethesda) **25**(2): 102-115.

Patapoutian, A., S. Tate, et al. (2009). "Transient receptor potential channels: targeting pain at the source." Nat Rev Drug Discov **8**(1): 55-68.

Peake, K. B. and J. E. Vance "Defective cholesterol trafficking in Niemann-Pick C-deficient cells." FEBS Lett **584**(13): 2731-2739.

Pelled, D., E. Lloyd-Evans, et al. (2003). "Inhibition of calcium uptake via the sarco/endoplasmic reticulum Ca2+-ATPase in a mouse model of Sandhoff disease and prevention by treatment with N-butyldeoxynojirimycin." J Biol Chem **278**(32): 29496-29501.

Perrotta, C. and E. Clementi (2010). "Biological roles of Acid and neutral sphingomyelinases and their regulation by nitric oxide." Physiology (Bethesda) **25**(2): 64-71.

Peters, C. and A. Mayer (1998). "Ca2+/calmodulin signals the completion of docking and triggers a late step of vacuole fusion." Nature **396**(6711): 575-580.

Petersen, N. H. and T. Kirkegaard (2010). "HSP70 and lysosomal storage disorders: novel therapeutic opportunities." Biochem Soc Trans **38**(6): 1479-1483.

Petersen, N. H., T. Kirkegaard, et al. (2010). "Connecting Hsp70, sphingolipid metabolism and lysosomal stability." Cell Cycle **9**(12): 2305-2309.

Pipalia, N. H., M. Hao, et al. (2007). "Sterol, protein and lipid trafficking in Chinese hamster ovary cells with Niemann-Pick type C1 defect." Traffic **8**(2): 130-141.

Piper, R. C. and J. P. Luzio (2004). "CUPpling calcium to lysosomal biogenesis." <u>Trends Cell Biol</u> **14**(9): 471-473.

Poccia, D. and B. Larijani (2009). "Phosphatidylinositol metabolism and membrane fusion." <u>Biochem J</u> **418**(2): 233-246.

Proikas-Cezanne, T., S. Ruckerbauer, et al. (2007). "Human WIPI-1 puncta-formation: a novel assay to assess mammalian autophagy." <u>FEBS Lett</u> **581**(18): 3396-3404.

Pryor, P. R., B. M. Mullock, et al. (2000). "The role of intraorganellar Ca(2+) in late endosome-lysosome heterotypic fusion and in the reformation of lysosomes from hybrid organelles." <u>J Cell Biol</u> **149**(5): 1053-1062.

Pryor, P. R., F. Reimann, et al. (2006). "Mucolipin-1 is a lysosomal membrane protein required for intracellular lactosylceramide traffic." <u>Traffic</u> **7**(10): 1388-1398.

Puertollano, R. and K. Kiselyov (2009). "TRPMLs: in sickness and in health." <u>Am J Physiol Renal Physiol</u> **296**(6): F1245-1254.

Puri, V., R. Watanabe, et al. (1999). "Cholesterol modulates membrane traffic along the endocytic pathway in sphingolipid-storage diseases." <u>Nat Cell Biol</u> **1**(6): 386-388.

Radchatawedchakoon, W., R. Watanapokasin, et al. (2010). "Solid phase synthesis of novel asymmetric hydrophilic head cholesterol-based cationic lipids with potential DNA delivery." <u>Bioorg Med Chem</u> **18**(1): 330-342.

Raiborg, C. and H. Stenmark (2009). "The ESCRT machinery in endosomal sorting of ubiquitylated membrane proteins." <u>Nature</u> **458**(7237): 445-452.

Ramsey, I. S., M. Delling, et al. (2006). "An introduction to TRP channels." <u>Annu Rev Physiol</u> **68**: 619-647.

Rao, S. K., C. Huynh, et al. (2004). "Identification of SNAREs involved in synaptotagmin VII-regulated lysosomal exocytosis." <u>J Biol Chem</u> **279**(19): 20471-20479.

Raychowdhury, M. K., S. Gonzalez-Perrett, et al. (2004). "Molecular pathophysiology of mucolipidosis type IV: pH dysregulation of the mucolipin-1 cation channel." <u>Hum Mol Genet</u> **13**(6): 617-627.

Reddy, A., E. V. Caler, et al. (2001). "Plasma membrane repair is mediated by Ca(2+)-regulated exocytosis of lysosomes." <u>Cell</u> **106**(2): 157-169.

Reynolds, L., C. Ullman, et al. (2003). "Repression of the HIV-1 5' LTR promoter and inhibition of HIV-1 replication by using engineered zinc-finger transcription factors." <u>Proc Natl Acad Sci U S A</u> **100**(4): 1615-1620.

Rohacs, T. and B. Nilius (2007). "Regulation of transient receptor potential (TRP) channels by phosphoinositides." <u>Pflugers Arch</u> **455**(1): 157-168.

Romanenko, V. G., G. H. Rothblat, et al. (2002). "Modulation of endothelial inward-rectifier K+ current by optical isomers of cholesterol." <u>Biophys J</u> **83**(6): 3211-3222.

Rosenbaum, A. I., C. C. Cosner, et al. (2010). "Thiadiazole carbamates: potent inhibitors of lysosomal acid lipase and potential Niemann-Pick type C disease therapeutics." <u>J Med Chem</u> **53**(14): 5281-5289.

Rosenbaum, A. I. and F. R. Maxfield (2011). "Niemann-Pick type C disease: molecular mechanisms and potential therapeutic approaches." <u>J Neurochem</u> **116**(5): 789-795.

Rosenbaum, A. I., M. Rujoi, et al. (2009). "Chemical screen to reduce sterol accumulation in Niemann-Pick C disease cells identifies novel lysosomal acid lipase inhibitors." <u>Biochim Biophys Acta</u> **1791**(12): 1155-1165.

Roth, M. G. (2004). "Phosphoinositides in constitutive membrane traffic." <u>Physiol Rev</u> **84**(3): 699-730.

Saftig, P. and J. Klumperman (2009). "Lysosome biogenesis and lysosomal membrane proteins: trafficking meets function." <u>Nat Rev Mol Cell Biol</u> **10**(9): 623-635.

Saito, M., P. I. Hanson, et al. (2007). "Luminal chloride-dependent activation of endosome calcium channels: patch clamp study of enlarged endosomes." <u>J Biol Chem</u> **282**(37): 27327-27333.

Sardiello, M. and A. Ballabio (2009). "Lysosomal enhancement: a CLEAR answer to cellular degradative needs." <u>Cell Cycle</u> **8**(24): 4021-4022.

Sardiello, M., M. Palmieri, et al. (2009). "A gene network regulating lysosomal biogenesis and function." <u>Science</u> **325**(5939): 473-477.

Saxena, S. K. and S. Kaur (2006). "Regulation of epithelial ion channels by Rab GTPases." Biochem Biophys Res Commun **351**(3): 582-587.

Sbrissa, D., O. C. Ikonomov, et al. (2007). "Core protein machinery for mammalian phosphatidylinositol 3,5-bisphosphate synthesis and turnover that regulates the progression of endosomal transport. Novel Sac phosphatase joins the ArPIKfyve-PIKfyve complex." J Biol Chem **282**(33): 23878-23891.

Schiffmann, R. (2010). "Therapeutic approaches for neuronopathic lysosomal storage disorders." J Inherit Metab Dis **33**(4): 373-379.

Schissel, S. L., G. A. Keesler, et al. (1998). "The cellular trafficking and zinc dependence of secretory and lysosomal sphingomyelinase, two products of the acid sphingomyelinase gene." J Biol Chem **273**(29): 18250-18259.

Schneider, L. and J. Zhang (2010). "Lysosomal function in macromolecular homeostasis and bioenergetics in Parkinson's disease." Mol Neurodegener **5**: 14.

Schuchman, E. H. (2007). "The pathogenesis and treatment of acid sphingomyelinase-deficient Niemann-Pick disease." J Inherit Metab Dis **30**(5): 654-663.

Schuchman, E. H. (2010). "Acid sphingomyelinase, cell membranes and human disease: lessons from Niemann-Pick disease." FEBS Lett **584**(9): 1895-1900.

Schultz, M. L., L. Tecedor, et al. (2011). "Clarifying lysosomal storage diseases." Trends Neurosci **34**(8): 401-410.

Settembre, C., E. Arteaga-Solis, et al. (2009). "Self-eating in skeletal development: implications for lysosomal storage disorders." Autophagy **5**(2): 228-229.

Settembre, C., A. Fraldi, et al. (2008). "A block of autophagy in lysosomal storage disorders." Hum Mol Genet **17**(1): 119-129.

Settembre, C., A. Fraldi, et al. (2008). "Lysosomal storage diseases as disorders of autophagy." Autophagy **4**(1): 113-114.

Shachar, T., C. Lo Bianco, et al. (2011). "Lysosomal storage disorders and Parkinson's disease: Gaucher disease and beyond." Mov Disord **26**(9): 1593-1604.

Shaughnessy, L. M., A. D. Hoppe, et al. (2006). "Membrane perforations inhibit lysosome fusion by altering pH and calcium in Listeria monocytogenes vacuoles." Cell Microbiol **8**(5): 781-792.

Shen, D., X. Wang, et al. (2011). "Pairing phosphoinositides with calcium ions in endolysosomal dynamics: phosphoinositides control the direction and specificity of membrane trafficking by regulating the activity of calcium channels in the endolysosomes." Bioessays **33**(6): 448-457.

Shen, J., W. M. Yu, et al. (2009). "Deficiency of MIP/MTMR14 phosphatase induces a muscle disorder by disrupting Ca(2+) homeostasis." Nat Cell Biol **11**(6): 769-776.

Shin, H. W., M. Hayashi, et al. (2005). "An enzymatic cascade of Rab5 effectors regulates phosphoinositide turnover in the endocytic pathway." Journal of Cell Biology **170**(4): 607-618.

Shisheva, A., B. Rusin, et al. (2001). "Localization and insulin-regulated relocation of phosphoinositide 5-kinase PIKfyve in 3T3-L1 adipocytes." J Biol Chem **276**(15): 11859-11869.

Simonsen, A., R. Lippe, et al. (1998). "EEA1 links PI(3)K function to Rab5 regulation of endosome fusion." Nature **394**(6692): 494-498.

Simonsen, A. and S. A. Tooze (2009). "Coordination of membrane events during autophagy by multiple class III PI3-kinase complexes." J Cell Biol **186**(6): 773-782.

Slagsvold, T., K. Pattni, et al. (2006). "Endosomal and non-endosomal functions of ESCRT proteins." Trends Cell Biol **16**(6): 317-326.

Smith, E. L. and E. H. Schuchman (2008). "The unexpected role of acid sphingomyelinase in cell death and the pathophysiology of common diseases." FASEB J **22**(10): 3419-3431.

Soyombo, A. A., S. Tjon-Kon-Sang, et al. (2006). "TRP-ML1 regulates lysosomal pH and acidic lysosomal lipid hydrolytic activity." J Biol Chem **281**(11): 7294-7301.

Spiric, A., D. Trbovic, et al. (2010). "Statistical evaluation of fatty acid profile and cholesterol content in fish (common carp) lipids obtained by different sample preparation procedures." Anal Chim Acta **672**(1-2): 66-71.

Stein, M. P., J. Dong, et al. (2003). "Rab proteins and endocytic trafficking: potential targets for therapeutic intervention." <u>Adv Drug Deliv Rev</u> **55**(11): 1421-1437.

Stenmark, H. (2009). "Rab GTPases as coordinators of vesicle traffic." <u>Nat Rev Mol Cell Biol</u> **10**(8): 513-525.

Storch, J. and Z. Xu (2009). "Niemann-Pick C2 (NPC2) and intracellular cholesterol trafficking." <u>Biochim Biophys Acta</u> **1791**(7): 671-678.

Strubing, C., G. Krapivinsky, et al. (2003). "Formation of novel TRPC channels by complex subunit interactions in embryonic brain." <u>J Biol Chem</u> **278**(40): 39014-39019.

Su, Z., X. Zhou, et al. (2009). "Mechanical force and cytoplasmic Ca(2+) activate yeast TRPY1 in parallel." <u>J Membr Biol</u> **227**(3): 141-150.

Sugimoto, Y., H. Ninomiya, et al. (2001). "Accumulation of cholera toxin and GM1 ganglioside in the early endosome of Niemann-Pick C1-deficient cells." <u>Proc Natl Acad Sci U S A</u> **98**(22): 12391-12396.

Suh, B. C. and B. Hille (2008). "PIP2 is a necessary cofactor for ion channel function: how and why?" <u>Annu Rev Biophys</u> **37**: 175-195.

Sun, M., E. Goldin, et al. (2000). "Mucolipidosis type IV is caused by mutations in a gene encoding a novel transient receptor potential channel." <u>Hum Mol Genet</u> **9**(17): 2471-2478.

Suudhof, T. C. (2008). "Neurotransmitter release." <u>Handb Exp Pharmacol</u>(184): 1-21.

Sztolsztener, M. E., A. Dobrzyn, et al. (2012). "Impaired dynamics of the late endosome/lysosome compartment in human Niemann-Pick type C skin fibroblasts carrying mutation in NPC1 gene." <u>Mol Biosyst</u> **8**(4): 1197-1205.

Tam, C., V. Idone, et al. (2010). "Exocytosis of acid sphingomyelinase by wounded cells promotes endocytosis and plasma membrane repair." <u>J Cell Biol</u> **189**(6): 1027-1038.

Tandon, R., D. P. AuCoin, et al. (2009). "Human cytomegalovirus exploits ESCRT machinery in the process of virion maturation." <u>J Virol</u> **83**(20): 10797-10807.

Tao, J. L., X. Z. Ruan, et al. (2010). "Lipids-induced apoptosis is aggravated by acyl-coenzyme A: cholesterol acyltransferase inhibitor." <u>Chin Med Sci J</u> **25**(2): 76-84.

Tassa, A., M. P. Roux, et al. (2003). "Class III phosphoinositide 3-kinase--Beclin1 complex mediates the amino acid-dependent regulation of autophagy in C2C12 myotubes." <u>Biochem J</u> **376**(Pt 3): 577-586.

te Vruchte, D., E. Lloyd-Evans, et al. (2004). "Accumulation of glycosphingolipids in Niemann-Pick C disease disrupts endosomal transport." <u>J Biol Chem</u> **279**(25): 26167-26175.

Teis, D., S. Saksena, et al. (2009). "SnapShot: the ESCRT machinery." <u>Cell</u> **137**(1): 182-182 e181.

Thomas, E. R., C. Shotton, et al. (2003). "CD4-dependent and CD4-independent HIV-2: consequences for neutralization." <u>AIDS</u> **17**(3): 291-300.

Thompson, E. G., L. Schaheen, et al. (2007). "Lysosomal trafficking functions of mucolipin-1 in murine macrophages." <u>BMC Cell Biol</u> **8**: 54.

Thongcharoen, P., P. Auewarakul, et al. (2011). "Cross-clade immunogenicity and antigen-sparing with an AS03(A)-adjuvanted prepandemic influenza vaccine in a Thai population." <u>J Med Assoc Thai</u> **94**(8): 916-926.

Tian, L., S. A. Hires, et al. (2009). "Imaging neural activity in worms, flies and mice with improved GCaMP calcium indicators." <u>Nat Methods</u> **6**(12): 875-881.

Tian, L., Y. Liu, et al. (2010). "Association of the low-density lipoprotein cholesterol/high-density lipoprotein cholesterol ratio and concentrations of plasma lipids with high-density lipoprotein subclass distribution in the Chinese population." <u>Lipids Health Dis</u> **9**: 69.

Trajkovic, K., C. Hsu, et al. (2008). "Ceramide triggers budding of exosome vesicles into multivesicular endosomes." <u>Science</u> **319**(5867): 1244-1247.

Trautwein, E. A., Y. Du, et al. (2010). "Purified black tea theaflavins and theaflavins/catechin supplements did not affect serum lipids in healthy individuals with mildly to moderately elevated cholesterol concentrations." <u>Eur J Nutr</u> **49**(1): 27-35.

Treusch, S., S. Knuth, et al. (2004). "Caenorhabditis elegans functional orthologue of human protein h-mucolipin-1 is required for lysosome biogenesis." <u>Proc Natl Acad Sci U S A</u> **101**(13): 4483-4488.

Truman, J. P., M. M. Al Gadban, et al. (2011). "Acid sphingomyelinase in macrophage biology." Cell Mol Life Sci **68**(20): 3293-3305.

van Meer, G., D. R. Voelker, et al. (2008). "Membrane lipids: where they are and how they behave." Nat Rev Mol Cell Biol **9**(2): 112-124.

van Zyl, L., P. V. Bozhkov, et al. (2003). "Up, down and up again is a signature global gene expression pattern at the beginning of gymnosperm embryogenesis." Gene Expr Patterns **3**(1): 83-91.

Vanier, M. T. (2010). "Niemann-Pick disease type C." Orphanet J Rare Dis **5**: 16.

Venkatachalam, K., T. Hofmann, et al. (2006). "Lysosomal localization of TRPML3 depends on TRPML2 and the mucolipidosis-associated protein TRPML1." J Biol Chem **281**(25): 17517-17527.

Venkatachalam, K., A. A. Long, et al. (2008). "Motor deficit in a Drosophila model of mucolipidosis type IV due to defective clearance of apoptotic cells." Cell **135**(5): 838-851.

Venugopal, B., M. F. Browning, et al. (2007). "Neurologic, gastric, and opthalmologic pathologies in a murine model of mucolipidosis type IV." Am J Hum Genet **81**(5): 1070-1083.

Venugopal, B., N. T. Mesires, et al. (2009). "Chaperone-mediated autophagy is defective in mucolipidosis type IV." J Cell Physiol **219**(2): 344-353.

Vergarajauregui, S., P. S. Connelly, et al. (2008). "Autophagic dysfunction in mucolipidosis type IV patients." Hum Mol Genet **17**(17): 2723-2737.

Vergarajauregui, S., J. A. Martina, et al. (2009). "Identification of the penta-EF-hand protein ALG-2 as a Ca2+-dependent interactor of mucolipin-1." J Biol Chem **284**(52): 36357-36366.

Vergarajauregui, S. and R. Puertollano (2006). "Two di-leucine motifs regulate trafficking of mucolipin-1 to lysosomes." Traffic **7**(3): 337-353.

Vergne, I., J. Chua, et al. (2005). "Mechanism of phagolysosome biogenesis block by viable Mycobacterium tuberculosis." Proc Natl Acad Sci U S A **102**(11): 4033-4038.

Vergne, I., J. Chua, et al. (2004). "Cell biology of mycobacterium tuberculosis phagosome." Annu Rev Cell Dev Biol **20**: 367-394.

Vestergaard, M., T. Hamada, et al. (2010). "Cholesterol, lipids, amyloid Beta, and Alzheimer's." Curr Alzheimer Res **7**(3): 262-270.

Vicinanza, M., G. D'Angelo, et al. (2008). "Function and dysfunction of the PI system in membrane trafficking." EMBO J **27**(19): 2457-2470.

Vieira, O. V., R. J. Botelho, et al. (2002). "Phagosome maturation: aging gracefully." Biochem J **366**(Pt 3): 689-704.

Vieira, O. V., R. E. Harrison, et al. (2004). "Acquisition of Hrs, an essential component of phagosomal maturation, is impaired by mycobacteria." Mol Cell Biol **24**(10): 4593-4604.

Vitner, E. B., F. M. Platt, et al. (2010). "Common and uncommon pathogenic cascades in lysosomal storage diseases." J Biol Chem **285**(27): 20423-20427.

Wang, Q., G. Liang, et al. (2011). "The common inhaled anesthetic isoflurane increases aggregation of huntingtin and alters calcium homeostasis in a cell model of Huntington's disease." Toxicol Appl Pharmacol **250**(3): 291-298.

Wang, S., A. Subramaniam, et al. (2003). "Increased fatty acid oxidation in transgenic mice overexpressing UCP3 in skeletal muscle." Diabetes Obes Metab **5**(5): 295-301.

Wang, Y. M., B. Zhang, et al. (2010). "The mechanism of dietary cholesterol effects on lipids metabolism in rats." Lipids Health Dis **9**: 4.

Weber, T., B. V. Zemelman, et al. (1998). "SNAREpins: minimal machinery for membrane fusion." Cell **92**(6): 759-772.

Wei, X., V. G. Henke, et al. (2003). "Real-time imaging of nuclear permeation by EGFP in single intact cells." Biophys J **84**(2 Pt 1): 1317-1327.

Whiteford, C. C., C. A. Brearley, et al. (1997). "Phosphatidylinositol 3,5-bisphosphate defines a novel PI 3-kinase pathway in resting mouse fibroblasts." Biochem J **323 (Pt 3)**: 597-601.

Wickner, W. (2010). "Membrane fusion: five lipids, four SNAREs, three chaperones, two nucleotides, and a Rab, all dancing in a ring on yeast vacuoles." Annu Rev Cell Dev Biol **26**: 115-136.

Willey, S. J., J. D. Reeves, et al. (2003). "Identification of a subset of human immunodeficiency virus type 1 (HIV-1), HIV-2, and simian immunodeficiency virus strains able to exploit an alternative coreceptor on untransformed human brain and lymphoid cells." J Virol **77**(11): 6138-6152.

Williams, R. L. and S. Urbe (2007). "The emerging shape of the ESCRT machinery." Nat Rev Mol Cell Biol **8**(5): 355-368.

Wollert, T., D. Yang, et al. (2009). "The ESCRT machinery at a glance." J Cell Sci **122**(Pt 13): 2163-2166.

Wu, J., H. P. Shih, et al. (2011). "Neuronal store-operated calcium entry pathway as a novel therapeutic target for Huntington's disease treatment." Chem Biol **18**(6): 777-793.

Wu, L., C. S. Bauer, et al. (2002). "Dual regulation of voltage-gated calcium channels by PtdIns(4,5)P2." Nature **419**(6910): 947-952.

Wu, L. J., T. B. Sweet, et al. (2010). "International Union of Basic and Clinical Pharmacology. LXXVI. Current progress in the mammalian TRP ion channel family." Pharmacol Rev **62**(3): 381-404.

Xu, H., M. Delling, et al. (2007). "Activating mutation in a mucolipin transient receptor potential channel leads to melanocyte loss in varitint-waddler mice." Proc Natl Acad Sci U S A **104**(46): 18321-18326.

Xu, Y., Y. Ramu, et al. (2008). "Removal of phospho-head groups of membrane lipids immobilizes voltage sensors of K+ channels." Nature **451**(7180): 826-829.

Yamaguchi, S. and K. Suzuki (1978). "A novel magnesium-independent neutral sphingomyelinase associated with rat central nervous system meylin." J Biol Chem **253**(12): 4090-4092.

Yang, Z. and D. J. Klionsky (2010). "Mammalian autophagy: core molecular machinery and signaling regulation." Curr Opin Cell Biol **22**(2): 124-131.

Yu, I. M. and F. M. Hughson (2010). "Tethering factors as organizers of intracellular vesicular traffic." Annu Rev Cell Dev Biol **26**: 137-156.

Yu, L., C. K. McPhee, et al. (2010). "Termination of autophagy and reformation of lysosomes regulated by mTOR." Nature **465**(7300): 942-946.

Yu, Z. F., M. Nikolova-Karakashian, et al. (2000). "Pivotal role for acidic sphingomyelinase in cerebral ischemia-induced ceramide and cytokine production, and neuronal apoptosis." J Mol Neurosci **15**(2): 85-97.

Zager, R. A., K. M. Burkhart, et al. (2000). "Sphingomyelinase and membrane sphingomyelin content: determinants ofProximal tubule cell susceptibility to injury." J Am Soc Nephrol **11**(5): 894-902.

Zamponi, G. W. (2003). "Regulation of presynaptic calcium channels by synaptic proteins." J Pharmacol Sci **92**(2): 79-83.

Zant-Przeworska, E., M. Stasiuk, et al. (2010). "Resorcinolic lipids improve the properties of sphingomyelin-cholesterol liposomes." Chem Phys Lipids **163**(7): 648-654.

Zeevi, D. A., A. Frumkin, et al. (2009). "A potentially dynamic lysosomal role for the endogenous TRPML proteins." J Pathol **219**(2): 153-162.

Zeidan, Y. H. and Y. A. Hannun (2007). "Activation of acid sphingomyelinase by protein kinase Cdelta-mediated phosphorylation." J Biol Chem **282**(15): 11549-11561.

Zeidan, Y. H., B. X. Wu, et al. (2008). "A novel role for protein kinase Cdelta-mediated phosphorylation of acid sphingomyelinase in UV light-induced mitochondrial injury." FASEB J **22**(1): 183-193.

Zhang, Y., S. N. Zolov, et al. (2007). "Loss of Vac14, a regulator of the signaling lipid phosphatidylinositol 3,5-bisphosphate, results in neurodegeneration in mice." Proc Natl Acad Sci U S A **104**(44): 17518-17523.

Zhu, M. X., J. Ma, et al. (2010). "TPCs: Endolysosomal channels for Ca2+ mobilization from acidic organelles triggered by NAADP." FEBS Lett **584**(10): 1966-1974.